1997-12-01

The Development of Electromechanical Batteries for Power System Support and for Short-term Standby Power

Michael Peter O'Leary
Technological University Dublin

THE DEVELOPMENT OF ELECTROMECHANICAL BATTERIES FOR POWER SYSTEM SUPPORT AND FOR SHORT-TERM STANDBY POWER

by

Michael Peter O'Leary BE MEngSc

under the supervision of

Mr R. O'Neill MA MSc (DIT Fitzwilliam Hse)

Mr G. Walker BA MRP (DIT Bolton Street)

in

The Bolton Street College of the Dublin Institute of Technology

For submission to

The Dublin Institute of Technology

in fulfillment of the requirements for a

Master of Philosophy degree

on

December 19, 1997

I certify that this thesis which I now submit for examination for the award of Master of Philosophy is entirely my own work and has not been taken from the work of others save and to the extent that such work has been cited and acknowledged within the text of my work.

This thesis was prepared according to the regulations for postgraduate studies by research of the Dublin Institute of Technology and has not been submitted in whole or in part for an award in any other Institute or University.

The Institute has permission to keep, to lend or to copy this thesis in whole or in part, on condition that any such use of the material of the thesis be duly acknowledged.

Signed:_____ Date: 19.12.97

Acknowledgements

I would like to thank both supervisors Mr. [illegible] and Mr. [illegible] for their invaluable contributions to this project. I would also like to thank the many others within [illegible] College who helped in varying degrees. Names that spring to mind include those of [illegible], [illegible] Leary [illegible] building: Mr. [illegible], Mr. [illegible], [illegible] and [illegible] and Jimmy in [illegible] Street. My thanks also to the librarians and to Jimmy in the Photocopying Room for their patience and good humoured assistance. [illegible] program, namely, [illegible] Mary [illegible] also [illegible] much [illegible].

Outside of the [illegible], my parents, brothers and sisters provided [illegible] support. The staff at Michael Leary's [illegible] good [illegible] Peter [illegible] and [illegible].

Above all though, my thanks to the Lord Jesus Christ for [illegible] in so many ways [illegible] like me. And finally, to all other contributors not mentioned above, my sincere thanks.

Peter [illegible] Leary

December [illegible]

Table of Contents

List of figures

Abstract

The slow move from a fossil-fuel powered society to a renewable-energy powered society is creating and will continue to create a demand for good energy storage technologies. The electromechanical battery (EMB), comprising a flywheel energy storage system with electrical input and output, is one of the many candidate technologies. Two different EMB types are evaluated in the present project. The first is a ring (or annular) flywheel to be constructed using fibre composite materials and to rotate at high speed in a vacuum. Energy is to be imported and exported electromagnetically based on linear electrical machine principles. Confinement of the annulus is to be performed electrodynamically using superconductors. The basic mechanical and electromagnetic considerations are summarised and the prospects of this composite annular flywheel are considered for different applications.

The second EMB evaluated is a more conventional system and is aimed at the standby power supply market. This EMB principally comprises the following off-the-shelf components--an induction machine, capacitors and a flywheel. The system is permanently connected on line, with the induction machine operating in its motoring mode so as to overcome rotational losses. In the event of a mains failure, the induction machine reverts to being a self-excited induction generator and extracts energy from the flywheel to power the load. Obviously, the extraction of energy from the flywheel causes deceleration and frequency and voltage reduction. These effects are examined in detail, and implications for this particular EMB are assessed.

CHAPTER 1

INTRODUCTION

1.1 General Background

The sun is the major source of power on the earth, providing about[2] 173,000 Terawatts (or the equivalent of 173 thousand billion electric fires) on a non-stop basis at the outer atmosphere. This power is directly or indirectly responsible for energising the ecological life cycle, for maintaining life-supporting temperatures at the Earth's surface, for the rain cycle, for the wind, etc. (Figure 1.1 - taken from Boyle[2]).

Figure 1.1 Solar radiation incident on Planet Earth is firstly filtered and then transformed into various other energy types, including electricity (hydro and wind-electric schemes are shown)

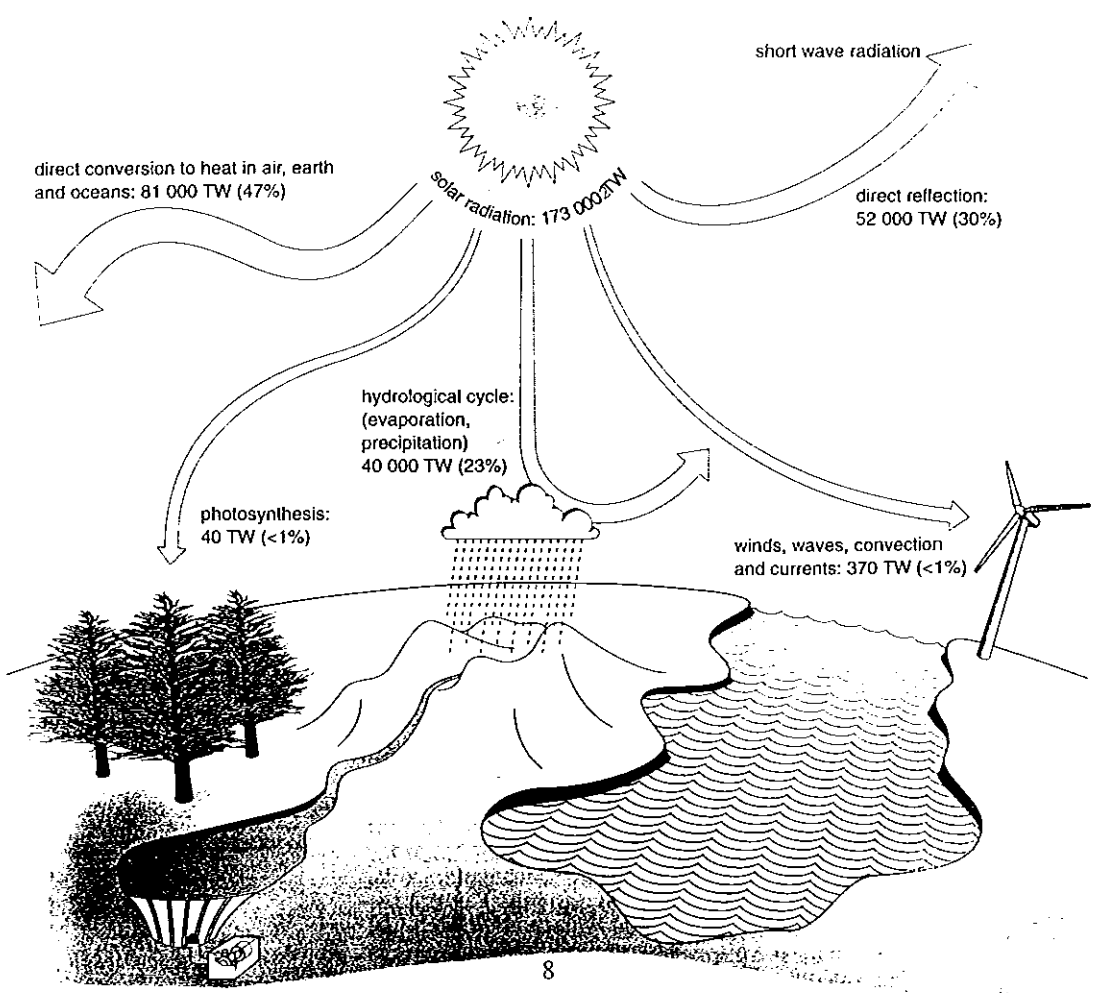

Despite its magnificence and general benevolence, however, the sun does not meet all of mankind's energy needs (and whims) for the following reasons:

(1) **Low density and high variability** The sun's light has a relatively low energy density—the maximum value is less than 1 kW/m^2—and this density varies according to the time of day and year, the latitude, the angle of incidence and the cloud cover.

(2) **Usability** The sun provides its energy in light form--a form that might not be compatible with many energy consuming systems.

Typically, therefore, solar-powered systems must be able to capture diffuse and irregular light energy, store that energy efficiently and then reconvert it as required. The most marvellous example of such a system is, of course, the ecological system—green leaves slowly capture the light energy by using it to create high-energy organic compounds (i.e. sugars, starches and cellulose) from carbon dioxide and water. That energy can be stored in those compounds for long periods without loss before being extracted by humans, animals, insects or bacteria.

Indeed, the clever humans not only extract the energy internally to power their own bodies, but they have also created devices that permit extraction of the energy from those organic compounds to provide heat, mobility and electricity. Compounds used for the latter purposes are generally known as biomass and include wood, straw, vegetable oils and their derivatives, animal wastes etc. In fact, even fossil fuels are generally assumed to be derived from biomass compounds of ancient ecosystems.

It might be expected therefore, as fossil fuel reserves dwindle, that the resulting void would be filled by biomass fuels, the technology of which is continually being improved. This will undoubtedly occur to some extent, but biomass is unlikely to ever enjoy the dominance currently being enjoyed by fossil fuels. The main reasons for this, apart from the increased cost of biomass, are related to pollution or, more importantly, the perceived polluting effects of the combustion process presently used to extract energy from both fossil and biomass fuels. (Fuel cell technology may allay fears somewhat, but the development of a viable biomass compatible fuel cell may be a long way off.)

The end result has been a huge drive to find alternative energy sources to support a 'sustainable' future. Some of the different possibilities were already shown in the Figure 1.1; a more complete list, including various nonsolar possibilities, is given in Table 1.1 (taken from Jensen[1]).

Table 1.1 Estimates of Global Energy Resources (in Terawatts or Terawatt-Years)

Resource	Estimated Recoverable Amount	Resource Base
Solar radiation at Earth's surface	1000 TW	90000 TW
Wind	10 TW	1200 TW
Wave	0.5 TW	3 TW[d]
Tides	0.12 TW[a]	3 TW
Hydro	1.5 TW[a]	30 TW
Salinity gradients		3 TW
Geothermal flow		30 TW
Geothermal heat	50 TWy[a]	1.6×10^{11} TWy
Kinetic energy in atmospheric and oceanic circulation		32 TWy
Biomass (standing crop)		450 TWy[c]
Oil	300 TWy[a], 2500 TWy[b]	
Natural gas	180 TWy[a], 1400 TWy[b]	
Coal	930 TWy[a], 7000 TWy[b]	
Uranium-235	90 TWy[a]	
Other fission resources	10000 TWy[b]	
Deuterium fusion	3×10^{11} TWy[b]	
Present rate of primary energy conversion: 10 TW		

SOURCE: Based on Sorensen (1979); Chesshire and Pavitt (1978).

[a] Estimated recoverable reserves (proven and possible).
[b] Estimated recoverable resources (ultimately minable).
[c] At present.
[d] Theoretical estimate.

In relation to the data shown in Table 1.1, it should be noted that both nuclear fission and fusion are unlikely to contribute extensively to meeting future energy needs—the former because of the perceived dangers, the waste disposal problems and the limited supply; the latter because of the huge lengths of time, the costs and the uncertainty associated with the development of a viable energy-conversion system. As a result, it will fall upon renewable energies, including some biomass, to take up the slack as fossil fuels are phased out. This is the basis of the 'fossil-free energy scenario' developed for Greenpeace International by the Stockholm Environment Institute's Boston Centre and published in 1993 (Figure 1.2--taken from Boyle[2]).

Figure 1.2 The Greenpeace fossil-free energy scenario, which foresees coal, oil, natural gas, and nuclear energy sources being replaced by renewable sources within 100 years

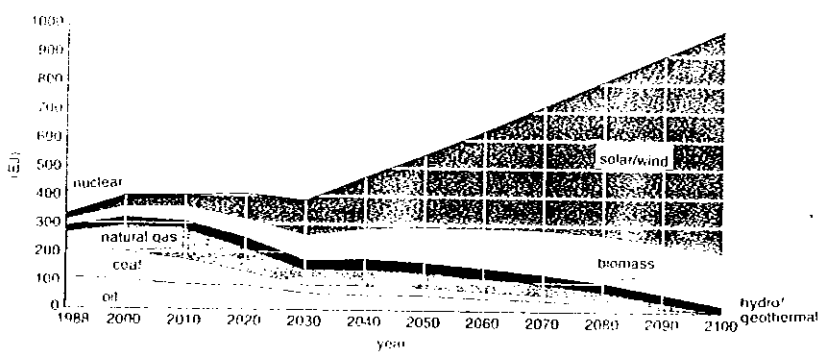

The transformation from a fossil-fuel-based energy supply to a renewable-energy-based supply has, however, two important implications:

(1) Electricity will become the dominant energy source at points of end use; at the moment that role is jointly shared with fossil fuels (Table 1.2), which are particularly strong in areas where the point of use is mobile. This is because of the

difficulty of making a continuous connection to an electrical grid and because of the lack of good electricity storage technology. (The performance of the conventional lead-acid battery, for example, is roughly two orders of magnitude below that of fossil fuels in terms of energy storage per unit mass.)

Table 1.2 Energy types and their sources at major points of end use

ENERGY TYPE	PRINCIPAL APPLICATIONS	MAIN ENERGY SOURCE
Thermal	Heating homes,offices, manufacturing processes etc.	Both hydrocarbon and electricity
Mechanical	Transportation (Road vehicles, ships, airplanes, trains)	Almost exclusively hydrocarbon fuels (apart from electric trains)
	Portable mechanical power (Drills, grinders, chainsaws, lawnmowers, etc)	Both hydrocarbon fuels and electricity
	Installed mechanical power (Pumps, fans, rollers, grinders)	Almost exclusively electricity
Other	Lighting and power for small appliances/electronic equipment	Almost exclusively electricity

(2) Utilities will have to find ways of matching the largely variable renewable energy sources (i.e. solar/wind) with the ever-varying energy-utilisation characteristics of consumers. This obligation arises because the inherent energy storing capability of fossil fuels is not replicated in the most important renewable energy sources—solar and wind. As in the previous point, the problem is at least partly one of storing electrical energy efficiently and cost effectively.

Not surprisingly, therefore, the looming need for good electrical energy stores is prompting huge research efforts into several different technologies, including advanced electrochemical batteries, supercapacitors (also known as ultracapacitors and double-layer capacitors), superconducting magnetic energy storage, compressed air storage, hydrogen storage and electromechanical batteries (EMBs). And some lines of demarcation are already appearing:

- The electrochemical battery is likely to continue to dominate the low-energy low-power market (watches, calculators, laptops) and, along with supercapacitors, will come to dominate the electric vehicle market and possibly even the power system energy-storage market
- Superconducting magnetic energy storage will probably be used to stabilise and bolster power systems
- Compressed air, if competitive, will be used as an energy store for power systems
- Hydrogen is being proposed as a future fuel for airplanes and even as a direct replacement to fossil fuels in the so-called hydrogen economy
- The EMB, which is focus of the present thesis, has been proposed as a suitable energy store for uninterruptible power supplies, for power systems, for electric cars and hybrid electric cars, for spacecraft, for pulse power supplies and other. (These areas of application are discussed in more detail in Section 1.2 below.)

As explained in more detail below, the EMB has long been recognised as a technology with huge potential in several different application areas. To make a detailed evaluation of that potential became the major aim of the research documented in the present thesis.

1.2 The background of the EMB

An electromechanical battery is basically a flywheel energy storage system with electrical inputs and outputs. The flywheel is a very old approach to storing energy (See Genta [3] for a history of flywheel technology), but only lately has serious consideration been given to using the flywheel as an on-line energy store for electrical systems. This revival of interest first began in the United States in the 1960s. A flurry of U.S. research and development activity, heightened by the oil crisis of the 1970s, ensued and enthusiasm among researchers was high. In 1973, for instance, Richard F. Post and Stephen F. Post wrote[4], "Advances in materials and mechanical design make it possible to use giant flywheels for the storage of energy in electric-power systems and smaller ones for the propulsion of automobiles, trucks and buses." This did not occur immediately, however, and almost 20 years later, the same authors wrote[5], "Most of these [vehicular flywheel] studies were terminated in the early 1980s and, as far as we know, no commercial products resulted from these programs. Overseas, there have been several developmental vehicular flywheel programs, with, at least until recently, no available commercial products to our knowledge."

Reasons for the slow development rate in the area of electric vehicles include the fact that the EMB simply could not compete with the fossil-fuel based internal combustion engine in terms of energy stored per unit mass, even though the EMB was,

on paper anyway, significantly better than the then electrochemical battery (conventional lead-acid). The slow development was also mirrored in applications involving electrical power systems where there was little demand for energy storage because of the favourable energy storage characteristics of coal, oil and gas (i.e. energy can be extracted any time and at short notice). Any demand that did exist for energy storage was met by pumped storage, the high price of which was not so important because of the small amounts required. Furthermore, EMB technical problems were being encountered in the areas of bearings and fibre composites.

In recent years, however, EMB development has received a second wind due, as was explained earlier, to a second oil crisis (except this one was pollution initiated) and also due to technology improvements in the areas of magnetic bearings, materials and electronics. There are many potential areas of application for the new EMB including

* Power system support. As explained above, huge energy stores will be needed for use in future electrical power systems. EMBs have been proposed for various support functions including diurnal load leveling[6], spinning reserve[7], power smoothing from variable energy sources such as the wind[8] and even transmission system stabilisation[9]

* Electric vehicles. The move away from fossil-fuel powered vehicles has resulted in the EMB being proposed as both the principal energy store[5] for the electric vehicle and the auxiliary energy store[10] for various hybrid electric vehicles.

* Uninterruptible power supplies. The flywheel has long been used to maintain/smooth the rotation speed in diesel-engine-powered back-up motor-generator sets[11, 12], but more recently high-speed EMBs have been proposed as

suitable short-term stand-alone energy stores for computers, remote telecommunication nodes and other critical loads[13-16].

* Other. The EMB has been used or has been proposed for use in several other areas, including spacecraft power supplies [17], pulse power supplies for thermonuclear fusion facilities and for other technological installations[18], and even pulse power supplies for electromagnetic guns;

Of all these possible areas of application, the big prize would appear to be the electric vehicle, and many researchers undoubtedly have that application targeted. However, an EMB for an electric vehicle has a much higher specification than an EMB for a static application, such as power system support. In particular, the vehicular EMB must be able to withstand all possible vibrational and gyroscopic forces associated with vehicle movement; it must also be safe in all crash scenarios; and it must be able to match the new advanced electrochemical batteries in its energy storage per unit mass. Not surprisingly, therefore, a number of researchers (such as O'Kain at the Oak Ridge National Laboratory in the U.S. and Post at the Lawrence Livermore National Laboratory also in the U.S.) are firstly concentrating their efforts on developing EMBs for static applications where the specification is less stringent and energy storage per unit cost rather than per unit mass is the most important parameter. This logical approach was also adopted in the present project, with power system support being initially targetted because of the huge potential in that particular area. After all, evolution to the electric vehicle could always be undertaken if the EMB is proven in simpler applications.

In power system support applications, the main competitors of the EMB may very well be the electrochemical battery and the superconducting magnetic energy storage (SMES) systems. It is difficult, however, to compare these technologies in terms of the cost because of the constant advances, but certain authors have made some definite statements that allow some positive conclusions to be made: Luongo[19], for example, states that

> "the costs of SMES are too high compared to fossil fuel-based peaking generation. .... Even in the long-term, advanced batteries and flywheels are likely to pose insurmountable competition to SMES in the diurnal load leveling market."

With similar optimism, Hull[20] says that

> "Superconducting bearings promise to reduce friction by up to two orders of magnitude..... [but] whether 10 MWh units will be composed of one large monolithic flywheel or of individual elements, each in the 10 kWh class, remains an open question"

The EMB is compared with the electrochemical battery by Post et al[5], who say that EMB advantages include a

> "far superior turnaround efficiency, maintenance requirements, and service lifetime."

Whether those advantages are maintained as both technologies advance remains to be seen, but on the basis of the evidence available, the EMB was deemed worthy of further investigation especially as some EMB ideas had already caught the imagination.

1.3 Scope of the work

Two major EMB ideas are explored in the present thesis. The first idea--a 'rim-supported EMB'-- involves shaping high-strength fibres into a ring or annular flywheel, which is held in a levitated position at all speeds by superconducting bearings. Energy is extracted from and imparted to the ring (i.e. deceleration and acceleration, respectively) via toroidal coils wound around the ring at its periphery. Speed is varied by varying the position of these coils with respect to one another, by pole changing or by pole amplitude modulation. Of course, the adoption of a ring-shaped flywheel is not new, but has been previously been explored by several investigators including Ball[44], Schlieben[47], Aaland and Lane[49] and Russell and Chew [6]. The ring shape is also currently being investigated by a Japanese group[46], who appear to be targeting large-scale energy storage for utilities, and by some of those researching other very low-loss magnetic-bearing EMBs[27, 33 , 43].

Unfortunately, the evaluation of this rim-supported EMB was cut short for a number of reasons, including the present unsuitability of high-temperature superconducting bearings and the unfavourable economics of commercial-scale applications. This prompted a change of focus to the other end of the EMB spectrum—a 'shaft-supported EMB' comprising the following off-the-shelf components: an induction machine, capacitors, and a conventional steel flywheel with suitable bearings and coupling. The aim was to use the flywheel to power a load for a short duration following a mains interruption by keeping the induction machine in a self-excited generation regime. This idea is explored quite comprehensively.

1.4 Thesis overview (See Table 1.3)

In Chapter 2, a classification scheme is first of all proposed for the various types of EMB. Then, the idea for the rim-supported EMB is mooted and various design features are discussed. Some experimental work is also briefly described before the reasons for suspending further development are explained.

In Chapter 3, the search that led to the proposal for an off-the-shelf EMB for short-term uninterruptible power supply applications is described. This shaft-supported EMB is then described in some detail.

In Chapter 4, the proposed shaft-supported EMB is modelled and tested. The results of the tests and any implications are discussed.

In Chapter 5, the concluding chapter, the outlook for both proposed EMBs is evaluated.

Table 1.3 The Project Path

Approx Timescale	*Work undertaken and the rationale behind it*	*Thesis Section*
Up to May 1996	It is projected that there will be a big future demand for good energy storage techologies in order to meet changes in electrical energy generation and consumption. The electromechanical battery (EMB) is proposed as a technology that could go some way towards meeting both the projected energy-storage demands of electric utilities and the energy-storage demands of other technology sectors.	Ch. 1
June-Dec 1996	One near-optimum EMB arrangement for large-scale energy storage comprises high-strength fibres configured in the shape of a rim , which is then supported by magnetic bearings and accelerated/decelerated by a linear tubular induction machine. Various experiments evaluating magnetic bearings are undertaken, and prototypes of the rim-supported EMB are constructed, but several difficulties are encountered.	2.1-3
Jan-Feb 1997	Further investigation presents more reasons for suspending further development of the rim-supported EMB: the unsuitability of present high-temperature superconducting bearings and the marginal economics of applying this EMB to a most desirable small-scale application--night energy storage. Other EMB research options and application areas are considered.	2.4
March-April 1997	The electric vehicle is deemed an unsuitable location for EMBs, even for regenerative energy storage purposes. Uninterruptible power supply technology is seen as being more suitable, and the idea for a simple low-cost high-reliability short-term EMB for use in standby power supplies is proposed. This shaft-supported EMB comprises an induction motor, which operates in the self-excited mode when delivering up its energy; excitation capacitors; a flywheel and a contactor /contactor controller .	3.1-2
May-June 1997	The new shaft-supported EMB is iteratively modelled in a spreadsheet format. The modelling method is later compared with the exact method proposed by Salama and Holmes[36] in their definitive paper on the self-excited induction generator.	4.1-2
July-Sept 1997	A physical model of the shaft-supported EMB is constructed. Various performance parameters are measured, and the results are compared with the predictions of the spreadsheet model.	4.3
Oct onwards	Future possibilities for both the shaft-supported EMB and the rim-supported EMB are explored	Ch.5

CHAPTER 2

EMB CLASSIFICATION AND A FIRST DESIGN EFFORT

2.1 *Introduction*

The electromechanical battery is an energy store and, as such, one of its important parameters is energy storage capability per unit mass $(E/m)_{max}$, which is measured in Joules.kg^{-1}. This parameter is dependent on both the flywheel shape—as given by a shape factor K—and on two characteristics of the flywheel material—maximum tensile stress (S_{max}) and density (ρ)--according to the equation[24]:

$$(E/m)_{max} = K \cdot S_{max}/\rho$$ (Appendix A gives a simple justification for this equation)

In the light of this equation, it is no surprise that one of the aims in EMB design is to maximise the product of the flywheel shape factor (See Figure 2.1) and the material stress limit per unit density (Table 2.1).

Figure 2.1 Flywheel shape factors for various flywheels (From [1] and [4])

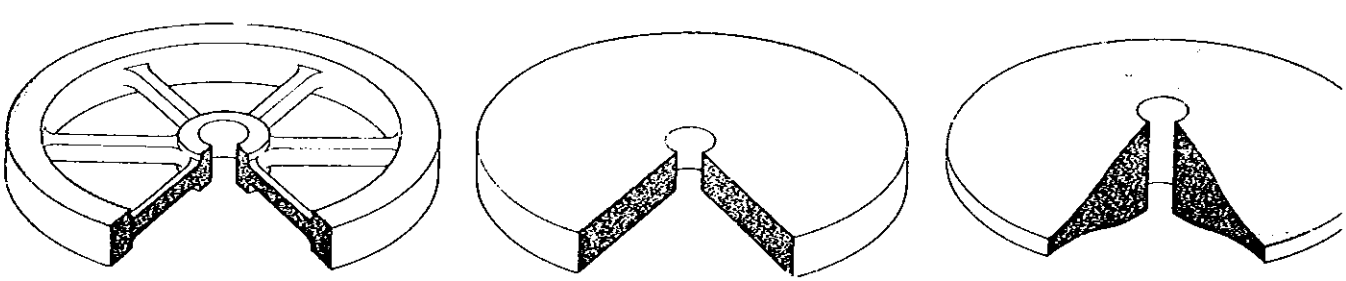

Thin rim
K ≅ 0.5

Flat disk
K ≅ 0.6

Constant Stress disk
K≅ 0.8

Table 2.1 Properties of some materials considered for flywheels (information gathered from [1], [5] and [44])

Material	Maximum Tensile Stress $[S_{max}]$ (GPa)	Density $[\rho]$ (kg/m^3)	Maximum Stress per unit Density $[S_{max}/\rho]$ (MN.m/kg)
Birch	0.13	700	0.18
Aluminium alloy	0.5	2,700	0.19
Maraging steel	2.7	8,000	0.34
Tyre wire	3.5	8,000	0.44
E-glass high-strength fibre	3.5	2,540	1.4
Graphite high-strength fibre	7.0	1,780	4.0

Obviously, the optimum combination is graphite fibre in a constant stress disk. Unfortunately, though, fibres are not suited to this particular shape because fibres only attain their maximum stress in the tangential direction whereas the constant stress disk places an approximately constant stress in both the radial and tangential directions. As a result, fibres can only be considered for flywheels where the bulk of the stress is unidirectional. The most obvious example is a thin-rim flywheel without any spokes, web or hub (Figure 2.2). Centrifugal stress in that particular flywheel is

Figure 2.2 The Thin-Rim Flywheel (taken from [46]), the basic component of one major category of EMBs--the rim-supported EMB

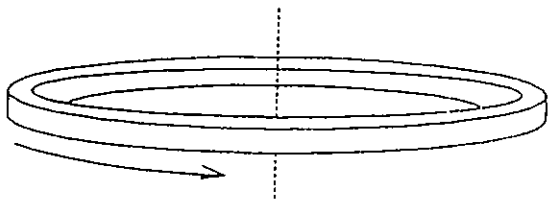

translated into a tangential (or hoop) stress because of the circular shape, and fibres that are wound around the rim experience only unidirectional stress during rotation. Not surprisingly, therefore, considerable EMB research has been concerned with the thin-rim flywheel [6-11], which is the basic component in one of the 3 proposed EMB categories (See the rim-supported EMB in Table 2.2) and, as will be seen, this particular EMB occupied much of the initial effort of the present project.

However, as was briefly explained in Chapter 1, the optimisation of the energy storage per unit mass is not the only goal in the design of EMBs. Cost is another very important consideration. In fact, the high cost of graphite fibre has prompted many developers to use the less desirable, but less expensive E-glass fibre as the principal rotor material. Cost and, to a lesser extent, weight and size implications have also prompted many developers to incorporate the electrical machine part of the EMB directly into the flywheel (Eg. Figure 2.3).

Another critical issue in EMB technology is the bearings—the flywheel must be supported in such a way that energy loss due to windage and friction is minimised and the working life of the flywheel maximised. Indeed, the bearings issue has particularly important implications for the simple thin-rim flywheel. This flywheel must be

Table 2.2 Different EMB types

CHARACTERISTIC	EMB Type		
	Shaft supported	Hub supported	Rim supported
Support Mechanism	Mechanical bearings	Mechanical or magnetic bearings	Usually magnetic bearings
Power Exchange Interface	Separate electrical machine	Embedded external-rotor electrical machine	Embedded linear electrical machine
Rotor material	Usually isotropic (steel)	Usually anisotropic high-strength fibre	Usually anisotropic high-strength fibre
Need for vacuum	Not usually (low-speed, short-term and efficiency not critical)	Usually necessary (high-speed, long-term)	Usually necessary (high-speed, long-term)
Energy storage per unit mass	LOW (<50 Wh/kg)	HIGH (≤150 Wh/kg)	Near MAXIMUM material strength (≤300 Wh/kg)
Technology status	Well-proven	Still under development but some products beginning to emerge (eg. [14], [56])	Still under development, and only by a limited number of researchers

supported at the rim (hence the generic name rim-supported EMB—see Table 2.2) where speeds can, depending on the flywheel material, exceed 1 km/second. Such speeds are unsuitable for mechanical bearings, so developers must usually design some proprietary magnetic bearing system for the rim-supported flywheels.

This, and other factors, has prompted many developers to abandon the idea of a pure thin rim in favour of flywheels that still accommodate the unidirectional stress constraints of fibre, but that could be supported near the hub where speeds would be only a fraction of the peripheral speeds. This permits the use of mechanical bearings, or magnetic bearings developed for conventional rotary machines. These particular EMBs constitute the second major class of EMB, namely, the hub-supported EMB. The typical layout of the hub-supported EMB is shown in Figure 2.3.

All the developmental work associated with applying fibres, incorporating electrical machines and choosing appropriate bearings has severely hampered the introduction of a first commercial generation of rim- or hub-supported EMB technology, and has ensured the survival of the more traditional EMB such as is used in standby power supplies (Figure 3.2) or power system support (Figure 2.4), where the electrical machine and the flywheel are kept separate and connected by a shaft. This third type of EMB is here called a shaft-supported EMB to distinguish it from its more sophisticated relatives. A comparison of the three different EMB classes is given above in Table 2.2.

Figure 2.3 The hub-supported EMB (Taken from Anonymous[40])

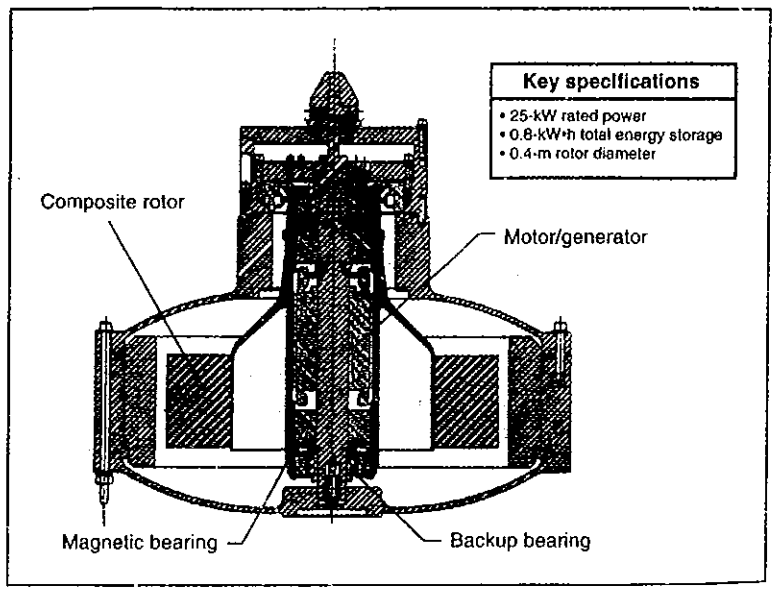

Figure 2.4 Example of the conventional shaft-supported EMB (Taken from[59])

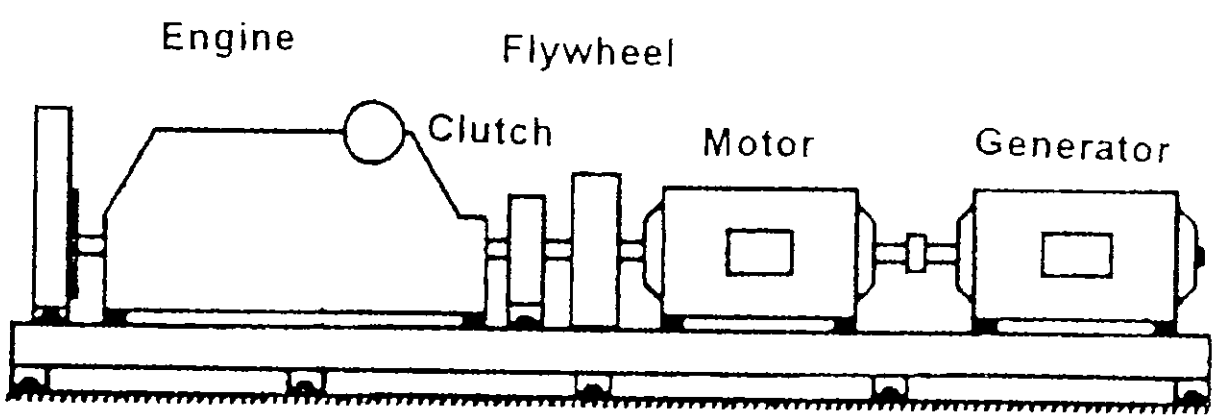

2.2 *Background to the development of a rim-supported EMB.*

Of the 3 different EMB types, the rim-supported EMB appeared to be the one to receive the least adequate attention while at the same time possessing the most favourable energy storage density. These factors prompted an evaluation of this particular EMB in the following 4 areas:

(1) The market

(2) The rotor fibre/matrix/sleeving

(3) The magnetic bearings

(4) The electrical interface.

The evaluation of each of these is described in the following 4 sections (Section 2.2.1-2.2.4) and resulted in a definite preference for the characteristics of a rim-supported EMB. First, though, it should be noted that the development and practical implementation of a rim-supported EMB is a major multidisciplined undertaking involving many more areas, including

- the specification of an appropriate support and containment structure
- the examination of the damping of rotor critical speeds
- the evaluation of rotor temperature rise due to the vacuum containment
- the specification of the vacuum equipment
- the determination of the optimal cross-sectional shape and rim radius
- comparative costs.

2.2.1 A realistic market

As explained in Chapter 1, energy storage is going to become a critical link in the world's energy supply infrastructure as energy consumption increases and renewable energy sources are increasingly relied upon. It is envisaged that there will, at the very least, be a need for a technology such as the EMB to meet spinning-reserve and diurnal-load-levelling requirements of future utility power systems. As a result, meeting the energy storage requirements of utility power systems is a logical long-term goal in the development of a rim-supported EMB.

A more logical short-term goal is the commercial night electricity storage market. This market exists because of present utility efforts to encourage consumers to use more electricity at night by providing night electricity at highly discounted rates. In many cases, however, these rates cannot be availed of, and electricity is used mainly during the day and is therefore paid for at the full premium. The development of an appropriate EMB would allow factories and businesses buy cheap night electricity and store it in the EMB until it was required during the day. The possible savings attainable in the Irish night energy storage market are evaluated in Appendix C and shown to be quite substantial--a 50-percent-plus reduction in the bill might typically be expected. More importantly from a designer's viewpoint, the development of such an EMB would be a natural stepping stone towards the ultimate goal of developing a utility-sized version.

Other markets, including those for electric vehicles or uninterruptible power supplies, were also considered, but the specifications for energy stores in the electric vehicle were considered too stringent (See also Section 3.2), and the shape and size of rim-supported EMBs were considered to be unsuitable for many uninterruptible power

supply applications. Of course, the envisaged night-storage EMB naturally provides a certain level of uninterruptible power protection anyway.

2.2.2 The fibre/matrix/sleeving combination for the rotor

As already seen, graphite is presently the best of the various commercially available fibres as a rotor material from the viewpoint of energy stored per unit mass. And, of course, the less weight the less energy that will be expended in supporting the rotor. However, graphite is expensive, costing perhaps ten or more times that of E-glass[40]. Nevertheless, graphite would still be our choice of fibre, not alone for its weight benefits but also for its low strain rate and possibly even for its good electrical conductivity (Section 2.4). Furthermore, the stress characteristics of graphite continue to improve, and prices should continue to fall in relative terms. Price drops should also be in order for the huge quantities required for a big EMB (>1,000 kg) such as would be the case in night storage and, ultimately, utility energy storage.

In relation to bonding for the fibres, one previously suggested option was the use a simple aluminium sleeving to hold and shape the fibres, allowing induced sleeving currents to both propel and suspend the rotor. Alternatively, a conducting fibre-matrix combination (eg. carbon-carbon) could serve the same function. Either of these simple rotor constructions would be very desirable from the viewpoints of manufacturability, balancing, temperature-induced fatigue, etc.

2.2.3 Suitable bearings

As explained in Section 2.1, the high peripheral speeds required to maximise the performance of fibre-based rotors effectively rules out the use of mechanical bearings near the periphery (except perhaps for emergency uses), making magnetic bearings compulsory. In relation to the choice of magnetic bearings, Jayawant[21] says that there are 4 realistic possibilities:

1. Permanent magnets in repulsion
2. Eddy current repulsion by means of the magnetic river
3. Superconducting methods
4 Attraction using controlled dc electromagnets

The first method is attractive for its simplicity, but is undesirable for a number of reasons including the need to mount permanent magnets in the rotor and possibly the unsuitability of the permanent magnets to upsizing[22]. The eddy current method is the easiest to implement -- the excitation system used to propel the rotor is also used to levitate and guide the rotor. It is expected that losses would be high, however, and control at very high speeds and low slips might prove to be a problem.

Superconducting levitation appeared interesting because of the promise of low losses and passive control. The possible suitability of superconductors in the power exchange system also (next section) was also seen as advantageous. In addition, this is the approach being adopted by the Japanese in their efforts to develop a Maglev train (in some senses a linear EMB), and several articles on the subject were very positive both

about the commercial introductions of high-temperature superconductors (eg. [57]) and about their application as flywheel bearings (eg.[20]).

The fourth possible method is attraction using controlled dc electromagnets. This is the approach being adopted by the German Maglev team and by some Japanese researchers[46] working in the area of large rim-supported EMBs for power systems and certainly appears to be another realistic possibility. Drawbacks, however, include the extra complexity of having iron in the rotor, the shorter air gap and, more importantly, the nonoptimal efficiency. (The Japanese researchers[46] did quote an efficiency figure of 82 percent, but that was for a flywheel some 320 meters in diameter, that weighed 320,000 tons and that could store 5 GWh.) This method was therefore rejected, and the superconductor method was earmarked as the most suitable.

2.2.4 The electrical interface

As is often the case in electrical machines, it is necessary to choose between synchronous and induction. In this case, a linear synchronous machine would be realised by incorporating a permanent magnetic structure in the rotor (eg.[52]) and by positioning pickup/driving coils along the stationary structure. An inverter would also be required to interface the variable frequency of this synchronous machine with the fixed frequency mains (unless the rotor rotated at near-constant speed so as to bolster the flywheel effect on the power system, but this approach has a small energy-storage utilisation figure).

An induction machine configuration was seen as the more preferable, because a direct-on-line connection would be possible. A high energy-storage utilisation figure could be attained by varying the rotor slip energy [46], by pole-changing [50] (including

pole-amplitude modulation) or by varying the pole pitch so as to obtain optimum rotor slip at all times.

This last approach, which has not been seen in the literature, is proposed as a very simple way of seamlessly controlling the rotor speed without the need for power semiconductor technology. This approach, which would of course not be a realistic proposition for small cylindrical machines, is illustrated for the rim-supported EMB in Figure 2.5.

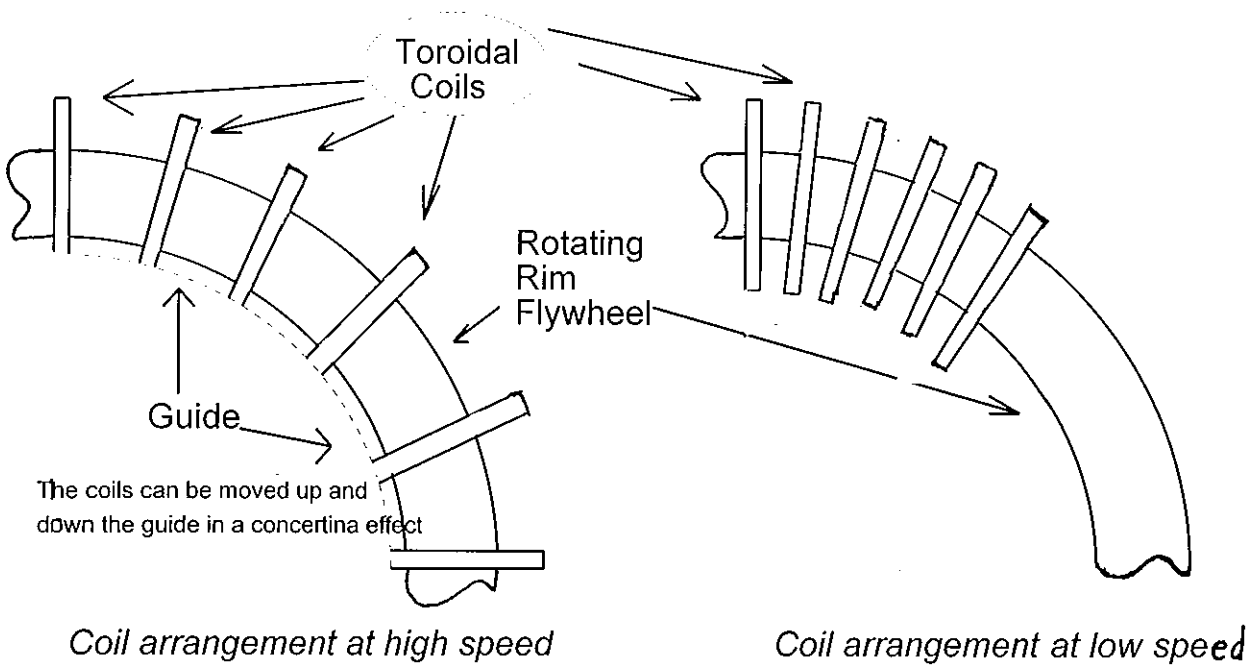

Figure 2.5 Proposed variable-pole-pitch system for a rim-supported EMB (Only the coil section of the rim is shown)

The coils would sit on a slide that would permit controlled coil movement such that all the inter-coil distances would always be the same at any one time. At low speeds, the inter-coil distances would be small, but as speeds increase so would the inter-coil distances thereby increasing the pole pitch and allowing the rotor to operate at optimum

slip continuously. The adjustable coil distance would give rise to large space harmonics in the MMF, which would subsequently affect the current. As with 3-phase power rectifiers, it should be possible to reduce these harmonics by introducing a second set of adjustable windings (Figure 2.7b) connected in an opposing formation so as to give a winding with a delta and another with a star formation.

As it would also be desirable to avoid including iron in the rotor, one is left with the old problem associated with large air-gap linear induction machines of low power factor and poor efficiency. However, as superconductors are already being used in the bearings, it may be possible to use them also in the tubular windings thereby maximising efficiency. Capacitors could be installed to improve the power factor and, possibly, reduce the generation of harmonics.

2.3 First steps in rim-supported EMB development process

Some of the huge variety of skills and resources required to properly develop a rim-supported EMB were outlined above. This task was beyond the remit of the present project, but it was decided to attempt the first steps in the developmental process. Accordingly, an experimental programme was initiated in DIT Bolton Street during the summer of 1996. With the help of a third year mechanical engineering student, some basic equipment was first of all assembled/constructed. This equipment included various transformers, power supplies and some measurement equipment, with the ultimate aim being the construction of the test system shown in Figure 2.6. (This figure shows the motor and flywheel as separate entities. Ideally, of course, we wanted to integrate both in the levitated thin-rim EMB.)

FIGURE 2.6 TEST SYSTEM FOR SMALL ENERGY-STORING FLYWHEELS

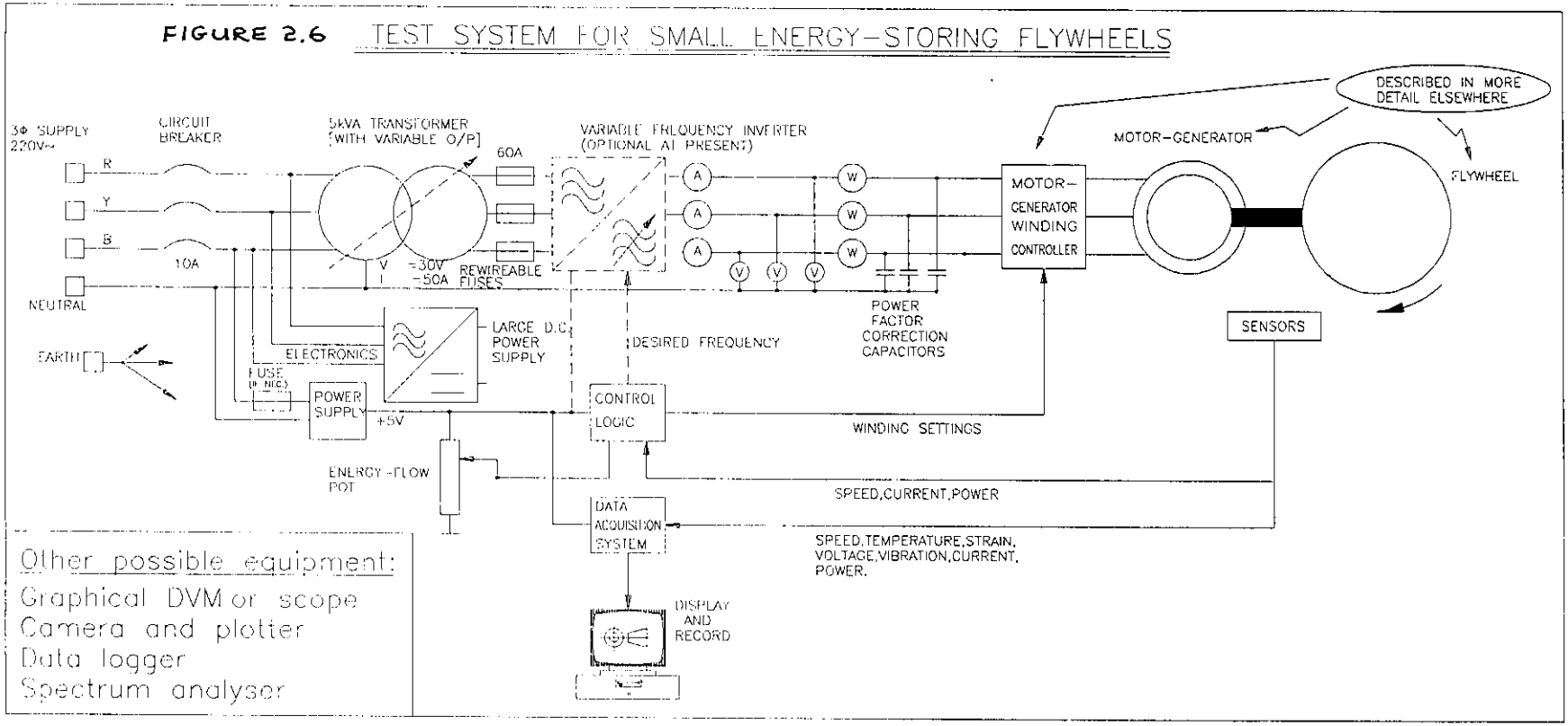

Some very simple levitation experiments were then conducted in an effort to "get a feel" for the whole levitation phenomenon. The experiments conducted included the well-known Jumping Ring experiment and other similar experiments in which levitation occurs in a conducting material by virtue of the eddy currents induced by a nearby alternating magnetic field. The main conclusion drawn from the experiments was that levitation is indeed easy to achieve, but controlled and stable levitation is quite another matter altogether. To tackle this issue more systematically, it was suggested that the next logical step in the development process should be simulation based. The aim would be to simulate the various forces involved in the levitation process and then to use this information to determine the magnetic field configuration that would be required to obtain stable and controlled levitation of conducting objects of specified shape (i.e. a thin-rim flywheel in this case).

Appropriate simulation work that had already been initiated was, therefore, continued (Appendix B) until it was learned that the European Commission, under its Joule R&D program, had issued a second call for proposals in the area of Non-Nuclear Energy (September 1996). More specifically, in the energy storage part of the renewable energy section of this latest call, flywheel technology was named as a research area that would be supported. Proposals for projects involving participants from different EU states had to be submitted by the end of January 1997. It was felt that this was an opportunity that could not be passed up. The expertise of people working in complementary areas in other EU states could be brought to bear on the problems of the project and, of course, financial resources would be made available for the implementation of a thorough research program. Accordingly, it was decided to delay

the simulation work and, instead, to try to develop some small working models that could be used to demonstrate the principles involved to potential research partners from different EU states.

Two prototypes of the rim-supported EMB (Figure 2.7-8) were assembled, with water-cooled copper wire being used instead of superconductors and a pure aluminum rim flywheel being used instead of a fibre-based rim. A single-phase linear induction machine winding was wound on the rim and magnetic bearings, based on ideas described by Laithwaite[23], were constructed. The use and nonuse of iron in these magnetic bearings was the essential difference between both prototypes.

However, it was all to no avail. The levitation instability problems previously experienced during the summer could not be overcome within the required timeframe, nor would the single-phase induction-machine winding give enough torque at low speeds to accelerate the flywheel. Would-be partners were contacted and advised that a proposal would not be submitted.

In hindsight, it was a mistake to take a short-cut on the simulation, but as things turned out, it all worked out for the good as the project soon took a major change in direction following a complete reappraisal of the proposal for a rim-supported EMB. (See Section 2.4 below.)

Figure 2.7 a Prototype No. 1--IRONSIDE

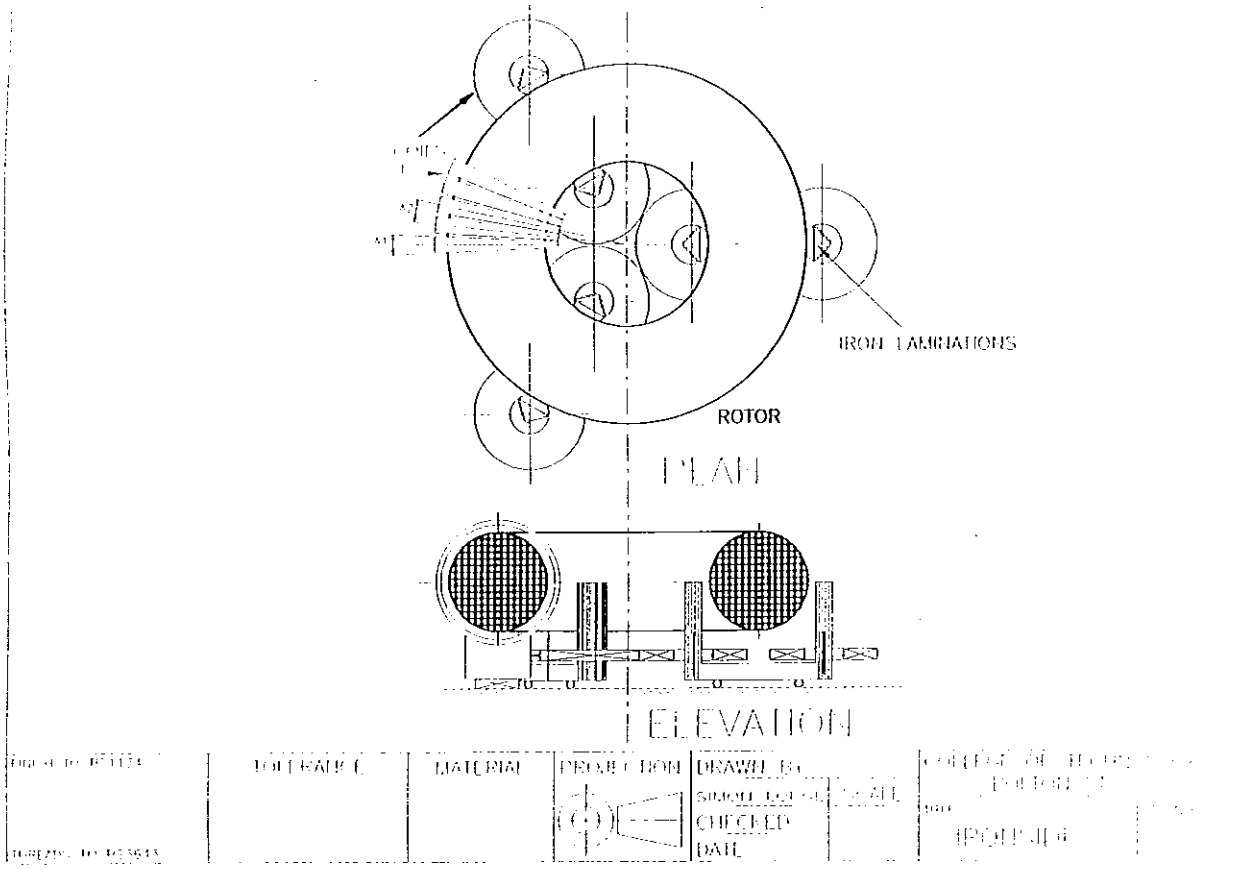

Figure 2.7b Prototype No. 2--The CRADLE

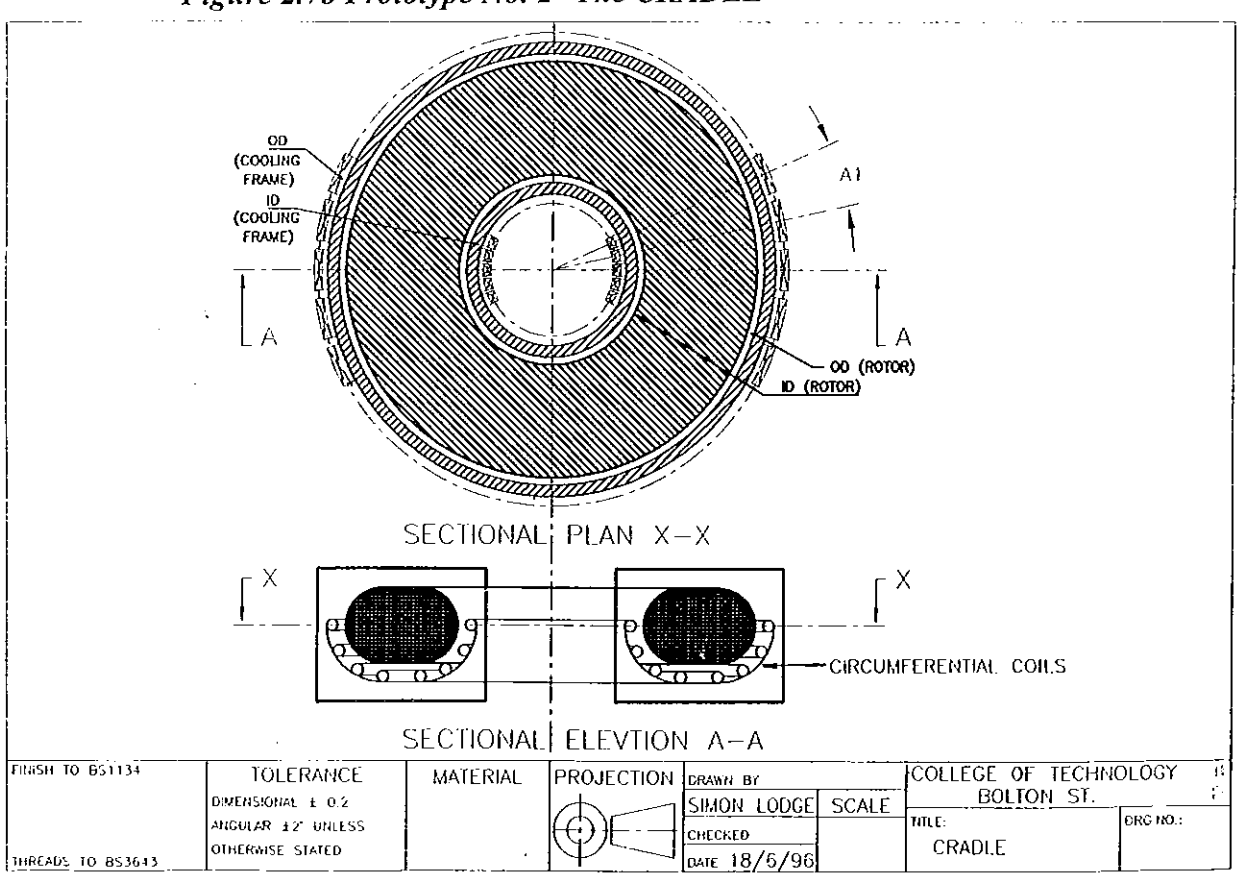

Figure 2.8a The aluminium ring flywheel with a single-phase induction-machine winding

Figure 2.8b The ring flywheel in its levitating position over the uncovered basin containing the water-cooled ironless bearing windings

Figure 2.8c The ring flywheel over 3 hollow iron cores with interspersed windings--one of the iron-based approaches to realising a stable bearing arrangement

2.4 *Reappraisal of the proposed rim-supported EMB*

The disappointment of the prototype prompted a complete reappraisal of the project. In particular, the so-called electrodynamic approach to levitating the flywheel was re-examined in an effort to lay to rest some latent doubts about the use of high-temperature superconductors. In adopting this mode of levitation, the aim had been to avail of the much vaunted high-temperature superconductors. The doubts originated in a previously quoted paper (Section 1.2) written by Luongo[19] in which superconducting storage systems are reviewed. In that paper, Luongo states that the use of high-temperature superconductors for superconducting storage is not likely until both costs and technical performance are improved. (This point was confirmed later when it was discovered that the Japanese continue to use low-temperature superconductors on their Mag-Lev trains.) Luongo also saw no future for superconducting magnetic energy storage systems in the diurnal load levelling market, which is the exact area being targeted in the present project, even if the superconductors are only being used for levitation and energy transfer. (Luongo did see a future for flywheels in the load-levelling market, but probably not flywheels that featured superconductor-based bearing systems.)

The reappraisal uncovered two further issues that were to seal the matter, at least for the purposes of the present project:

1. The stiffness of superconducting bearings
2. The economics of EMBs in commercial night-storage applications

These two issues are discussed in the following sections.

2.4.1 The stiffness of superconducting bearings

In a paper published by three researchers from the University of Sheffield[55], the wisdom of using flywheels as energy storage systems in electric vehicles is questioned. The reasons for this are given as

- The magnetic bearings together with the system dynamics
- The strength and integrity of the rim material

The second reason is easy to understand and, in effect, means that if the rim material is to be operated with reasonable safety margins and in an appropriate containment, energy storage per unit mass of the EMB will simply not match that of advanced electrochemical batteries. This reason has special relevance to the EMB for electric vehicles and, indeed, was one of the reasons that this project concentrated on static EMB applications. However, the first reason cited had not been anticipated although it does have relevance to static applications.

Basically, the natural frequency w_n of undamped transverse vibrations in a mass mounted between bearings of total radial stiffness k_r, rotational speed w, energy stored E and flywheel radius r are related by the following equation:

$$\frac{\omega_n}{\omega} = \sqrt{\frac{k_r . r^2}{2.E}}$$

where both ω and ω_n have units of rad.s^{-1}.

Because of uncertainty about the integrity of the flywheel around the critical speeds, the aim is to design a flywheel energy system so that w_n is above the operating speed, which in effect means that $E < ½ . k_r . r^2$. This design condition, rather than that related to the maximum fibre stress, may then limit the energy storage capability of the

flywheel and make it less than desirable especially for small-radius applications (i.e. electric vehicles). For the large-radius systems planned for static applications, such as the rim-supported EMB of the present thesis, high values of stiffness k_r would be required to maximise energy storage. However, the stiffness of electrodynamic levitation based on current superconducting bearings is relatively low, a characteristic that would limit the energy storage capability of the rim-supported EMB. The idea of using banks of small devices with ratings as low as 10 kWh to increase the energy storage capability to utility level, as suggested by Hull[20], is not expected to be a financially viable prospect given the marginal economics of the large energy-storing EMB--as explained in the next section.

2.4.2 The economics of applying EMBs to night energy storage

As explained in Section 2.3.1, the construction of medium-sized rim-supported EMBs for the night energy storage market should be a good stepping stone towards the ultimate goal of construting large rim-supported EMBs for utility usage. The whole question of the night energy savings was also examined in Appendix C, and it was shown that, at best, about £10 in annual savings might be expected for every kWh of installed EMB capacity. This saving must, at least in part, compensate for the cost of the energy storage system. How does the saving compare with the cost?

Figures given by Post[5] put the cost of the fibre and resin for a low-cost E-glass flywheel at about £15 per kWh, which means that 1.5 years of operation might be required to pay for a low-cost rotor material alone (the more desirable graphite fibre might be up to 5 times more expensive). No account has yet been taken of installation

costs, magnetic bearing costs, propulsion structure costs, vacuum housing costs, site costs, cooling costs etc. To account for these, it is assumed that fibre costs would be a substantial fraction of the overall project costs. Knowing this 'substantial fraction' information, it is possible to roughly estimate the payback period of any EMB night-storage project for a reasonable fraction range and for EMBs of different energy turn-around efficiencies (Figure 2.9). For example, if we were to assume that an efficiency of 0.7 could be attained for E-glass fibre and that the total system costs were minimised to 4 times the fibre costs, the payback period would then be about 5 years. However, that 5 years does not include any manufacturer's profit or the expense associated with development. As a result, this night-energy storage technology was deemed insufficiently attractive for commercial enterprises to install. (Although the efficiency of graphite fibre would be greater because less mass is required to give the same energy storage capability, graphite would be even less competitive because its cost is nearly an order above that of E-glass.)

Summary and Conclusion

The rim-supported EMB is the EMB with the best energy storage per unit mass capability. This means that the rotor weight is at a minimum, which in turn means that the energy required by magnetic bearings to support the rotor should also be minimised and efficiency optimised. Furthermore, the size and shape of the rim-supported EMB suggest that the larger static energy-storage applications would be most suitable niche for this EMB. Indeed, the slow move of utilities away from fossil fuels and towards renewable energy sources with their attendant need for energy storage support would appear to provide a most lucrative market for well-proven rim-supported EMB

Figure 2.9 Payback Time vs. Fiber Cost Fraction (E-glass Fibre)

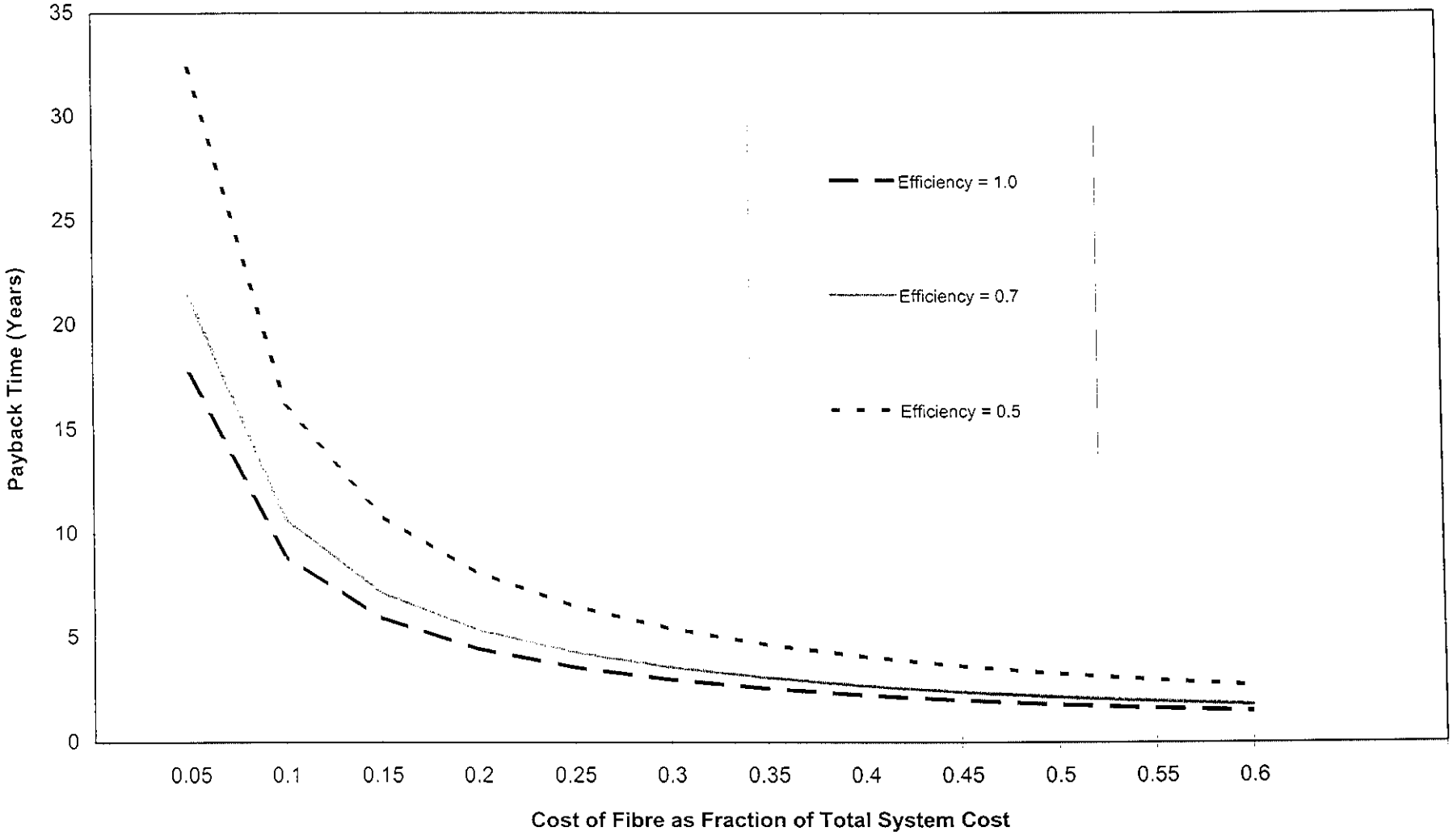

technology. Moreover, the discounted night-electricity charges of commercial enterprises would appear to be an ideal interim market for proving the rim-supported EMB with a view to its ultimate use by utilities. Accordingly, preliminary efforts in the process of constructing a rim-supported EMB for night-storage applications were undertaken.

However, 3 obstacles were encountered:

1. High-temperature superconducting technology does not appear to be commercially viable just yet
2. When used in magnetic bearings, these superconductors have a low stiffness, while the rim-supported EMB requires a high bearing stiffness to permit the storage of large amounts of energy
3. Payback periods for night-storage applications are too long.

It was felt that these factors would make any further development of the rim-supported EMB untenable. Accordingly, further effort into the rim-supported EMB was suspended, and a new campaign aimed at applying a novel configuration for a shaft-supported EMB was initiated. This new shaft-supported EMB is the subject of the Chapter 3.

CHAPTER 3

AN EMB FOR SHORT-TERM UNINTERRUPTIBLE POWER SUPPLIES

3.1 Introduction

As explained in the previous chapter, it was decided to suspend further exploration of the proposed rim-supported EMB because of difficulties with the magnetic bearings and because of the marginal economics of the most suitable application in the short term--night energy storage. Of course, one could evaluate various other rim-supported EMB options, such as the approach suggested by Russell and Chew[6] in which steel or reinforced concrete is the rotor material and mechanical rather than magnetic bearings are used (Figure 3.1). Ultimately though, the inevitably long payback period may make the huge development task associated with constructing a functional rim-supported EMB from the ground-up an unattractive proposition. It was decided, therefore, not to pursue further development of the rim-supported EMB, but to focus instead on either the hub-supported or the shaft-supported EMB. The choice between these two EMBs was then considered.

As with the rim-supported EMB, any developmental work on a hub-supported EMB would only be of a preliminary nature because of the huge amount of man-hours required in developing those EMBs from the ground up. Furthermore, it was felt that this particular EMB, unlike the rim-supported EMB, is receiving adequate attention from researchers (Table 2.2).

Figure 3.1 This 1981 proposal by Russell and Chew[6] for a rim-supported EMB with mechanical bearings was called the Kinetic Ring Energy Storage System and was designed for use in diurnal load leveling on power systems

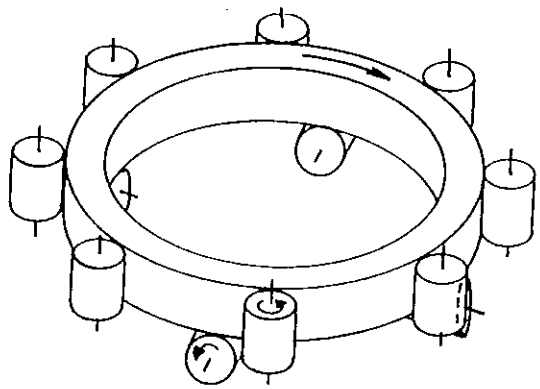

SIDEBAR related to Figure 3.1 *Russell and Chew[6] proposed that the bearings used to support the ring should not be lubricated, presumably because of lubricant outgassing in any vacuum introduced to limit aerodynamic drag. However, it was subsequently found that this particular approach would cause excessive bearing wear[26]. Russell felt that the solution to the problem would be the introduction of superconducting bearings, but it would be interesting to find out about advances in lubricant technology that might allow the introduction of a vacuum lubricant onto the bearings. Another possibility would be to reduce the radius (Russell and Chew proposed a ring radius of 1km) to the minimum point allowable from imbalance considerations, while simultaneously increasing the cross-sectional area of the ring to maintain the same mass and energy-storage potential. This should reduce the drag effects as indeed would the choice of a reinforced concrete rotor rather than a steel rotor. In relation to the choice of concrete or steel, however, there are other issues to be considered including the reduced energy storage capability and the proportional increase in the effect of bearing friction, the reduction in rotor material cost, the contribution of the latest approaches to concrete technology including prestressing to rotor strength, the effect on an electromagnetic power interface (Russell and Chew proposed a gearing interface) of a reduction in rotor steel, etc. Despite the intricacies involved, this idea cannot be dismissed and, indeed, given experiences with more sophisticated rim-supported EMBs, this could ultimately prove to be the best approach to rim-supported EMB technology.*

The shaft-supported EMB, on the other hand, was seen as a much more realistic development proposition. After all, the components for the shaft-supported EMB could be purchased off-the-shelf, and it would be possible to assemble, test and evaluate any idea for a shaft-supported EMB within the time remaining for the project.

Having chosen the shaft-supported EMB, it was then necessary to find a market and to come up with an appropriate product for that market. Two markets were considered--that for the electric vehicle and that for the uninterruptible power supply (UPS). These evaluations are given below in Sections 3.2 and 3.3.

3.2 The EMB and the Electric Vehicle

As reported in [28], California adopted a zero-emission vehicle mandate in 1990 that required major automakers to make at least 2 percent of their vehicles emission-free by 1998, 5 percent by 2001 and 10 percent by 2003. New York and Massachusetts adopted similar rules shortly thereafter. Although the Californian mandate was relaxed somewhat in March 1996, it still "seems certain that electric-drive technology will eventually supplant internal-combustion engines."[28] This inevitability has prompted much research into electrochemical batteries and, to a lesser extent, the EMB.

However, the EMB is not a suitable primary energy source for electric vehicles for the following reasons: the energy density is significantly less than that of advanced electrochemical batteries especially when an appropriate containment is included[29]; the present EMB generation also has a relatively high energy leakage rate compared to electromechanical batteries; and there are some uncertainties about the abilities of the EMB to withstand the various forces experienced by road vehicles and about an

appropriate containment for all crash scenarios. There is, though, considerable interest being shown [30, 31, 40, etc.] in using the EMB as a secondary power source in electric vehicles. In such a role, the good power exchange characteristics of the EMB would be used to complement the good energy storage characteristics of the advanced electrochemical battery, which has a limited power density. In other words, the EMB would absorb vehicle braking energy and use that energy to improve the vehicle acceleration profile. The lower energy storage density and energy retention characteristics of the EMB would not be important because of the relatively small amount and the transience of any energy stored in the EMB. Any doubts about the durability of the EMB in road service could also be dissipated by using mechanical rather than magnetic bearings.

Despite this compatibility with electrochemical batteries in electric vehicle applications, however, the newly developed supercapacitor appears to be an even more appropriate mate for the electrochemical battery in electric vehicles[32, 51] because the supercapacitor is also a DC device whereas the EMB with its rotating member is more naturally an AC device and requires a semiconductor converter/inverter to interface with the electrochemical battery. Indeed, the ultracapacitor not alone has an excellent power density, but it also boasts a good and continually improving energy density. Ultimately, therefore, this device could displace the advanced electrochemical battery and become the only energy store in the electric vehicle. It was concluded that an effort to apply the EMB even to secondary storage functions in the electric vehicle was pointless.

3.3 The EMB and the UPS

Standby power seems to be an altogether more appropriate technology for the EMB. Indeed, the conventional flywheel and motor-generator UPS (which has been categorised amongst shaft-supported EMBs in the present thesis) have, in configurations similar to that shown in Figure 3.2 (and Figure 2.4), long been used to provide emergency or standby power to industrial processes, office buildings, hospitals, supermarkets, etc. So much so, that one might reasonably ask what further contribution could be made to this already well-proven technology.

Figure 3.2 Typical configuration of the no-break diesel-generator set (Taken from Bishop[11])

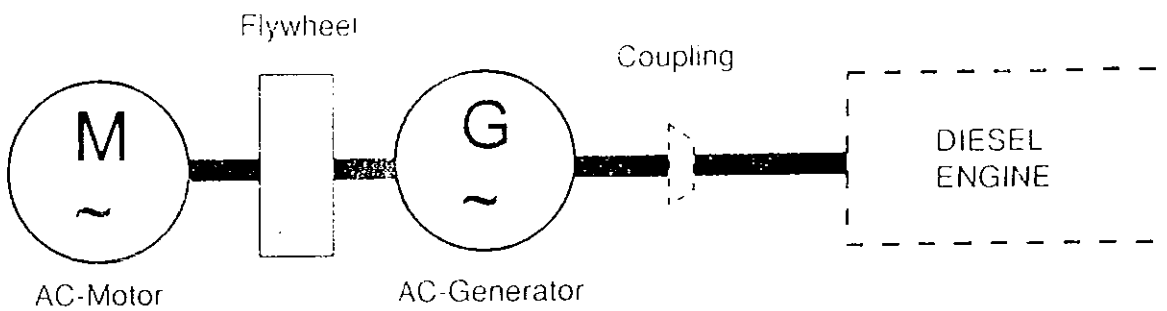

A possible answer to that question is found in Ken Bishop's recent article, "UPS:short-term or diesel?"[27]. In that article, Bishop explains that, from an industrial viewpoint, the major problems with mains power in Europe are caused by sags and short interruptions (Figure 3.3). Protecting an industrial process against such interruptions using a dedicated short-term UPS rather than the expensive and somewhat overspecified no-break diesel-generator set could yield considerable cost savings.

Figure 3.3 Typical statistics on mains failures (Taken from Bishop[11])

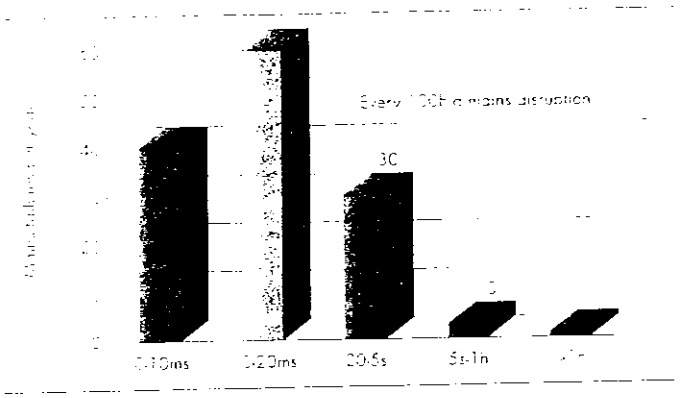

Figure 3.4 Typical electrochemical-battery-based uninterruptible power supply (Taken from Platts and St. Aubyn[12])

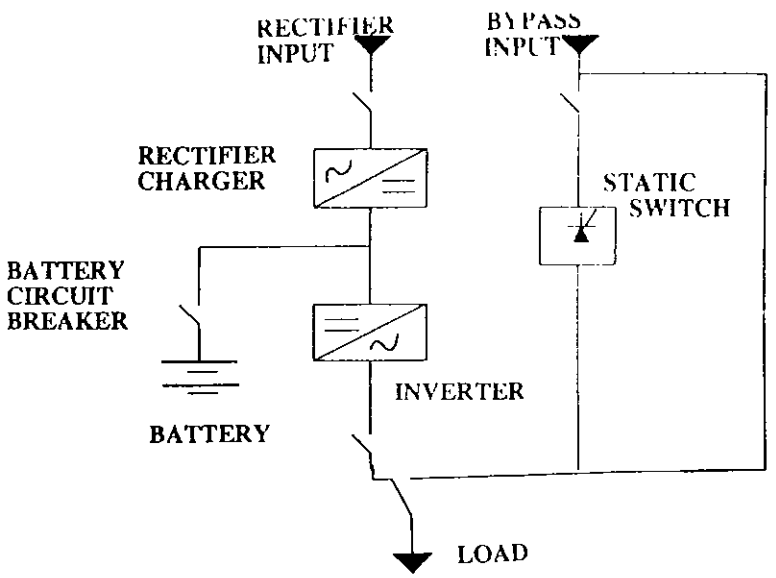

Such a short-term UPS could, at present, be realised in several different ways:

(1) **A synchronous generator coupled to a flywheel and a starter motor**

This trimmed-down version of the no-break system in Figure 3.2 has the advantage of being well proven, and reasonably easy to repair and maintain. As with most other rotary UPSs, this system would also generate ac naturally and it would have the ability to provide short-circuit current[12]. Disadvantages might include the high price due to the need for a starter motor; the high price of synchronous machines, especially in the low-power ratings, compared to squirrel-cage induction motors; and the need for controllers for both electrical machines. In addition, as this system provides energy to the electrical load, its speed and, hence, its frequency will fall. Finally, noise and safety considerations mean that this system must often be sited in a separate or an enclosed area.

(2) **An electrochemical battery and an inverter/converter** (Figure 3.4 above) This approach is already dominant in UPS systems for computers and, as both battery and inverter technologies mature, this approach will become even more dominant in the whole UPS area. One weakness of the system is the price, which is a little on the high side at present. (Table 3.1). Another is reliability or even the perceived reduction in reliability introduced by the inverter electronics. Yet another is the inability of the user to repair or maintain much of the system because of the complexity and the proprietary nature of the inverter. (See also Darrelman[45])

Table 3.1 Some information from a table given in an article published in Byte magazine[37] that compared the various characteristics of computer UPS systems from different suppliers

	MODEL	PRICE	CAPACITY (VOLT AMPS)	PRICE PER VOLT AMP	BATTERY RUNDOWN TIME (MINUTES, 70% LOAD
Line-Interactive Systems					
Asme Electronics	SM 800	$799	800	1.00	4.0
American Power Conversion	Smart-UPS 1000	$769	1000	0.77	6.0
Best Power	Fortress FI 1020S	$779	1000	0.78	5.5
Clary	OnGuard LI-1000	$849	1000	0.85	6.0
Deltec Electronics	PowerRite Pro 1000VA	$869	1000	0.87	
Hewlett-Packard	PowerWise UPS L900VA	$649	900	0.72	10.5
International Power Technologies	I-UPS 1250	$899	1250	0.72	4
Liebert	UPStation O	$972	900	1.08	5.5
Oneac	ON900A	$949	900	1.05	5.0
Para Systems	Minuteman Alliance A1250	$689	1250	0.55	4.5
Para Systems	Minuteman Powermind PML1250	$879	1250	0.70	7.0
Powercom America	UPS 1200-A	$599	1200	0.50	7.5
Square D-EPE	Topaz SV 1200	$999	1250	0.80	7.5
Superior Electric	Stabiline SL 1000	$695	1000	0.70	14.0
Tripp Lite Manufacturing	Smart 1050	$664	1050	0.63	10.0
Upsonic	LAN 100	$699	1000	0.70	4.0
On-Line Systems					
Alpha Technologies	CFR 1000	$1649	1000	1.65	8.0
Best Power	Ferrups 1.15	$1789	1150	1.56	8.0
C-Power Products	Guardian CPG-750	$1255	750	1.67	10.0
Controlled Power Company	LT-1200	$1165	1200	0.97	18.0
Exide Electronics	Powerware Prestige 1000P-1	$889	1000	0.89	9.0
Hewlett-Packard	PowerWise 1000 VA UPS	$1099	1000	1.10	7.0
IntelliPower	Bright-UPS IQ 1100	$1099	1100	1.00	6.0
Liebert	UPStation GX	$1485	1000	1.49	8.0
Para Systems	Continuous Power CP1K	$1399	1000	1.40	6.5
Powercom America	ONH-1000	$969	1000	0.97	12.0
Powercom America	ONL-1250	$1095	1250	0.88	14.0
Square D-EPE	Topaz SX 900	$1390	900	1.54	10.0
Toshiba International	1400S Series 1000VA	$2049	1000	2.05	9.5
Tripp Lite Manufacturing	Unison MPS 1200	$1399	1200	1.17	8.0
Upsonic	System 100	$999	1000	1.00	9.5

(3) **The Concycle alternator** Bishop's aforementioned article[11], which delineates the need for a good fast-responding short-term power, introduces the Concycle alternator (Figure 3.5a)--a doubly-fed machine that keeps the output

Figure 3.5a The Concycle generator of German company AVK/SEG complete with flywheel and diesel engine (Adapted from Bishop[11])

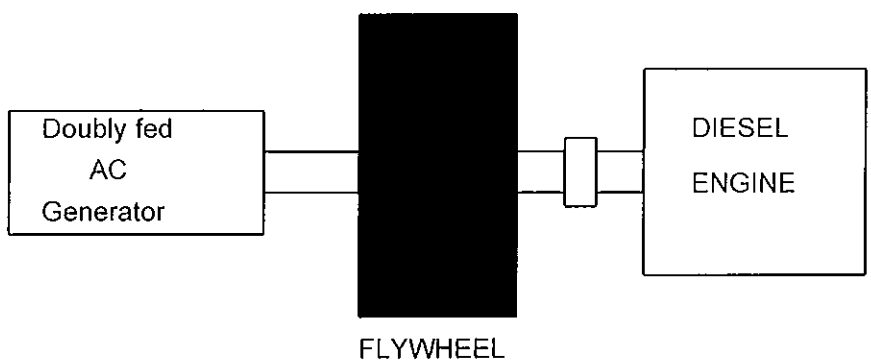

Figure 3.5b Comparison of three flywheel systems by percentage kinetic energy utilisation (Copied from Bishop[11])

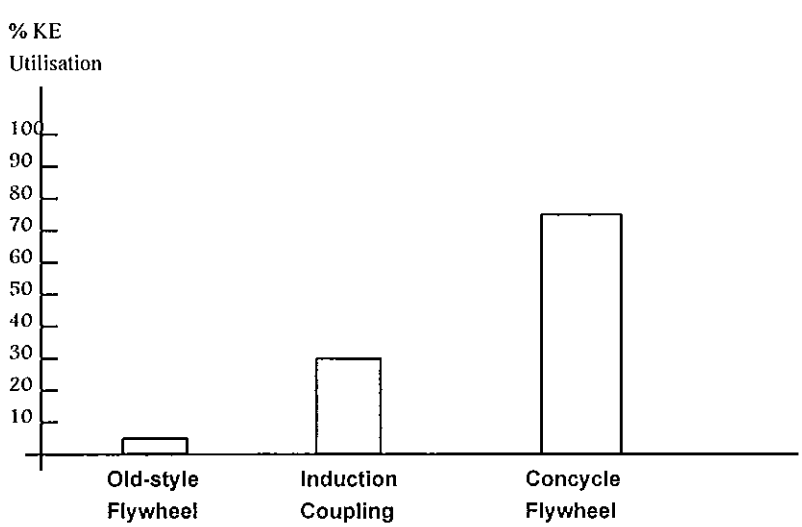

frequency regulated while utilising up to 75 percent of the energy stored in a mechanically coupled flywheel (Figure 3.5b above). Disadvantages are likely to include the expense and the fact that the technology is proprietary.

(4) **Other solutions** Platts and St.Aubyn[12] describe two other technologies that could be used to provide short-term energy: the Uniblock convertor (Figure 3.6) and the induction coupling (Figure 3.7). Again, however, both are undoubtedly expensive and involve the use of proprietary technology.

It is clear from the above, therefore, that there is still room for a low-cost non-proprietary short-term UPS that could be used to 'ride through' short-duration sags and interruptions in the mains power supply. One such system, which could be called a rotary UPS but is here categorised as a shaft-supported EMB, is described below (Section 3.4).

Figure 3.6 UPS system with Uniblock Converter (Taken from Platts and St. Aubyn[12])

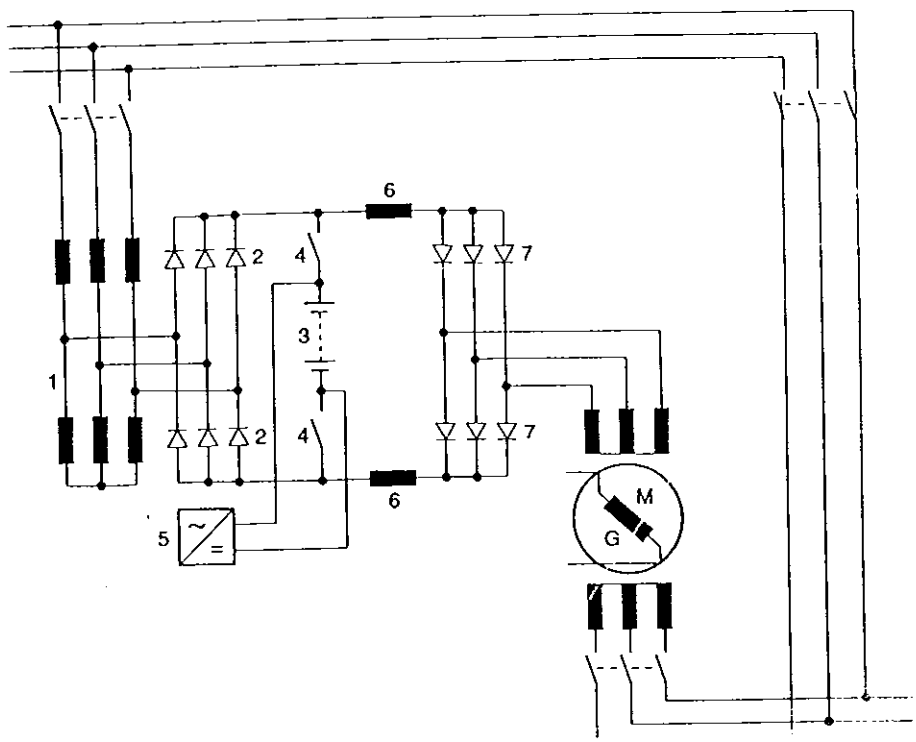

Figure 3.7 Schematic of the induction coupling in a no-break long-term (Taken from Platts and St. Aubyn[33])

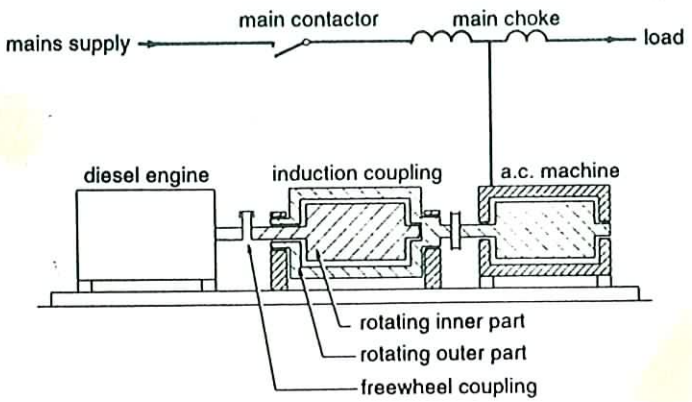

Figure 3.8 One of the principal applications of the self-excited induction generator is in wind turbines located in remote areas where the turbine is the major energy provider

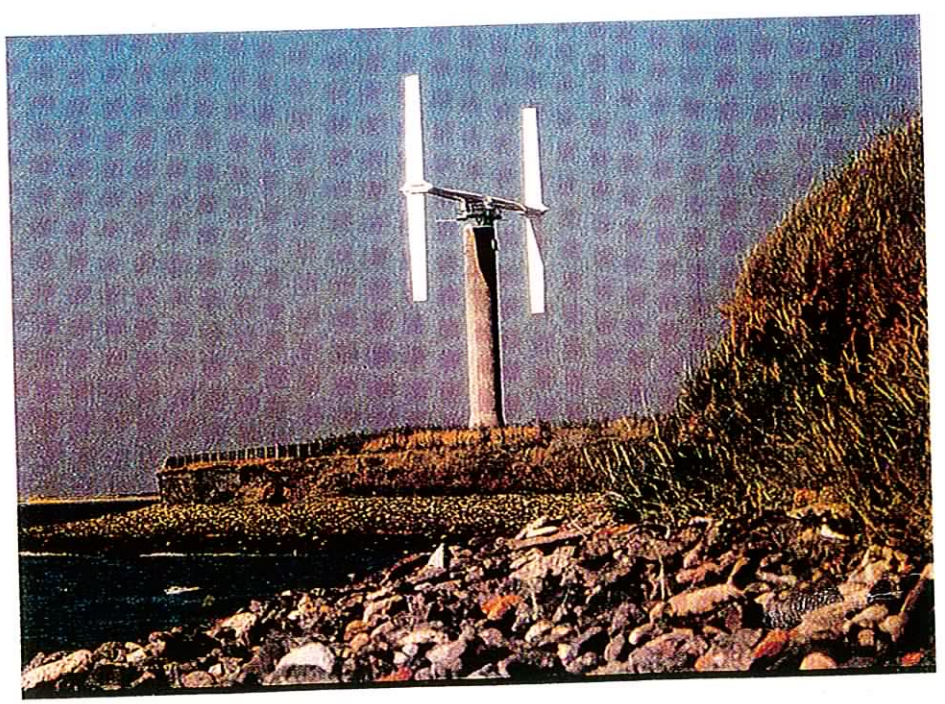

3.4 A new short-term UPS system based on the shaft-supported EMB

3.4.1 Introduction

The induction motor has long been the dominant electrical motor in industry. Reasons for this include the low cost, the passive control capability, the self-starting characteristic, the ease of application and the availability of single-phase versions. These favourable characteristics have also seen this machine being applied to the generation of electricity, particularly microhydro and wind-turbine generation (Figure 3.8). In these applications, the induction machine can be connected to a grid or operate in a stand-alone or self-excited mode. In the self-excited mode, the main obstacle that had to be overcome was the need to maintain a constant var balance between the load and the generator so that the voltage would not collapse or the current exceed its rating.

Much work was done in this area however, and the application of the induction machine to these systems has proved successful. Indeed, application of the induction machine as a generator is likely to increase even more as commercially available induction motors continue to improve in their performance. This improvement will be due to a move both in the U.S.[34] and Europe towards high-efficiency machines. For example, according to [60]

> "work sponsored by the U.K. Government in collaboration with industry has pioneered the development of higher efficiency motors which are sold at standard prices"

Given this background, it was decided to evaluate the possibility of applying the induction motor to UPS systems. In particular, it was proposed to replace the synchronous generator of the first option described above with an induction generator.

That particular arrangement should result in a reduction in capital cost because induction machines are of lower cost than synchronous machines and because induction machines are self-starting, which means no need for a starter motor provided it can be ensured that the motor will not overheat during start-up. Additionally, the system should be much easier than all the other solutions to repair and maintain. One big disadvantage, however, as with the synchronous machine, is that a reduction in flywheel speed will be accompanied by a reduction in electrical output frequency. Moreover, in the case of the induction machine, it is more difficult to maintain a constant voltage in the event of a reduction in frequency or a change in load. As a result, a prerequisite to the success of this proposal is that the load must be fairly robust to voltage and frequency variations.

Nevertheless, it is projected that the new system could find a niche as an interim energy store following a power supply interruption and until a diesel generator comes on line (e.g. sensitive manufacturing process) or until a load can be de-energised in a controlled manner (computer ups or emergency lighting supply).

The proposed induction-machine-based short-term UPS system is described in detail below (Section 3.4.2 onwards).

3.4.2 Apparatus and Operation

Figure 3.9 is a schematic of the shaft-supported EMB that is here proposed as a short-term UPS. The complete product comprises an induction machine (which could be an off-the-shelf induction motor Figure 3.10), a flywheel, a capacitor bank that may or may not be variable depending on the voltage regulation required and the knowledge of the load, a circuit breaker, one or more contactors, and a controller to oversee operation of the contactors and the capacitor bank. The complete system may have an appearance that is not unlike the conventional flywheel used to smooth speed variations in piston-driven engines (Figure 3.11).

Operation of the proposed EMB is as follows. When the circuit is first powered up, the contactor energises and the contacts close, allowing power to flow to the load and to the capacitor-induction machine combination. Being in its motoring mode, the induction machine accelerates the flywheel almost up to the machine's synchronous speed. The large inertia of the flywheel makes a continuous acceleration impossible, so the contactor opens at regular intervals to allow the machine windings to cool down during the acceleration process. When acceleration is complete, the capacitor-induction machine combination draws only enough current from the supply needed to compensate for eddy current and hysteris losses in the machine, for windage and friction losses, and for the slight non-unity power factor. (Obviously, the expense associated with this current could be greatly reduced by using a premium efficiency motor or by keeping the combination in a de-energised state with only the occasional "charge-up" to maintain the speed near synchronous speed.)

In the event of a mains failure or dip, the main contactor opens and, assuming var balance, the induction machine operates in a self-excited state with the

Figure 3.9 ***Schematic of the self-excited-induction-generator-based EMB proposed for use as a low-spec short-term standby power supply***

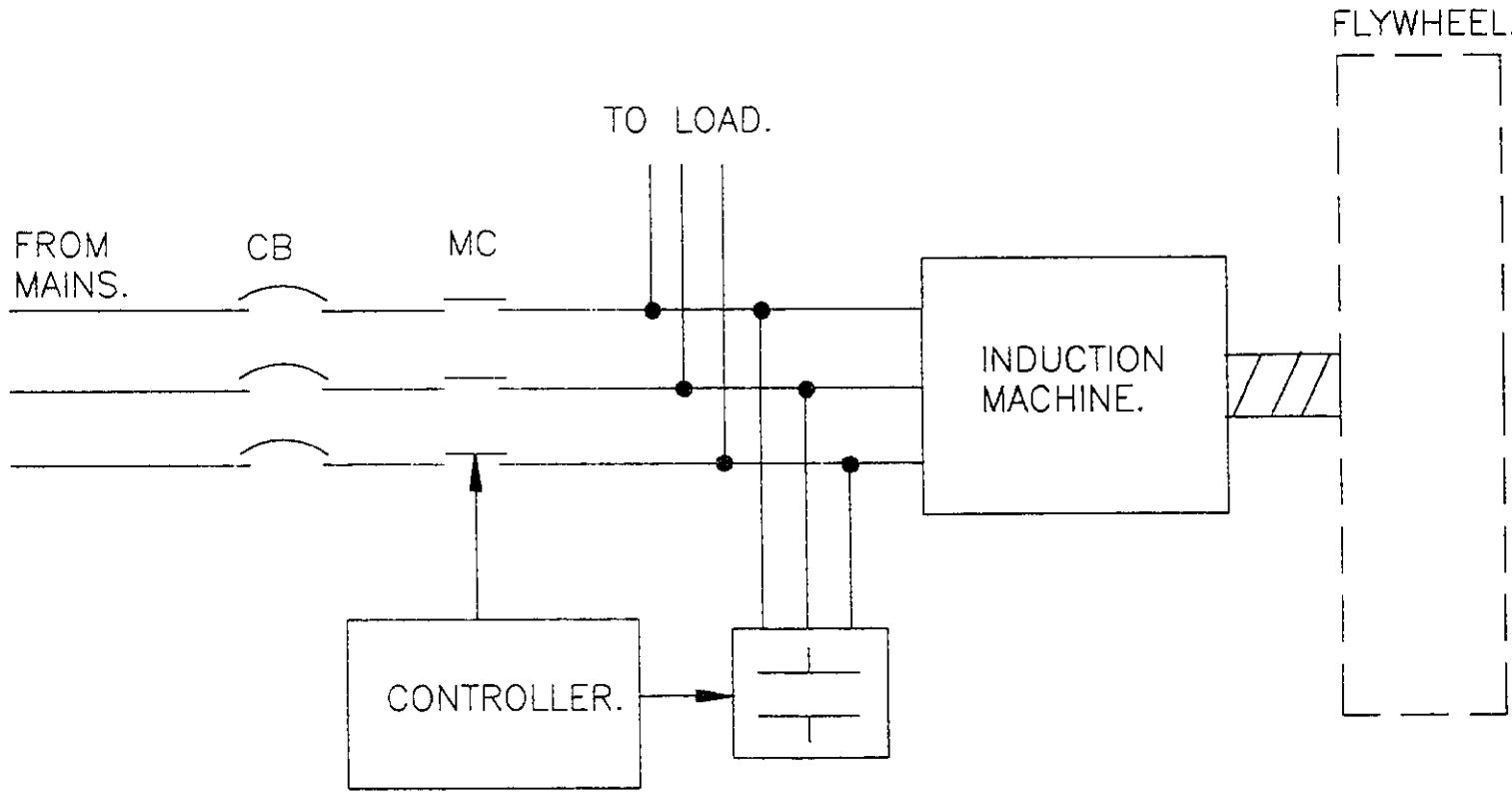

Fig 3.10 **Typical modern totally-enclosed three-phase squirrel-cage induction motor** (From [38])
Type MBT 180, 22 kW, IP 54, IC 51, 1470 r/min, weight: 145 kg

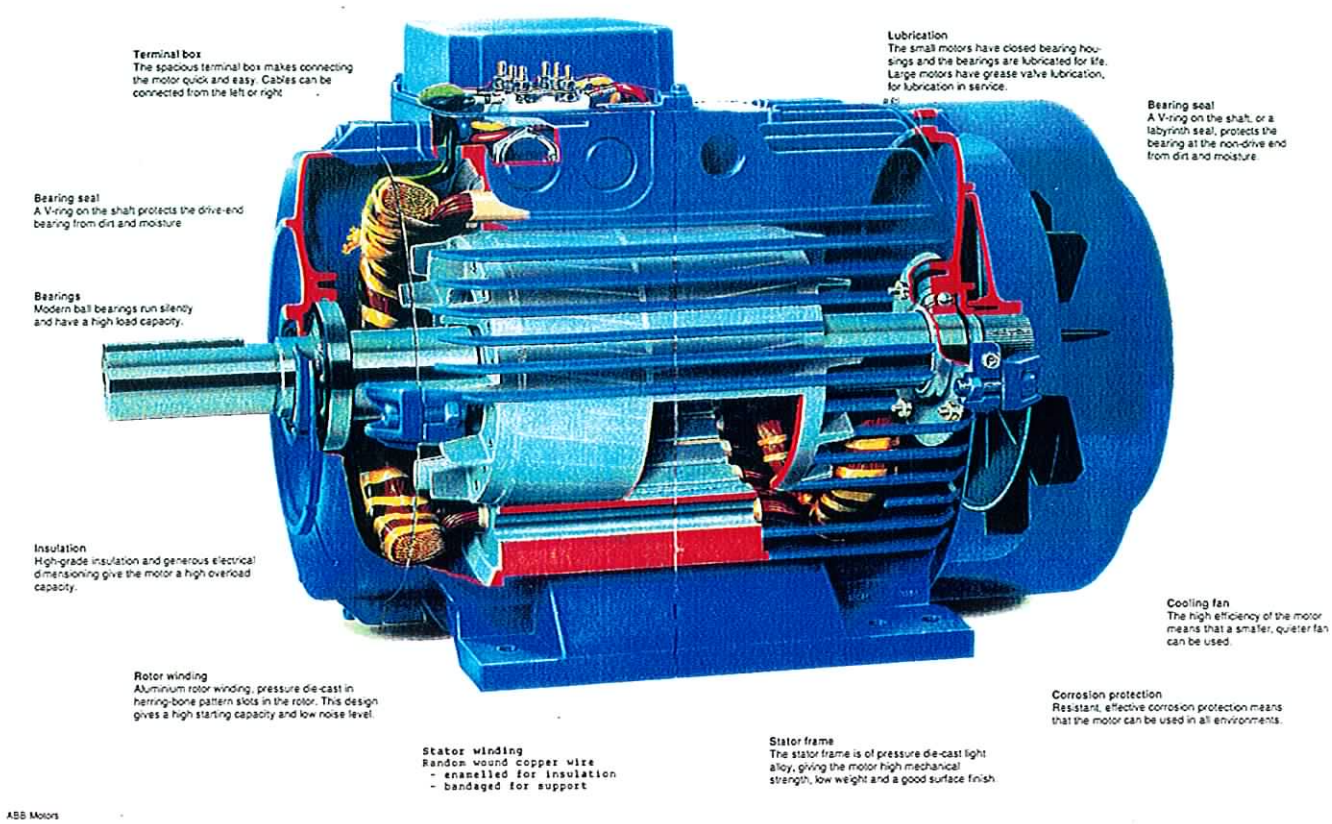

Figure 3.11 Internal combustion engine with large steel flywheel to smooth speed variations between piston strokes

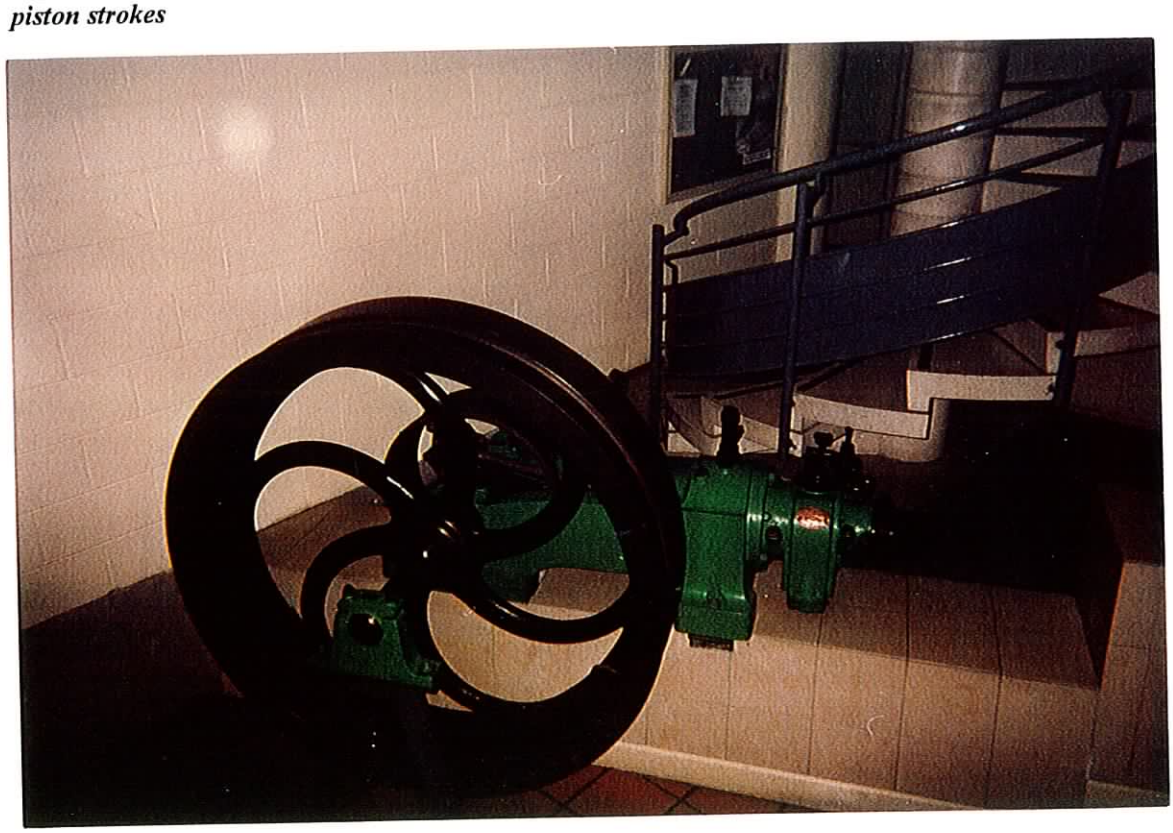

load now being powered by means of the flywheel kinetic energy. As a result, the flywheel begins to lose speed at a rate dictated by the load, the flywheel inertia and speed, and the losses. The reduction is speed is accompanied by a reduction in frequency, which has implications for the var balance--the vars generated by the capacitor must be adjusted so as to balance the vars being absorbed by the load and the motor.

It would be hoped though, as would be the case for a specially designed induction generator[35], that premium efficiency motors, soon to be available off the shelf[34,60], may be able to cover the complete frequency range with a single excitation capacitor because of the relatively small variation in the vars required by the induction machine, but this would have to examined in more detail when those machines become available. Conventional induction motors, by contrast, have deliberately been designed to have a high leakage reactance, and hence a wide var range.

Using information in [36], these issues will be analysed in more detail, allowing prediction to be made of both the load and frequency windows for various 3-phase machines connected to different load types. This theoretical analysis will be described in Chapter 4 along with corroborating experimental work.

Chapter 4

Simulation and Testing

4.1 Introduction

The function of the electromechanical battery proposed in the previous chapter is to provide power to a load in the event of a power failure. In such an event, the frequency and voltage will no longer remain fixed as the induction machine is in its self-excited mode. Instead, both frequency and voltage will be determined by a combination of the following: the load characteristics, the inertia and speed of the flywheel, the size of the excitation capacitors and the parameters of the induction machine. This self-excited mode of operation of the induction machine has been the subject of many studies into the use of the induction machine as the principal electromechanical energy converter in autonomous electrical generation schemes. In one of the most recent of those studies, Salama and Holmes[36] (henceforth denoted 'Holmes') presented a very thorough and general analysis of the induction machine. In much of this chapter and in Appendix E, Holmes' work is adapted to the self-excited induction generator in the proposed flywheel energy storage system.

4.2 Application of Holmes' analysis

In Section 10 of Holmes' paper, a node voltage analysis is performed on the well-know lumped-parameter per-phase circuit of the induction generator. That analysis produces the following two-equation model of the self-excited induction generator as follows: (The complete analysis is given in Appendix E)

$$\frac{R}{R^2+X^2}+\frac{1}{R_C}+\frac{R_2/s}{(R_2/s)^2+X_2^2}=0 \qquad \textbf{Model Equation One}$$

and:

$$X_M=-\left(\frac{X}{R^2+X^2}+\frac{X_2}{\left(\frac{R_2}{s}\right)^2+X_2^2}\right)^{-1} \qquad \textbf{Model Equation Two}$$

where R + jX is the combination of the following impedances:

the equivalent series load impedance
the excitation capacitive reactance
and the stator resistance plus leakage reactance

and
X_m is the machine's nonlinear magnetising reactance
R_c is core loss
R_2 is the referred rotor resistance
X_2 is the referred rotor reactance ($=\omega.L_2$)
s is the machine slip

Assuming the speed of the machine and the characteristics of both the machine and load are known, the easiest way of solving the above two equations is to solve the first equation to get the slip, which can then be used to calculate the magnetising reactance. From a knowledge of the magnetising characteristic of the machine, it would then be possible to calculate the air-gap flux and thence the air-gap voltage. With the air-gap voltage, it is possible to calculate output voltage and current, efficiency, power factor etc.

The main task, therefore, is to solve the first equation. The approach adopted by Holmes was to expand this equation into its natural polynomial, which is of degree 6. Some root searching method could then be used to find the slip. There is a simpler way of finding the solution, however. Model Equation 1 is first of all rearranged (See Appendix E) to give:

$$s = -R_2 \cdot \left(1 + \left(s \cdot X_2 / R_2\right)^2\right) \cdot \left(\frac{R}{R^2 + X^2} + \frac{1}{R_C}\right) \qquad \textbf{Iterative slip equation}$$

This equation could then be used as the basis for an iterative approach to finding the slip, but it was felt that rewriting the equation in terms of the electrical frequency ω_e and the mechanical frequency ω_m before performing the iterations, would prove to be a more stable approach. The reason for this is that, for a lightly loaded self-excited induction generator, the slip can easily be shown to be roughly proportional to the square of the frequency (and speed), simply because R_2/s would be much greater than X_2, R_c could be neglected without much loss of accuracy and X would be expected to be a capacitive reactance significantly bigger than R. The resulting near-square-law relationship between the slip and the frequency is in contrast to the near-linear relationship between the speed and the frequency irrespective of the loading. Furthermore, the reasonably accurate initial guess required by the iterative approach is much easier to make with an iterative frequency equation rather than the iterative slip equation.

The above equation in slip is therefore rewritten as (See Appendix E):

$$\omega_e = \frac{p.\omega_m}{1 + R_2.\left(1 + \left((\omega_e - p.\omega_m).\frac{L_2}{R_2}\right)^2\right).\left(\frac{R}{R^2 + X^2} + \frac{1}{R_C}\right)}$$ **Iterative freq eqn**

This equation was then implemented on a spreadsheet (See Appendix E). This approach is proposed as being simpler, but it should be equally as accurate and more transparent than the method used by Holmes.

4.2.1 Holmes comparison

It was wished to compare the results of the iterative method with those of Holmes to validate the proposed iterative approach. To that end, the induction machine parameters used by Holmes were first duplicated:

Stator resistance (R_1)	=	8.5 ohms
Stator leakage reactance (X_1)	=	15.715 ohms
Magnetising reactance (X_m)	=	133.7 ohms
Core losses (R_c)	=	Neglected in this case
Referred rotor resistance (R_2)	=	3.95 ohms
Referred rotor reactance (X_2)	=	18.06 ohms

Then various points on Holmes' motor curve of air-gap voltage vs. magnetising reactance were estimated and used to produce a similar curve (Figure E.2). With all of these data and the same loads as were used by Holmes (ie. Resistive loads of 200, 400 and infinite ohms), it was possible to produce plots similar to those presented by Holmes.

To compare results, various points on some of the graphs presented by Holmes were estimated and plotted next to the points produced by the iterative method being proposed here. The results are shown for various on Figures 4.3-5. In the first two figures, the output voltage is graphed against rotation speed and capacitance respectively for different loads. In Figure 4.5, the efficiency of the induction generator is graphed against capacitance for different loads. The correlation is very good between both predictive approaches, with any differences being explicable by the various estimating phases undertaken reproducing Holmes' data, by Holmes' use of exact-fit polynomials to produce curves from discrete data and by the discrete nature of the magnetising data in the spreadsheet.

Figure 4.3 Output Voltage Comparison--Variable Rotation Speed

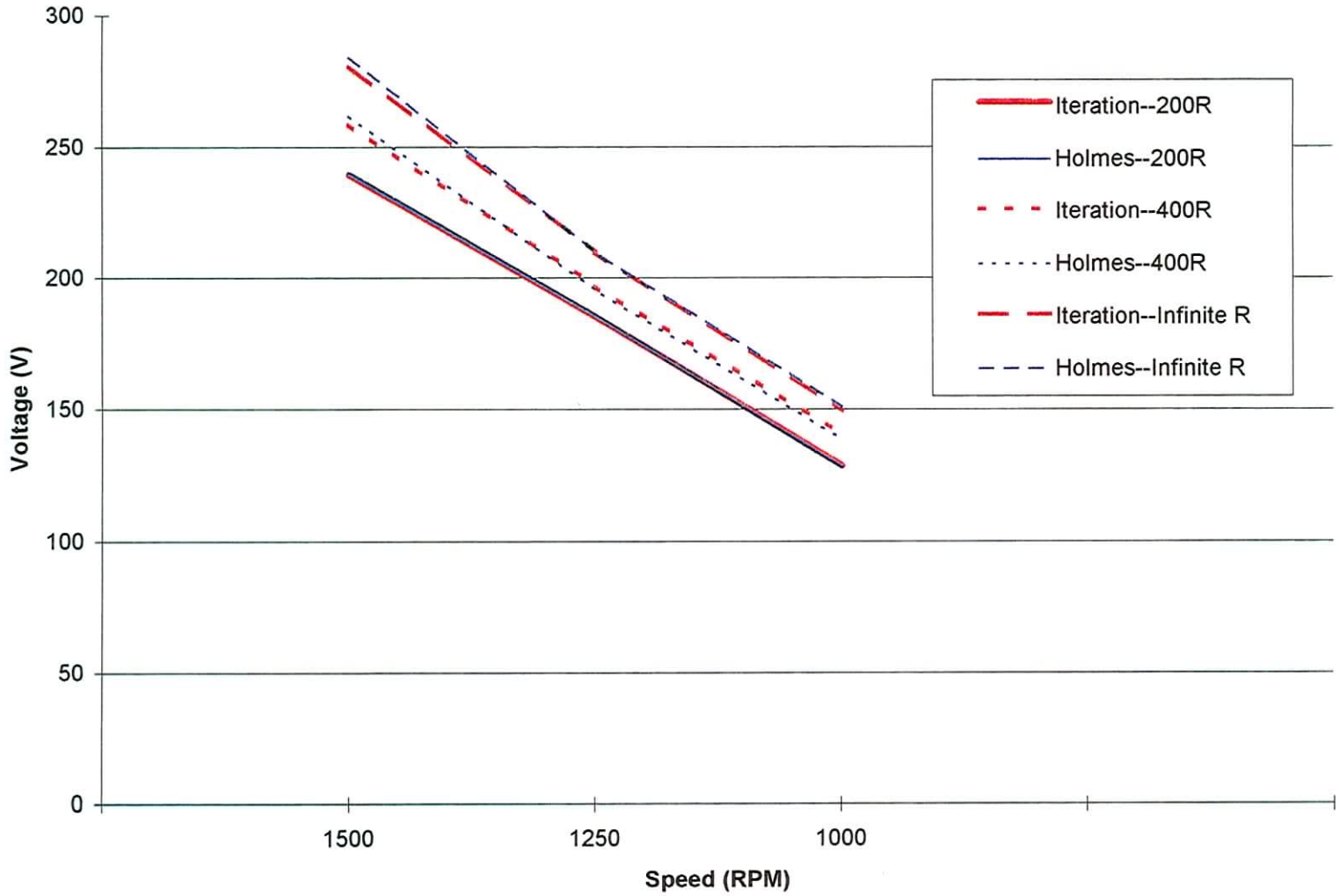

Figure 4.4 Output Voltage Comparison--Variable Excitation Capacitance

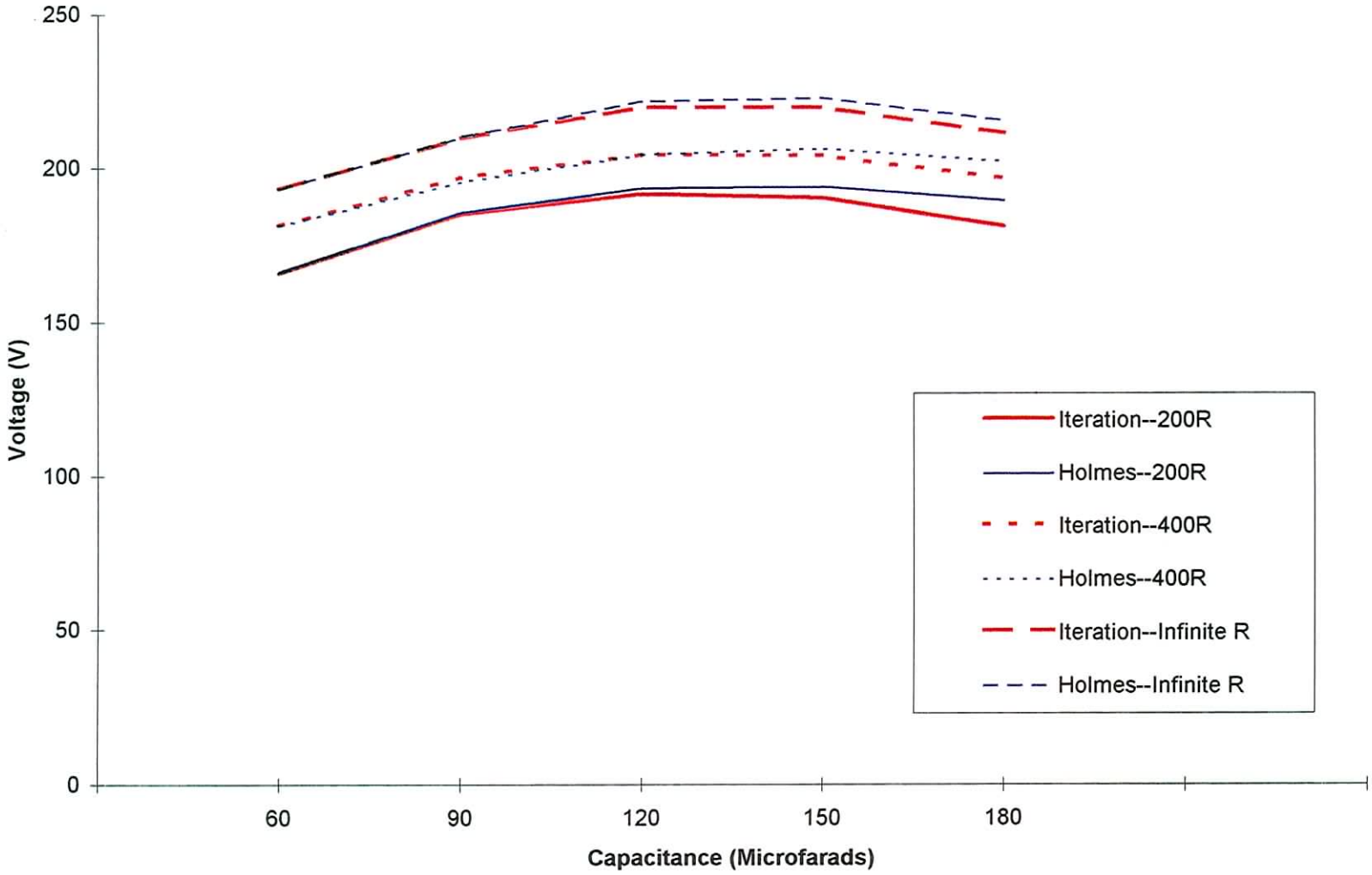

Figure 4.5 Efficiency Comparison--Different Loads

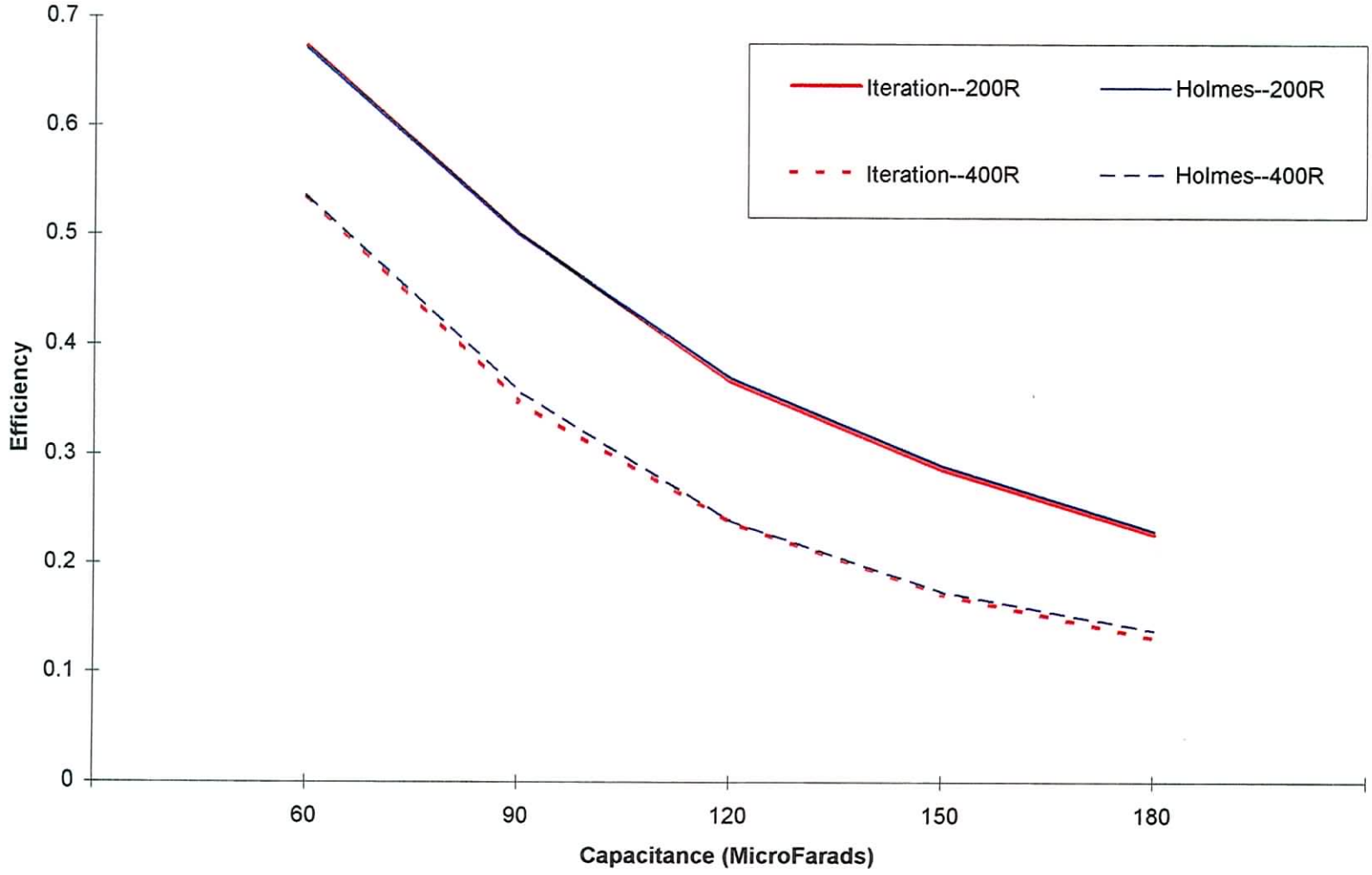

4.3 *Experimentation*

An experimental program was undertaken during the summer of 1997. The aims of this program were to:

(1) Demonstrate the principle of the voltage and frequency persisting, albeit declining, following the disconnection of the mains voltage.

(2) Further validate the model adapted from that proposed by Holmes

(3) Identify problems not immediately evident from the theory but which could be encountered in practical implementations

4.3.1 Apparatus

Having thought about ways of satisfying the aims of the experimental campaign, one simple solution to the problem of acquiring a flywheel and mounting that flywheel between suitable bearings emerged. It was decided to try a car wheel mounted on its own bearings and connected to an inducation motor via its own drive shaft. Accordingly, a suitable secondhand car wheel and its support accessories were purchased from a scrapyard. These were mounted on a suitable base and coupled to a small induction machine. Unfortunately though, there was too much play in the wheel bearings resulting in excessive vibration of the system. It was felt that the bearings were faulty, but an examination of several other bearings revealed a similar amount of play and, under some time pressure, the car-wheel flywheel was put aside.

Instead, it was decided to revert to a conventional steel flywheel with double-sided bearing support. To that end, an old truck flywheel was obtained, its gear cog was

removed, and a suitable collar was machined to allow the flywheel to be held in place between two bearings. The bearings were then mounted on a base constructed from box-section steel and featuring mechanical slides that permitted variation of the width in order accommodate wider flywheels (Figure 4.6).

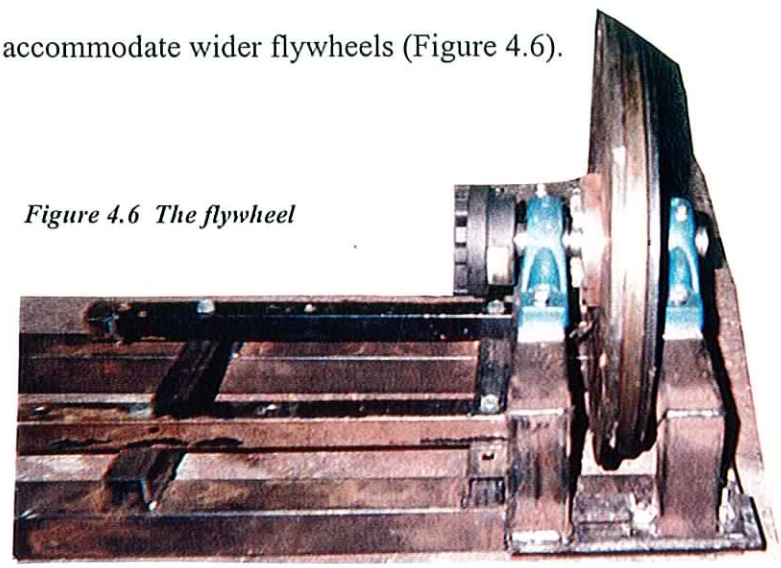

Figure 4.6 The flywheel

The base was also designed to support a small induction machine that would be mechanically coupled to the flywheel. The complete assembly was then placed in an open-topped steel box (Figure 4.7) that came complete with castors making the assembly somewhat mobile. Furthermore, it was deemed desirable to evaluate the aerodynamics of the rotating system at reduced atmospheric pressure, so the box was upgraded to a vacuum chamber (See Section 4.3.6 for results and discussion) . This involved fitting the box with a reinforced steel top and applying an expandable foam seal and silicone to make the chamber air tight. Evacuation of the chamber was effected using an old refrigerator pump connected up in reverse. Other connections to the inside of the chamber included the electrical wires to the motor and a vacuum gauge. A window was also cut into the

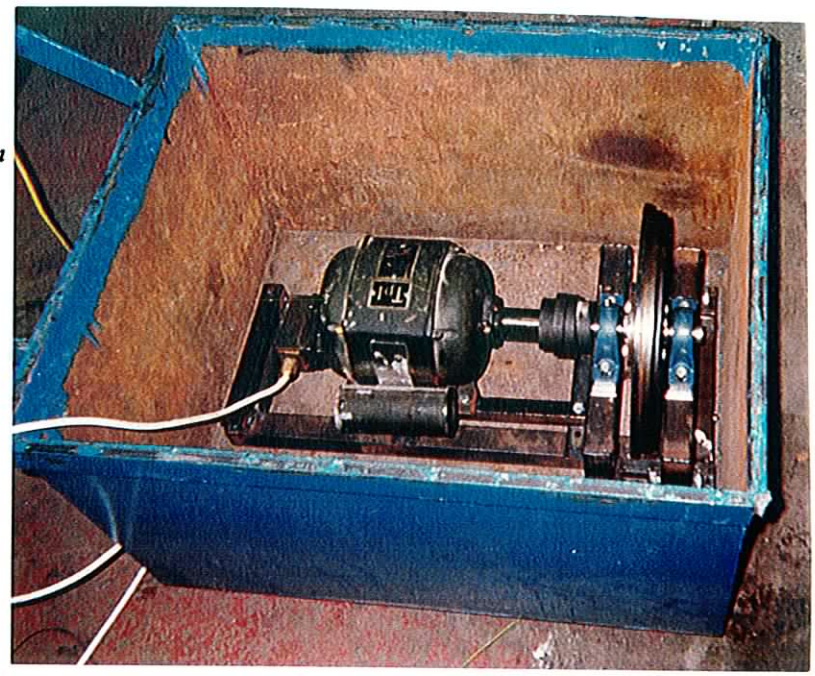

Figure 4.7 The flywheel and induction machine in a steel box

Figure 4.8 Reinforced box top with a window aperture for flywheel speed measurement and with other interfaces for the vacuum pump, pressure gauge and electrical connections to the motor

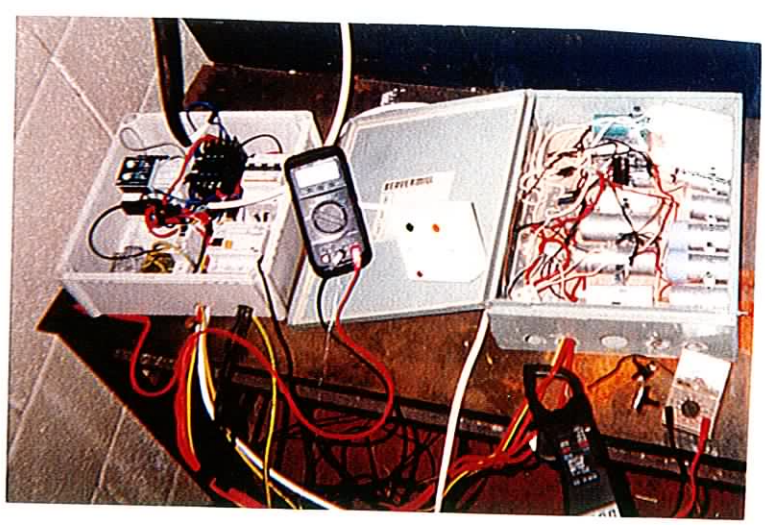

Figure 4.9 The electrical control panel

steel top to allow external monitoring of the flywheel speed using an optical tachometer (Figure 4.8). Finally, some electrical panels were assembled to oversee and control the mains connection to the system (Figure 4.9). Components of the electrical panel included an earth-leakage circuit breaker, a convential circuit breaker, contactors, a double timer relay, and a capacitor bank. Voltage, current, power, frequency and distortion were monitored using voltmeters, a clamp-on ammeter and an energy analyser.

It has already been explained that the mechanical structure supporting the flywheel and motor was designed for a small induction machine. Three different types were tried. The first was an approximately 1 kW, 1000 rpm, 3-phase machine. This machine proved unsuitable because of the small amount of energy stored in the flywheel due to the relatively low synchronous speed. As a result, the self-excitation process only lasted a few seconds because of relatively high parasitic losses, and self-excitation looked more like a blip in the aftermath of mains switch-off. Accordingly, the remaining two motors tried had a 3,000 rpm synchronous speed, which meant that about nine times more energy was stored in the flywheel.

The first of those machines was an old single-phase machine with a rating of less than 250 W. One might expect that such a machine with its high speed, low rating and low efficiency might be at risk of burning out during the starting process. This is exactly what happened despite the use of intermittent energisation of the coil of the starting contactor to allow the windings to cool during startup. One of the problems with that approach was that the rotor tended to slow down too quickly when the mains was not being applied. The complete starting problem is discussed more fully in the concluding chapter.

The second high-speed machine had a higher rating (1.2 kW) and was 3-phase and was far more robust during startup. Nevertheless startups were minimised and spread out to reduce the thermal loading on the windings. The self-excitation performance of this machine was much longer (10-20 seconds depending on load and capacitors), and this machine became the main focus of all the experiments carried out.

4.3.2 Equivalent-circuit parameter determination

The first experimental task was to provide the information required to calculate the parameters of the per-phase equivalent circuit and thereby enable machine simulation. This task was accomplished by performing some standard tests:

Blocked Rotor

A G-clamp was first connected to the flywheel to stop rotation. A low voltage was applied by means of a resistor divider circuit, and the resulting current and power inputs are noted.

DC Resistance

With the copper still hot from the previous test, the dc-resistance of stator windings is measured.

No Load

The motor is connected directly on line and allowed to rotate close to synchronous speed. Per-phase values of voltage, current and power on each of the three phases are noted.

The most remarkable point about these tests was the large imbalance in each of the three phases as exemplified by results from a No Load test:

Table 4.1 Results from the no-load test

			PHASE	
		One	Two	Three
	Voltage (V)	234.5	232.1	233.2
	Current (A)	1.28	0.96	0.97
	Power (W)	111	35.5	124.2

The large difference between some of the measurements (especially those of the per-phase powers) was somewhat mystifying. All the readings were double-checked so it was concluded that the problem lay within the machine itself. Presumably, therefore, each of the phases on the machine had been wound differently--perhaps with a different gauge wire or with a different number of turns--and/or there were differences in the magnetic circuits on each phase. It was felt that, at such low power ratings, the

manufacturer would not have been overly concerned about imbalances in the no-load per-phase powers. After all, this motor was destined to spend its working life driving a small fan--before we borrowed it.

From the point of view of our experimental accuracy, the large imbalance in each of the phases was somewhat unsatisfactory. Apart from that, however, the machine was nearly ideal for our needs, and it was decided to continue using it. We would average all of the test results to obtain average per phase voltages, currents and powers. Of course, this approach would compromise the accuracy slightly, but we would still be able to satisfy the aforementioned aims of the experimental programme.

Standard calculation procedures (See Fitzgerald et al. [39]) were applied to the averaged quantities to obtain values for each of the lumped parameters of the per-phase equivalent circuit. The following 50 Hz parameter set was obtained:

Stator resistance (R_1) = 3.6 ohms

Stator leakage reactance (X_1) = 5.4 ohms

Magnetising reactance (X_m) = 224 ohms

Core losses (R_c) = 529 ohms

Referred rotor resistance (R_2) = 5.35 ohms

Referred rotor reactance (X_2) = 5.4 ohms

4.3.3 Magnetising Curve Construction

Another test was conducted in order to obtain the magnetising curve of the motor. This test is not quite so straightforward as the above tests because the voltage output from the self-excited induction generator can initially rise substantially above the nominal mains value. As a result, this test required a device that would provide an input voltage that was, perhaps, 30 percent higher than the mains voltage. In other words, the mains voltage in the area was around 230 volts, but it was desirable to plot the magnetising curve of the motor at an input of up to 300 volts. Not having a suitable 3-phase transformer or variac, it was decided to examine the possibility of using series capacitors to bolster the effective input voltage to the induction machine. It was felt that 2 points would be ample for constructing an accurate magnetising curve above 230 volts.

With both a series and a shunt capacitive connection to a non-loaded induction machine, the resonant frequency of the circuit of both can be approximated by

$$1/\sqrt{L.C}$$

where C is the value of the capacitor and L that of the machine's magnetising inductance. This means that the capacitance required to give resonance can be written as:

$$\frac{1}{w.X_m}$$

At mains frequency and a magnetising reactance of 224 ohms (230 volt value), the required resonating capacitance is about 14 microfarads. Theoretically, this value of

capacitance or values close to it are potentially dangerous, because of the possibility of very high values of input voltage. For example, 13.5 microfarads should theoretically give an input voltage of 4,300 V (Table 4.2). In practice, though, it was found that 13.5 microfarads only gave about 300 volts on the input, so the Q-factor is quite low in the circuit. Details of the two points on the magnetising curve found by this method are given in Table 4.2.

Table 4.2 This table shows the series capacitance values tried, the theoretical input voltage (i.e. voltage produced by an ideal series LC circuit) and the actual voltage along with the resulting current and power

Capacitance (Microfarads)	Input Voltage [Infinite Q] (V)	Input Voltage [Measured] (V)	Average Input Current (A)	Average. Input Power (W)
10	550	266	1.47	110
13.5	4300	298.8	2.21	388

With this data, as well as the data for 230 V mains excitation and for excitation below mains (135 V), a magnetising curve was interpolated (Figure 4.10). This curve, along with the machine parameters, was used to model the machine in its self-excited mode.

Figure 4.10 The magnetising curve of the 3-phase 2-pole 1.2 kW induction motor

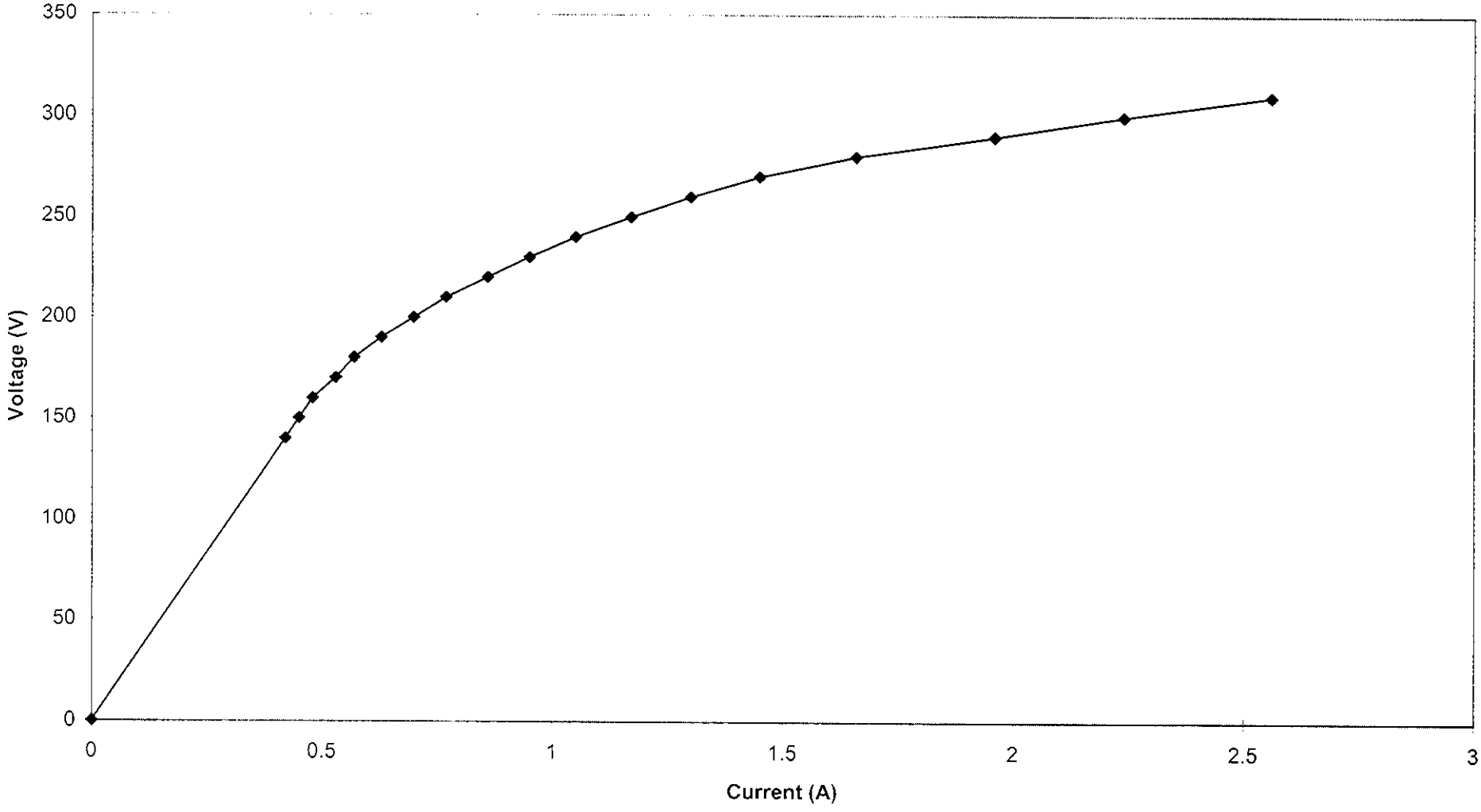

4.3.4 Self-excitation measurements

Excitation capacitors can be estimated in a manner similar to that used for choosing series resonance capacitors. Once again, the 50 Hz resonance frequency occurs at about 14 microfarads because the resonance frequency for series and shunt connections is identical. In the present self-excitation scenario, however, only capacitors approximately equal to and greater than 14 microfarads are viable propositions because the self-excited frequency will always be less than 50 Hz here—even just after the point of changeover from mains excitation. Of course, the larger the excitation capacitor the wider the excitation frequency range and the larger the initial voltage. Both of these points are evident in the graphs of Figures 4.11 and 4.12, which compare measured and calculated output voltage for 17 and 30 microfarad excitation capacitors.

The graphs also demonstrate a good correlation between measurement and theory. The graph of the 30 microfarad excitation, in particular, is particularly accurate except around the frequency of de-excitation, where shortcomings of using a linear spline to approximate the initial section of magnetisation curve are evident. The graph of the 17 microfarad excitation is somewhat inaccurate in its voltage calculation—an error that is attributable to the use of one of the phases to measure the voltage (the measured voltage for the 30 microfarad graph is an average of the three phase voltages). It should also be noted that the spreadsheet model has also been improved since.

Figure 4.11 Theoretical and experimental no-load output voltages (17 μF per phase)

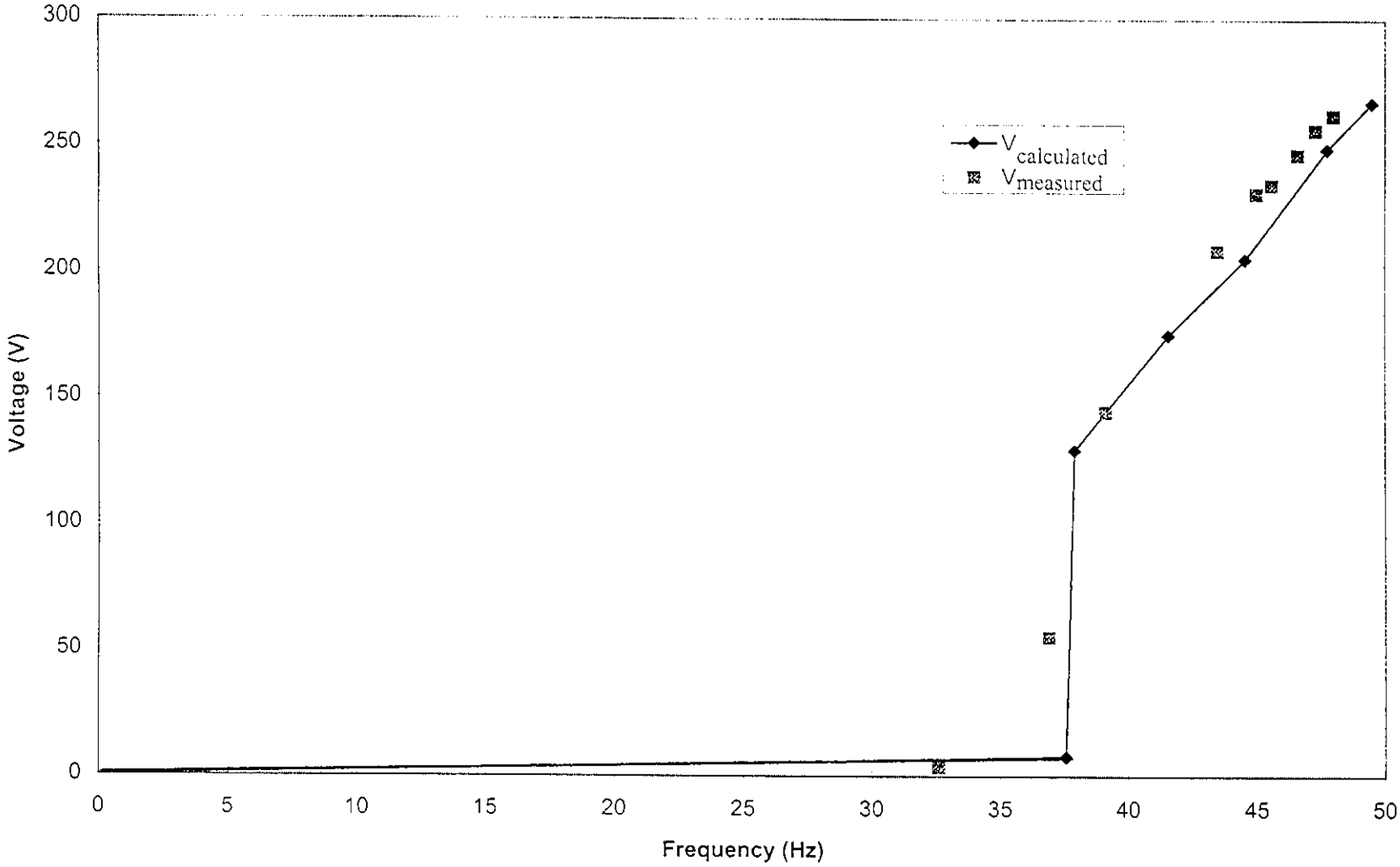

Figure 4.12 Theoretical and experimental no-load output voltages (30 μF per phase)

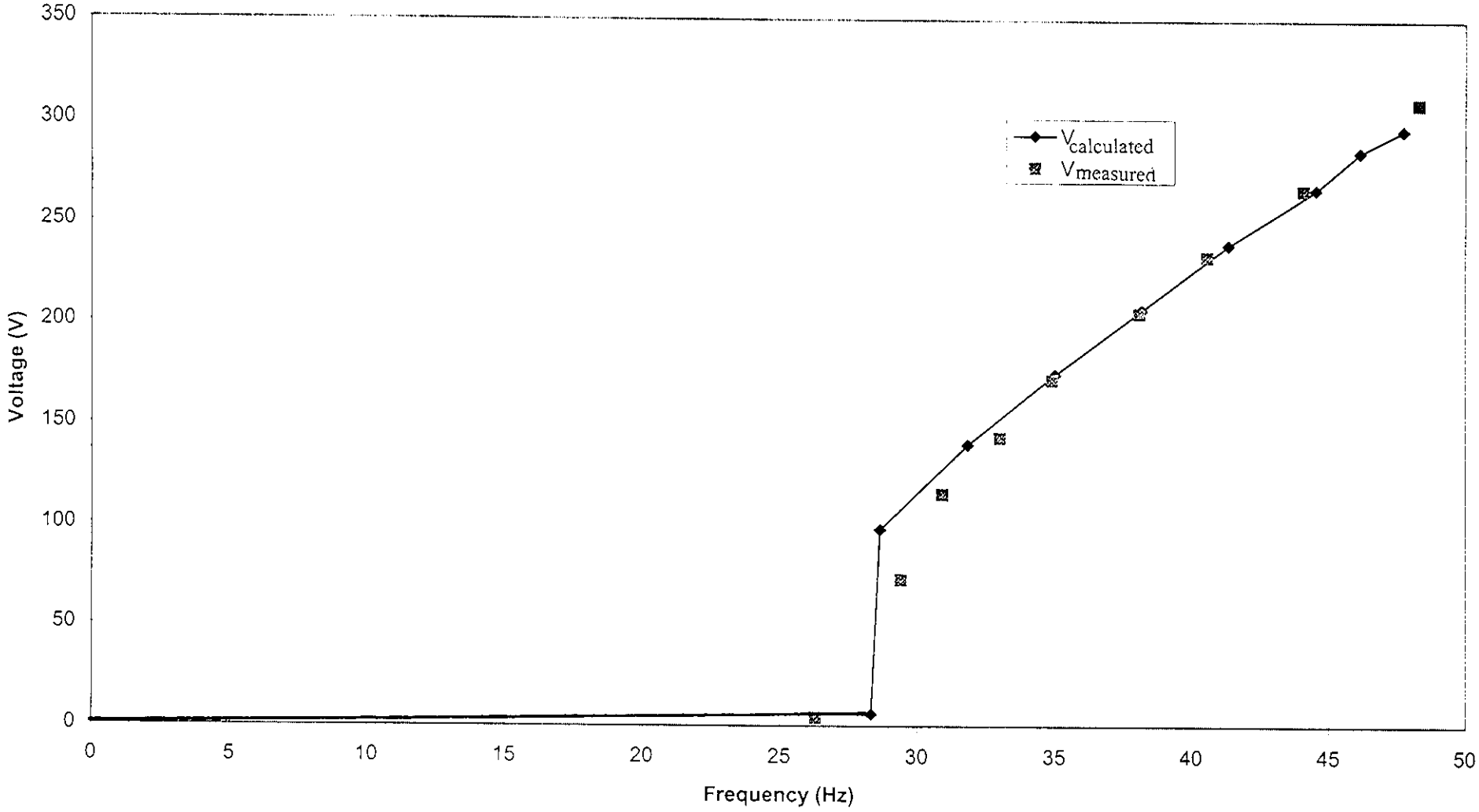

Time, equipment and other constraints prohibited detailed measurements of the output voltages for different 3-phase loads. This is recommended as future research work but, for the purposes of the present project, it was felt that the objective of further validating the simulation software had already been sufficiently satisfied.

4.3.5 Lighting load demonstration

One of the principal applications targetted by the present application is emergency lighting loads. It was, therefore, logical to examine the effect of the falling voltage and frequency on different light sources. Such an experiment also provided a somewhat illuminating demonstration of the principles involved in the proposed EMB.

Examples of some of the main light sources in commercial buildings were used in the experiment, namely, an incandescent bulb, a fluorescent tube with a wirewound choke and a fluorescent tube with an electronic ballast. The effects on the light output after the changeover to self-excitation are shown in Figure 4.13. Several points are noteworthy:

1. Following changeover, the light output of the incandescent jumped dramatically to over double its original value due to rise in the voltage (Figure 4.12). The change in output from the fluorescents was far less marked particularly for the electronic ballast compact fluorescent.

2. Variation in light output is most noticeable with the incandescent where it appears to fall almost exponentially from its initial high to zero. Light output from both fluorescents is nearly constant throughout.

3. All of the bulbs gave light for considerable durations, but the output from the incandescent gradually faded whereas the output from both fluorescents was more constant and had definite cut-off points (at approximately 20 seconds, 200 V and 40 Hz), with the wirewound-choke fluorescent slightly outlasting the compact fluorescent.

It would be difficult to quantitatively predict the results of such an experiment because of the nonlinear nature of each light source---even the incandescent bulb is nonlinear, having a low resistance at room temperature and a very high resistance (perhaps 10 times greater) at operating temperature. As a result, no effort was made to measure the light output against frequency or voltage. However, it is possible to qualitatively understand the characteristic of each source:

The fluorescent tube with the wirewound choke The characteristic of this ubiquitous light source is seen to be well suited to the proposed EMB. The reason is that the light output is dependent on the current flowing through the tube. This current is in turn largely determined by the impedance of the wirewound choke, which drops off proportionally with frequency in the frequency of the power and should be compensated for by a proportional drop in the voltage so as to maintain the same current. In other words, when a variable-

when a variable-frequency power source is feeding

loads containing a saturable iron core, a constant voltage-to-frequency ratio should be maintained to give maximum performance. Fortunately, the voltage-to-frequency ratio of the proposed EMB is quite constant over a large frequency range, making this EMB suitable not just for these fluoresent tubes, but most loads containing a saturable iron core (motors, transformers and chokes) provided the drop in frequency can be tolerated.

The compact fluorescent The compact fluorescent is also seen to have characteristics that appear quite favourable to the proposed EMB. The reason is that the input to the compact fluorescent is usually rectified to dc, which means that the supply frequency is not so important. This dc is then inverted to high-frequency ac and fed to the fluorescent tube. A current controller on the inverter limits the voltage being applied to the tube so as to maintain an approximately constant current. This controller is probably not designed to bolster the voltage however and, below a certain voltage, the tube current collapses.

The incandescent bulb The output from this source is extremely variable and, for that reason, probably the least suited to the proposed EMB, despite its having the longest duration and no sudden loss of light. Another reason for the

Figure 4.13 Light Output from different light sources as frequency and voltage drop (C=30 micro farads)

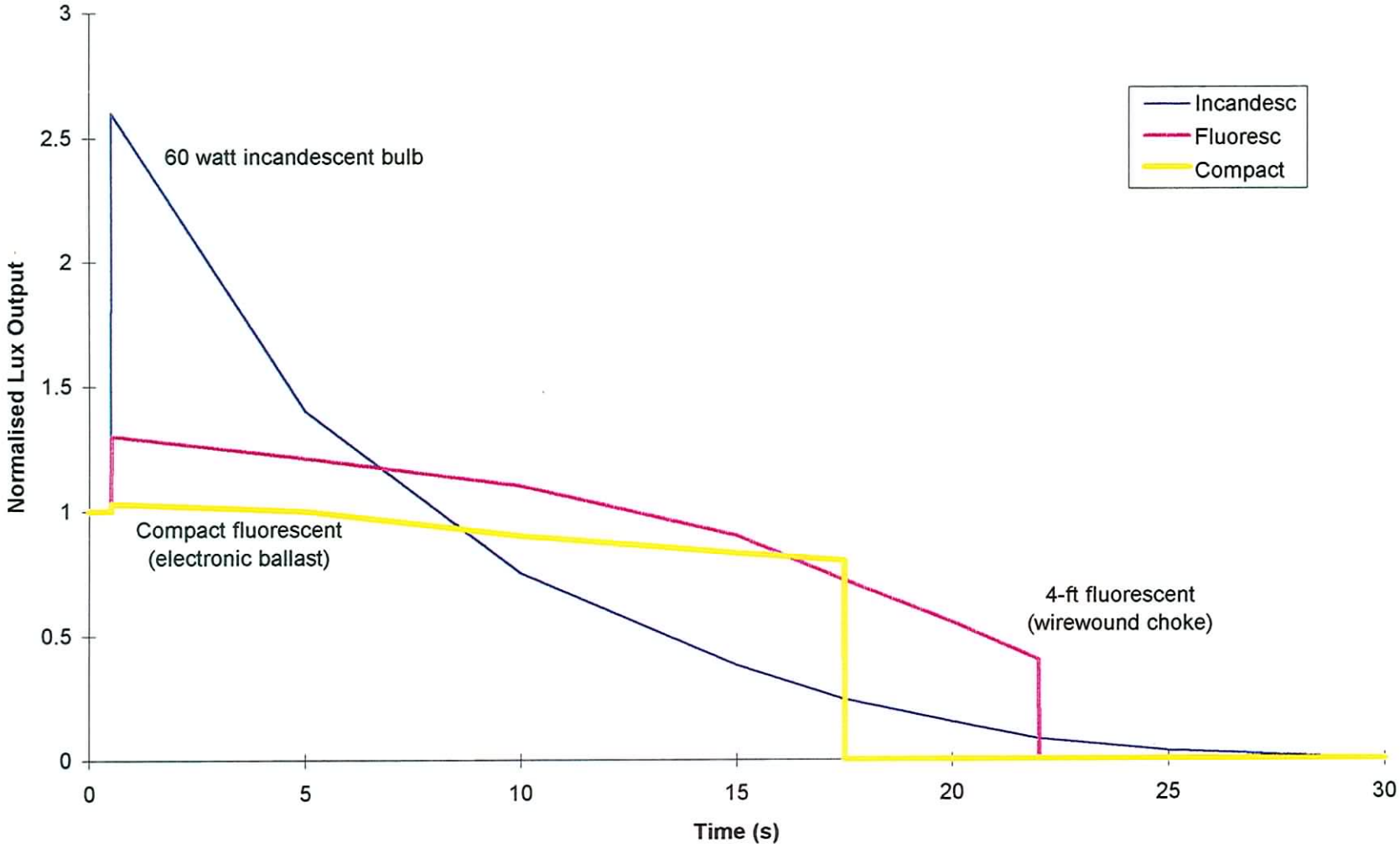

unsuitability of this source is that the large voltages at switchover would draw equally large currents that might reduce the life of the bulb—a characteristic that might have a similar effect on the fluorescent tube with the wire wound choke.

4.3.6 Aerodynamics and friction considerations

Measurements were also taken of the deceleration of the flywheel under two different ambient pressures—one at atmospheric and the other at half an atmosphere (0.56 atmospheres to be exact--further reductions were not possible with the chamber used in the present experimental programme because of doubts about the integrity of vessel for larger pressure differentials.) With the measurements, it was possible to create a simple model of aerodynamic drag and friction on the flywheel by assuming that aerodynamic drag was proportional to the square of rotation speed and friction was constant over the speed range i.e.

$$T_{drag} = k_1.\omega^2 \qquad \text{and} \qquad T_{fric} = k_2$$

It is possible to get accurate estimates for both constants k_1 and k_2 by creating curves that fit both sets of measurements best (Figure 4.14). And with the values for these constants, it is then possible to predict the effects of changes in flywheel size and dimensions, and the effects of different vaccuum pressures. This information can then be used to size flywheels for different installations (See Appendix D).

Figure 4.14 Measured and Simulated Deceleration Rates at pressures of one atmosphere and of half an atmosphere

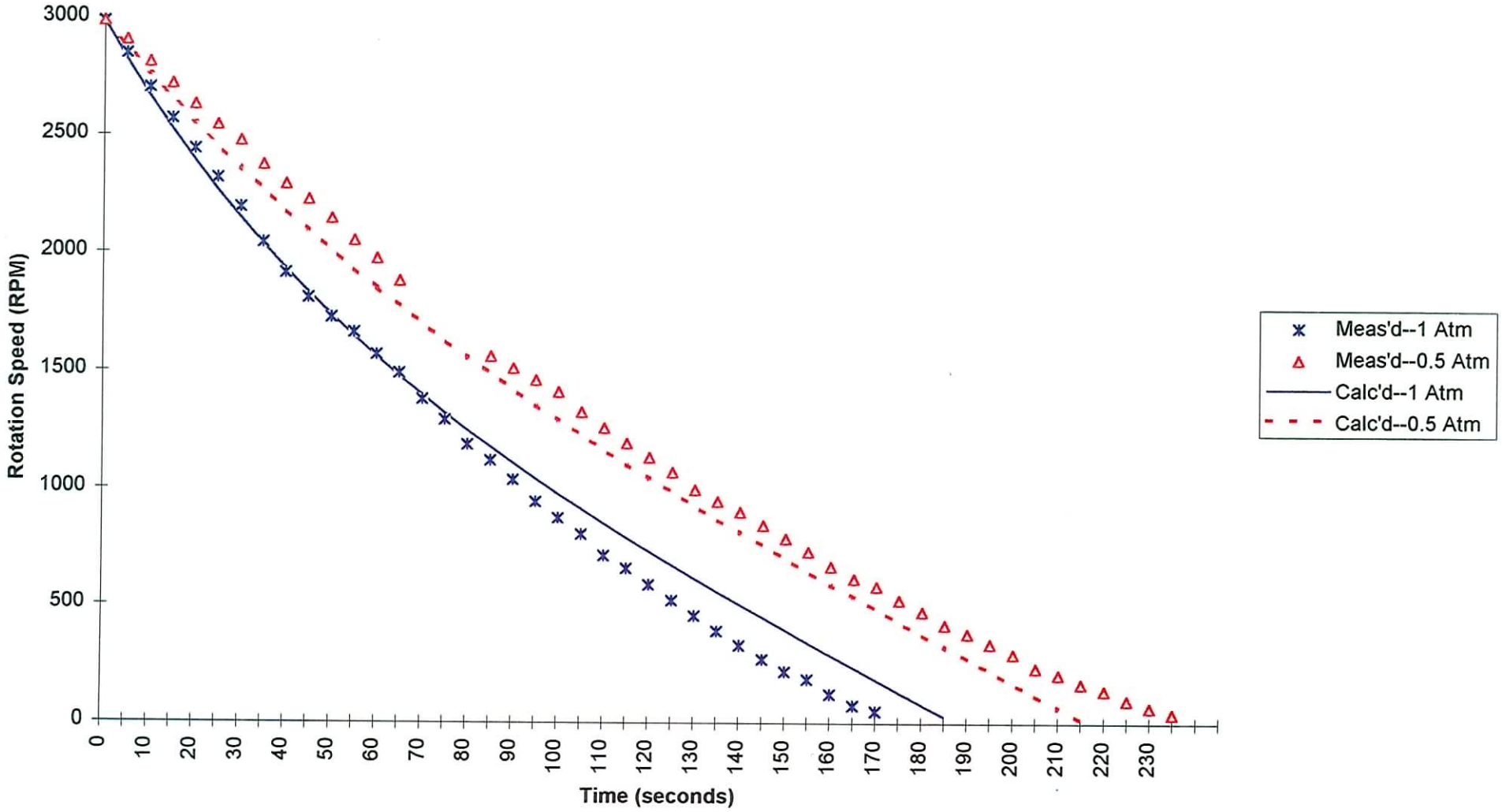

CHAPTER 5

CONCLUSION

5.1 Introduction

This thesis was designed to review the present state of the EMB sector and likely future developments within this sector. The thesis also focused on 2 particular EMB devices, both of which are still at the development stage. The first was a high-specification high-speed rim-supported ring flywheel that would be suitable for use as an energy store in small and large power systems. The second was a relatively low-specification steel flywheel connected to an induction machine, which was capable of operating in a self-excited mode to power a critical electrical load. The outlook for both of these EMBs is described in this chapter.

5.2 The rim-supported EMB

The availability of a rim-supported EMB capable of storing large quantities of energy could obviate the need for spinning reserve on power systems, smooth the fluctuations in power system energy demand and reduce the need for transmission system reinforcement. Although previous efforts to develop such an EMB have largely proved unsuccessful, the thesis developed novel ideas for the application of recently developed high-temperature superconductors to both levitation and energy-conversion and sought to apply these to a rim-supported EMB. As a first step towards the ultimate goal of developing such an EMB for use in power systems, it was proposed that efforts

should be made to develop smaller EMBs that would allow the commercial sector avail of cheap night electricity. Unfortunately though, high-temperature superconductors were found to be a long way from easy and economic application--particularly for this project's purposes.

These superconductor difficulties were compounded by the low stiffness of such superconducting bearings. In addition, an examination of the economics of night storage revealed the unfavourable economics of night storage and resulted in the postponement of further development of this particular rim-supported EMB. It is concluded that the commercial application of such EMBs are some years away and even the development of a practical prototype will depend on big advances being made in the development of superconductor technology.

5.3 The shaft-supported EMB

The shaft-supported EMB idea is closer to commercial development. In its simplest form, this EMB consists of the following off-the-shelf components: an induction motor, flywheel, capacitors, and associated mechanical and electrical components. The low-cost and rugged induction motor was, for the first time to our knowledge, going to be used in its self-excited mode to transfer kinetic energy from a flywheel to power an electrical load. This electrical load would, therefore, have to be able to withstand significant changes in both voltage and frequency, although the voltage-to-frequency ratio would be nearly constant over the operating range. Nevertheless, this EMB was shown to be reasonably compatible with the most common

light sources in a laboratory experiment. Several other advances were also made for this EMB:

(1) A model to simulate the operation of the EMB was developed,

(2) Model results were shown to compare favourably with the model results of Salama and Holmes[36]. The model results also compared well with experimental results.

(3) Guidelines on applying this EMB were drafted and these are included in Appendix D.

Suitable applications for this EMB include critical loads that require standby power in order to avoid the adverse consequences of the loss of mains voltage. The standby power provided by the EMB could then be used either to bring a process to a controlled and safe stop or to allow a second, slower-responding power source to come on-line. Typical applications might include:

(1) Uninterruptible power supplies for computers

(2) Emergency lighting supplies for offices, factories etc.

(3) Manufacturing processes that require controlled stops because sudden power losses could, for example, cause processed material to get stuck in machines with undesirable consequences

(4) Standby power supplies where it is required to provide power for several seconds until a diesel engine comes on line. New, high-efficiency induction generators could prove very suitable to this task and, indeed, to other diesel-generator systems.

(5) Pulse power supplies. This is not a standby power application, but is a particular power supply occasionally required by industry, researcher and the military to provide widely spaced, but large pulses of power to different applications. The EMB has often been used to service these applications, and the proposed EMB might do so at a lower cost.

The exact implementation of the EMB would depend on the application. Ideally, the simple shaft-supported EMB illustrated in Figure 3.9 would be sufficient for most applications. In some cases though, this simple configuration may require some alteration. There are 2 likely reasons for this: the maximum break in power that the load can tolerate is exceeded, and the required duration of the energy delivery is too long. For loads that can tolerate no break or a very short break, it would be necessary to connect a second induction motor to the shaft--an arrangement that is briefly discussed in the next section (Section 5.3.1). For loads where the duration of flywheel energy delivery is of the order of hours rather than minutes, the system might be described as a medium-term system, and the special requirements of such implementations are discussed in Section 5.3.2.

5.3.1 No-break implementations

With this approach (Figure 5.1), the system is connected in line and power flows through both induction motors before reaching the load. A diesel engine could also be coupled to the shaft via a clutch to provide power after the flywheel deceleration. This would provide isolation to the load in almost the same way as the synchronous-

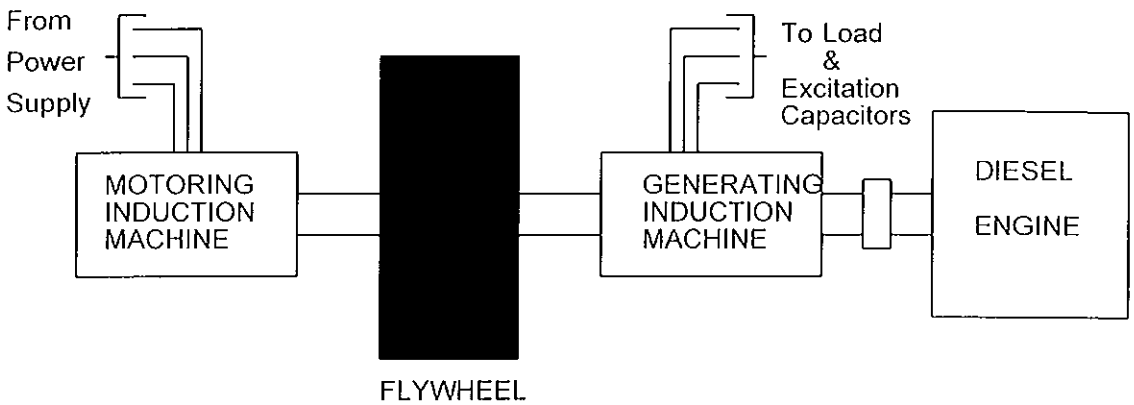

Figure 5.1 No-break short-term system

generator no-break systems do (Figures 3.2 and 2.4), but with some differences (e.g. clocks that derive their references from the mains frequency would be slow etc.)

To simulate the effect of the new induction machine, the model described in Appendix E would have to be slightly modified to include the effects of slip in the machine connected to the mains, but that should not be a difficult exercise if the torque-speed curve of this machine were available. It should also be noted that, with this particular double-induction-machine system, it may also be possible to connect both induction machines to the mains during startup to reduce the winding temperature rise.

5.3.2 Medium-term Standby EMBs

Another common application that would require alterations to be made to the simple short-term EMB is that of emergency lighting. Two particular difficulties arise:

(I) Emergency lighting systems might typically be required to provide power to lights for up to 3 hours (see British Standard on Emergency Lighting System--BS5266: Part 1: 1988), and the power-to-energy ratio is

quite low. This would make the simple EMB unsuitable because of its high parasitic losses, namely, aerodynamic drag, core and winding losses and friction.

(II) The low power-to-energy ratio means that a small induction motor is having to start a large flywheel. However, because induction motors incur high losses during starting, manufacturers place a limit on the size of flywheel connected so as to minimise starting time. The flywheel required for an emergency lighting power supply would exceed this limit many times.

These difficulties can be overcome in the following way. First of all, the motor and flywheel could be enclosed in a partial vacuum to eliminate aerodynamic losses (some derating of motor may be required to avoid rotor overheating and special lubricant may be required for the bearings--depending on the air pressure), a high-efficiency motor could be used to minimise losses (these motors will soon become compulsory in the U.S. to reduce that nation's energy consumption) and low-loss bearings could be used. Then, a timer relay could be installed to open the motor contactor periodically during the start-up sequence to allow the motor to cool before its next acceleration run. (The present research work did not manage to verify the full extent of aerodynamic losses as the minimum operating pressure was only half an atmosphere, but there is no reason to believe that the inclusion of low-loss bearings and the use of low air pressures should give a highly effective and low-cost emergency-lighting power supply.)

5.4 Conclusions

The rim-supported EMB will require substantial improvements to be made in superconductor technology before a successful prototype could be developed. In contrast, the shaft-supported EMB has several short-term applications and, indeed, could replace battery or synchronous generator systems in many uninterruptible power supply applications. Much development work is still outstanding though, including

- The evaluation of the robustness of various loads to voltage and frequency changes (Light sources were shown to be very resilient to these changes)

- The examination of voltage collapse during changeover to the standby system (the contactor with overload would take ~300 ms to open) and during a short circuit

- The upgrading and validation of the software to cater for different loads, including nonlinear ones, and for the no-break system

- The development of a contactor control algorithm and implementation to ensure the motor does not overheat during start up

REFERENCES

1 Jensen, J; Sorenson, B; "Fundamentals of Energy Storage," published by Wiley-Interscience (1984)

2 Boyle, G.; "Renewable Energy: Power for a Sustainable Future," published by Oxford University Press (1996)

3 Genta, G.; "Kinetic Energy Storage," Published by Butterworth (1981)

4 Post, R.F.; Post, S.F.; "Flywheels," *Scientific American*, December 1973, Vol. 229, No. 6

5 Post, R.F.; Fowler, K.; Post, S.F.; "A High-Efficiency Electromechanical Battery", *Proceedings of the IEEE*, March 1993, Vol. 81, No. 3, pp. 462-4

6 Russell, F.M.; Chew, S.H.; "Kinetic Ring Energy Storage System;" *International Conference on Energy Storage,* Brighton , U.K., April 29-May 1, 1981; Organised by BHRA Fluid Engineering

7 Bornemann, H.J.; Sander, M.; *IEEE Transactions on Applied Superconductivity,* June 1997, Vol. 7, Iss. 2, Pt. 1, pp. 398-401

8 Bleijs, J.a.M.; Dutton, A.G.; Ruddell, A.J.; "Variable speed operation of wind turbine for power smoothing," *Wind Energy Conversion 1996. Proceedings of the 18th British Wind Energy Association Conference,* pp. 323-8

9 Takahashi, O.; Sato, K; Goto, K; Shirasaki, T.; Sanekata, J.; Amano, M.; Endo, M.; "Stabilization of a large-capacity and long-distance transmission system by an adjustable speed flywheel generator," *Transactions of the Institute of Electrical Engineers of Japan,* July 1997, Part B, Vol. 117-B, Iss. 7, pp. 930-7

10 Acarnley, P.P.; Mecrow, B.C.; Burdess, J.S.; Fawcett, J.N.; Kelly, J.G.; Dickinson, P.G.; IEEE Transactions on Industry Applications, Nov-Dec 1996, Vol. 32, Iss. 6, pp. 1402-8

11 Bishop, K.; "UPS: short-term or diesel," *Electrotechnology*, Oct/Nov 1992, pp. 30-2

12 Platts, J; St. Aubyn, J; "Uninterruptible Power Supplies," Published by Peter Peregrinus (1992)

13 Post, R.F.; Bender, D.A.; Merrit, B.T.; "Electromechanical Battery Program at the Lawrence Livermore National Laboratory;" *Proceedings of the 29th IECEC*, Livermore, California, 1994, Vol. 4, pp. 1367+

14 Horner, R.E.; Proud, N.J.; "The key factors in the design and construction of advanced flywheel energy storage sytems and their application to improve telecommunication power back-up," *INTELEC. Eighteenth International Telecommunications Energy Conference*, 1996, pp. 668-75.

15 Kusko, A.; Fairfax, S.; "Survey of rotary uninterruptible power supplies," *INTELEC. Eighteenth International Telecommunications Energy Conference*, 1996, pp. 416-19

16 Hockney, R.L.; LeBlanc, P.L.; "Powering of remote node locations using flywheel energy storage," *INTELEC. Eighteenth International Telecommunications Energy Conference*, 1996, pp.662-7

17 Rose, M.F; "Space power technology," *Conference Record of the 1996 Twenty-Second International Power Modulator Symposium*, pp.9-14

18 Rutberg, P.G.; Kasharskiy, E.G.; Platonova, M.Yu.; Hutoretskiy, G.M.; "Choice of the technical decision in the process of power supply source design on the basis of synchronous flywheel generator," *Digest of Technical Papers, Tenth IEEE Internation Pulsed Power Conference*, 1995, Vol.2, pp. 1309-12.

19 Luongo C.A., "Superconducting Storage Systems: An Overview," *IEEE Transactions on Magnetics*, Vol.32, No. 4, July 1996, pp. 2214+

20 Hull, J.R.; "Flywheels on a roll," *IEEE Spectrum*, July 1997, Vol. 34, Iss. 7, pp. 20-5

21 Jayawant, B.V.; "Electromagnetic Levitation and Suspension Techniques," Published by Edward Arnold (1981)

22 Laithwaite, E.R.; "Magnetic or electromagnetic? The great divide," *Electronics and Power*, 9 August, 1973

23 Laithwaite, E.R.; "Electromagnetic Levitation," *Proceedings of the IEE*, Vol. 112, No. 112, December 1965

24 Ter-Gazarian, A.; "Energy Storage for Power Systems " Published by Peter Peregrinus on behalf of the IEE; Copyright 1993

25 Oman, Henry; "Batteries vs Alternatives for storing energy"; *IEEE AES Systems Magazine*, August 1996

26 Russell, F.M.; Private Communication, 13 April 1996

27 Nagaya et al; "Fundamental Study on high Tc superconducting magnetic bearings for flywheel systems;" *IEEE Transactions on Applied Superconductivity*, Vol. 5, Iss. 2, Pt. 1, pp. 643-9, June 1995

28 Sperling, D.; "The case for Electric Vehicles," *Scientific American*, vol. 275, November 1996, pp. 36-41

29 Ashley, S.; "Designing safer flywheels," *Mechanical Engineering*, Vol 118, November 1996, pp.88-91

30 News and Notes; "Cheaper composite flywheels, *Mechanical Engineering*, Vol. 118, June 1996, pp.10

31 Fowler, D.;"Spin-off saves on car costs," The Engineer, Volume 283, 5 September 1996, pp. 22

32 Adams, W.A.; "Exploratory research and development of batteries and supercapacitors for electric/hybrid applications," Proceedings of the Symposium on Exploratory Research and Development of Batteries for Electric and Hybrid Vehicles, 1996, pp. 1-15.

33 Hull et al; "Low rotational drag in high-temperature superconducting bearings;" *IEEE Transactions on Applied Superconductivity*, Vol. 5, Iss. 2, Pt. 1, pp. 626-9, June 1995

34 Babb, M.; "Premium-efficiency motors promise to save billions," Control Engineering, Vol. 42, pp. 59-60+, May 1995

35 Singh, S.P.; Singh, B.; Jain, M.P.; "Comparative study of the performance of a commercially designed induction generator with induction motors operating as self excited induction generators," *IEE Proceedings* Part C, Vol. 140, No. 5, September 1993

36 Salama, M.H.; Holmes, P.G.; "Transient and steady-state load performance of a stand-alone self-excited induction generator," *IEE Proceeding on Electrical Power Applications*, Volume 143, Number 1, January 1996

37 Baldazo, R. et al; "Sudden Darkness," *Byte Magazine*, November 1995, pp 227-31

38 ABB Catalogue for totally enclosed squirrel cage induction motors; Cat no. B10-2003E; Sizes 63 to 250 (0.18-55kW)

39 Fitzgerald, AE. et al; "Electric Machinery," Published by McGraw-Hill (1990)

40 Technical Briefs; "Composite flywheel rotors for hybrid EVs," *Automotive Engineering*, October 1995, pp.25+

41 "Electricity Prices ...Non-Domestic for Supplies at Low Voltage," a brochure issued by ESB Customer Supply & Marketing, April 1996

42 "Electricity Prices ...Non-Domestic for Supplies at Medium and High Voltage," a brochure issued by ESB Customer Supply & Marketing, April 1996

43 Weh, H; Wrede, C.; Steingrover, A.; Mosebach, H.; Meins, J; "Magnetically levitated flywheel energy storage system with an integrated energy converter," ICEM96 Proceedings. International Conference on Electrical Machines, 1996 pp. 331-5, vol. 3

44 Ball, N.E.; "No Spokes, No Hub, No Axle, No Bearings - The Rim as the Energy Storage Flywheel;" IECEC-93. Proceedings of the 28th Intersociety Energy Conversion Engineering Conference, August 1993, pp. 223-8, vol.2

45 Darrelman, H.; "Alternative power storages," *Telescon 97. Second International Telecommunications Energy Special Conference*, 1997, pp. 33-40

46 Ogata, T.; Takahashi, T; Shimada, R. "New Concept Flywheel - Ring Flywheel Generator;" *PCC*, Yokohama, Japan 1993, pp. 587-592

47 Schlieben, E.W.; "System Aspects of Energy Wheels;" *Proceedings of the 1975 Flywheel Technology Symposium*, Lawrence Hall of Science, Berkeley, California, Nov 10-12, 1975

48 Ashley, S.:"Flywheels put a new spin on electric vehicles," *Mechanical Engineering,* October 1993

49 Aaland, K.; Lane, J; "Ideas and Experiments in Magnetic Interfacing;" *Proceedings of the 1975 Flywheel Technology Symposium,* Lawrence Hall of Science, Berkeley, California, Nov 10-12, 1975

50 Hampton, D.E.; Tindall, C.E.; McArdle, J.M.;"Emergency Control of Power System Frequency using Flywheel Energy Injection," *IEE International Conference on Advances in Power System Control, Operation and Management*, Nov 1991, Hong Kong

51 Di Napoli, A.; Caricchi, F.; Crescimbini, F.; "Ultracapacitor based bidirectional DC-DC converter prototype for recovery of the braking energy in EV motor drives," *EPE '95. 6th European Conference on Power Electronics and Applications,* 1995, Vol. 2, pp. 141-6

52 Dettmer, R; "Spinning Reserve," *IEE Review*, January 1997, pp. 36-37

53 Anon; "Flywheels are back," *Compressed Air Magazine*, June 1993, pp 16-21

54 News Trends; "Better Batteries may make Electric Cars a Success," *Machine Design,* August 22, 1996

55 Howe, D.; Mellor, P.H.; Peel, D.J.; "High-Speed Electromechanical Storage Systems for Electric Vehicles," *Stockholm Power Technology Conference,* June 18-22, 1995

56 Hogan, Brian J., "Flywheel design challenges batteries," *Design News*, 8 November 1997, pp. 89+

57 Kenward, M.; "High-Temperature Superconductors set to transform industry," *Physics World,* June 1996.

58 Kreyszig, E.; "Advanced Mathematics for Engineers;" Published by Wiley

59 Kusko, A.; Fairfax, S.; "Survery of Rotary Uninterruptible Power Supplies;" *INTELEC. Eighteenth International Telecommunications Energy Conference,* October 1996, pp. 416-19

60 Anon.; "High Efficiency Motors", *IEE News*, 4 December 1997, pp. 10

Appendix A

SOME SIMPLE ENERGY STORAGE CONSIDERATIONS FOR A RIM-SUPPORTED ELECTROMECHANICAL BATTERY

The rim-supported electromechanical battery consists of a rim flywheel that rotates at high speed and, when accelerating and decelerating, respectively imports and exports electrical energy. If the rim or annulus is such that most of its mass (m) is concentrated at the point of maximum radius (r), the energy (E) stored at a rotation speed of w is approximately $^1/_2 . m . r^2 . w^2$ ($= {}^1/_2 . m . v^2$), and the energy stored per unit mass (E/m) is approximately $^1/_2 . r^2 . w^2$. The corresponding tensile stress (S) in the annulus, which is has a density ρ , due to the centrifugal force can easily be shown to be $\rho . r^2 . w^2$. This means that

$$E/m = S/2.\rho$$

and the maximum energy per unit mass of the annulus is limited by the maximum tensile stress per unit density of the annulus material:

$$\left[E/m\right]_{max} = S_{max}/2.\rho$$

Fibre composite materials that feature maximum tensile stresses higher than that of steel, but with much lower densities, are therefore the obvious choice of material for this type of rotational energy storage system.

[Graphite fibre example: $\left\{ S_{max} / 2.\rho \right\}$ for graphite fiber could be as high as 2.0 x 10^6 J/kg [3], which is over 500 Whr/kg.]

In practice, it would not be possible to reach the maximum energy storage density because of build imperfections, the inclusion of other materials in the annulus (eg. the matrix for the fibers), the finite rotor thickness, uneven weight support, acceleration/deceleration tensions and fatigue effects. Accordingly, a contingency (α) called the safety factor is included in the equation for energy stored per unit mass:

$$\left[E/m \right]_{max} = \alpha . S_{max} / 2.\rho$$

[Graphite example: If α is close to 0.5, (See [4]) the maximum energy storage per unit mass is about 250 Whr/kg ($\cong 10^6$ J/kg), which would not include the mass of the supporting/protecting structure, which could be substantial.]

Knowing energy storage per unit mass, it is possible to determine the peripheral speed because, as already noted, $E = {}^1/_2 . m . v^2$:

$$\Rightarrow \qquad v = \sqrt{\frac{2E}{m}} = \sqrt{\frac{S}{\rho}}$$

and $$v_{max} = \sqrt{2.\left[\frac{E}{m}\right]_{max}} = \sqrt{\frac{S_{max}}{\rho}}$$

And the radial thrust caused by any mass imbalance (m_i) in the annulus is $m_i . v^2/_r$, which can also be written as $2.\frac{E}{m}.\frac{m_i}{r} = \frac{S}{\rho}.\frac{m_i}{r}$

.

[Graphite example: From these equation we can obtain the maximum safe peripheral speed for graphite fibre composite (= 1.4 x 10^3 m/s) and the radial thrust at maximum speed (=2.0 x 10^6 . m_i/r).]

And knowing that v = r.ω, allows one to determine the maximum safe radius of the flywheel when the maximum rotation speed is known, i.e.

$$r = \frac{1}{\omega}.\sqrt{\frac{2.E}{m}} = \frac{1}{\omega}.\sqrt{\frac{S}{\rho}}$$

and

$$r_{max} = \frac{1}{\omega_{max}}.\sqrt{2.\left[E/m\right]_{max}} = \frac{1}{\omega_{max}}.\sqrt{\frac{\alpha.S_{max}}{\rho}}$$

• • • •

Although the above expressions have been derived for a rim flywheel, these expressions can be generalised to differently shaped flywheels by including a constant K, called the shape factor, into the expression for energy storage per unit mass (and any derivatives of that expression):

$$E/m = \frac{K.S}{\rho}$$

$$\left[E/m\right]_{max} = \frac{\alpha.K.S_{max}}{\rho}$$

Obviously, K for a rim flywheel is 0.5 while it is about 0.6 for a flat-disk flywheel.

This means that for a flat-disk flywheel made out of maraging steel (See Table 2.1), the maximum energy storage per unit mass is, assuming a safety factor of 0.5, about one tenth that of graphite fibre or 25 Wh/kg. Other generalised equations become:

$$v_{\max} = \sqrt{2.\left[\frac{E}{m}\right]_{\max}} = \sqrt{\frac{2.K.S_{\max}}{\rho}}$$

$$r_{\max} = \frac{1}{\omega_{\max}} \cdot \sqrt{2.\left[E/m\right]_{\max}} = \frac{1}{\omega_{\max}} \cdot \sqrt{\frac{2.K.\alpha.S_{\max}}{\rho}}$$

If the flywheel is connected to the mains so that the mains frequency is some multiple p times the rotation speed, it is possible to calculate the maximum safe radius:

$$r_{\max} = \frac{p}{\omega_{mains}} \cdot \sqrt{2.\left[E/m\right]_{\max}} = \frac{p}{\omega_{mains}} \cdot \sqrt{\frac{2.K.\alpha.S_{\max}}{\rho}}$$

For example, the maraging steel disk will have a maximum radius given by:

$$r_{\max} = 1.4 \times p$$

This means that the minimum radius to obtain the maximum utilisation of the maraging steel while operating with a 50 percent safety margin is 1.4 metres, and this is valid only when $p = 1$ and the flywheel is rotating at 3,000 RPM or 314 r/s.

Appendix B

SIMULATION OF THE MAGNETIC FIELDS CREATED BY BALANCED MULTIPHASE CONDUCTORS IN AN IRONLESS ELECTRICAL MACHINE

B.1 Introduction

Up until recently, ironless electrical machines driven by power frequency currents would never have been contemplated because of the large conductor sizes demanded by the high magnetising currents, because of the suitability of iron both to the task of coupling the torque developed by the rotor to a mechanical load/prime mover and to the task of supporting the stationary windings, and because of the transposition of forces created by the mechanically weak current-carrying conductors on to the stronger iron structures. Now, however, the development of high-temperature superconductors has still prompted much research into the development of ironless machines. The reason is, of course, the low losses and the corresponding high efficiencies of superconductor-based machines. The main problems with superconductor-based electrical machines are the high costs and the unsuitability of most superconducting material to the high stresses caused by the high current densities. If these problems can be overcome, superconductors may become commonplace in electrical machines, particularly in machines where superconductors are already being used as magnetic bearings for the rotor. A good example of such a machine is the electromechanical battery (EMB)--a flywheel energy storage system with electrical inputs and outputs. Indeed, the rim-supported EMB, the main component of which is a rim flywheel (See Section 2.1 in main text), with its huge surface area, may even allow for the traditional copper conductors--depending on the resulting efficiency and cost. To explore these issues more fully, efforts are here made to evaluate the fields within such hypothetical ironless machines. The ultimate aim would be to predict the various machine stresses, the power factor, the efficiency etc.

B.2 Problem and Solution

The aim is to determine and visualise the magnetic fields generated by current-carrying conductor turns that are fed from a balanced multiphase ac supply and that are arranged thinly and sinusoidally over a smooth surface in a homogeneous medium. It is assumed that the surface can be parametrically represented as: (Kreyszig[58])

$$\mathbf{r}(\theta,\phi) = x(\theta,\phi)\mathbf{i} + y(\theta,\phi)\mathbf{j} + z(\theta,\phi)\mathbf{k} \quad \text{(vectors shown in bold)}$$

and that the sum of the phase currents flowing in the turns at any point can be represented in scalar form as:

$$J(\theta,\phi,t) = n.N.I.\ F(\theta,\phi,t)$$

and in vector form as:

$$\mathbf{J(r)} = J(\theta,\phi,t)\ .\ \mathbf{r'}/|\mathbf{r'}| \quad [=J(\theta,\phi,t)\ .\ (u\mathbf{i} + v\mathbf{j} + w\mathbf{k})]$$

where N is half the number of turns per pole per phase

n is the number of phases (> 2)

I is the peak current per phase

$F(\theta,\phi,t)$ is the space/time distribution of the current

w is the supply frequency in radians/second

t is the time in seconds

$\mathbf{r'}$ is the tangent to $\mathbf{r}$ in direction of winding (Constant ϕ in example).

Located in a region of homogeneous permeability, the magnetic field (**H**) at any point **p** (li + m**j** + n**k**) can be found from the law of Biot and Savart:

$$H(\mathbf{p}) = \iint \frac{J(\mathbf{r}).\overline{pr}.|\mathbf{r}|}{4.\pi.|pr|^3}.d\theta.d\phi$$

If we write the vectors for **r**, **J(r)** and **p** in matrix form,

[ie **r** = (x y z), **J(r)** = $J(\theta,\phi,t)$.(u v w) and **pr** = (x-l y-m z-n)] this equation becomes:

$$H(l,m,n) = \frac{1}{4\pi}\iint \frac{J(\theta,\phi,t).\begin{vmatrix} i & j & k \\ u & v & w \\ x-l & y-m & z-n \end{vmatrix}.(x^2+y^2+z^2)^{1/2}}{((x-l)^2+(y-m)^2+(z-n)^2)^{3/2}}.d\theta.d\phi$$

The determinant in the above equation can also be written in matrix form as (u.(v.(z-n)-w.(y-m) v.(w.(x-l)-u.(z-n)) w.(u.(y-m)-v.(x-l))). This integral is not directly solvable for the surfaces of interest to us, but an accurate approximation should be possible by replacing the double integral with a double series and performing the associated calculations on a computer.

Example - Toroid of major radius a, minor radius b (Kreyszig[58])

$\mathbf{r}(\theta,\phi) = \underbrace{(a+b.\cos\theta).\cos\phi}_{x}\ \mathbf{i} + \underbrace{(a+b.\cos\theta).\sin\phi}_{y}\ \mathbf{j} + \underbrace{b.\sin\theta}_{z}\ \mathbf{k}$

And $\mathbf{J(r)} = J(\theta,\phi,t).(\underbrace{-\sin\theta.\cos\phi}_{u}\ \mathbf{i} + \underbrace{-\sin\theta.\sin\phi}_{v}\ \mathbf{j} + \underbrace{\cos\theta}_{w}\ \mathbf{k})$

With $J(\theta,\phi,t) = J_m.\cos(\phi - w.t)$, where $J_m = n.N.I$

So:

$$H(l,m,n) = \frac{J_m}{4\pi}\int_0^{2\pi} Cos(\phi-\omega t)\int_0^{2\pi} \frac{\begin{vmatrix} i & j & k \\ u & v & w \\ x-l & y-m & z-n \end{vmatrix}.(x^2+y^2+z^2)^{1/2}}{((x-l)^2+(y-m)^2+(z-n)^2)^{3/2}}.d\theta.d\phi$$

(A typical computer program to solve this equation is given at the end of this appendix.)

If this approach is used to find the field at every point, it should then be possible to find the flux density (B) in this homogeneous system and, from the flux density, it is possible to find both the flux and the flux linked by any winding of cross-sectional area A in the region:

$$\psi = \sum N.Cos\phi.(\sum_{A(\phi)} B.\Delta A).\Delta\phi)$$

Knowing the flux linkages of the windings, it is possible to calculate the low-frequency equivalent circuit of the system. This equivalent circuit could serve as a model for use in the design of prototypes.

B.3 Some Final Comments

The above approach presently utilises some simplifying assumptions, namely, that currents are sinusoidal and that the winding distributions are sinusoidal and infinitely thin. If those assumptions do not hold accurately enough for the physical realisation, it should be possible to extend the simulation to include for current and winding harmonics. It may also be desirable to extend the simulation so as to be able to include iron in either the stator or the rotor or indeed both, for comparison as well as evaluation purposes. Unfortunately, the computer program to implement the above equations was not realised during the course of the thesis. The equations and the sample program structure below may, however, be of use in the future.

B.4 Structure of program to compute the magnetic field (H) in and around a toroid

INTERACTIVELY INPUT N, n, I_{rms}, frequency (f), and toroid radii a,b

PRODUCE TOROID PLOT IF REQUIRED

FIND w (= 2 x Pi x f), I (= 1.414 x I_{rms}), AND $J_m = n.N.I$

PRODUCE A COLOUR PLOT OF CURRENT DENSITY VARIATION WITH TIME IF REQUIRED. USE THE ABOVE EQUATION FOR **J**(**r**) AND A TIME LOOP (SIMILAR TO ONE FOR COMPUTING FIELD BELOW).

Compute the field in the region as follows:

CONSTANT1 = $J_m/(4.Pi)$

FOR t = 0 TO AN INTERRUPTION IN STEPS OF 0.001

FOR l = [-2(a+b), 2(a+b)]; FOR m = [-2(a+b), 2(a+b)]; FOR n = [-2b,2b]

FOR ϕ = 0 TO 2.Pi IN STEPS OF 0.1 RADIANS

CONSTANT2 = Cos (ϕ - w.t)

FOR θ = 0 TO 2.Pi IN STEPS OF 0.1 RADIANS

CONSTANT3 (a 3-D vector)= CONSTANT3 + 3-D VECTOR GIVEN BY VALUE OF INNER SUMMATION IN H EQN

θ LOOP

CONSTANT4 (a 3-D vector)= CONSTANT4 + CONSTANT3.CONSTANT2

CONSTANT3 = 0

ϕ LOOP

H(l m n) = CONSTANT4

CONSTANT4 = 0

l, m AND n LOOPS

PLOT H(l m n) IN A 2-D PLANE

PAUSE (ONLY IF SPEED TOO FAST)

t LOOP

****

APPENDIX C

THE ECONOMICS OF VARIOUS TARIFFS AND OF NIGHT ENERGY STORAGE TECHNOLOGIES FOR NON-DOMESTIC ESB CUSTOMERS

C.1 Introduction

This appendix looks at the economics of energy storage for non-domestic users of electricity. Finding a niche for flywheel energy storage among this group would provide an ideal stepping stone towards the ultimate goal of using huge flywheels in utility power systems for the purposes of load levelling and spinning reserve.

C. 2 Background

In an effort to encourage consumers to use more electricity at night, electric utilities usually provide night electricity at highly discounted rates. To avail of these rates, consumers can presently either install night storage heaters or night refrigeration storage systems, or initiate night shift work. In many organisations, however, neither of those approaches are suitable or desirable, and electricity is paid for at the full premium. Soon, however, it may be possible to use highly efficient and reasonably priced temporary stores of electrical energy, in the form of electrochemical or electromechanical batteries, to buy the cheap night electricity and store it until it is required during the day. The economics of this process are examined below with respect to connections to the Irish Electricity Supply Board (ESB) power system. First, though, a brief description of the relevant electricity charges or tariffs.

C.3 Non-domestic ESB Tariffs

For the purpose of tariffs, the ESB divides its non-domestic customers into two basic groups: those with a low-voltage connection to the grid (Section C.3.1 below) and those with a medium- or high-voltage connection (Section C.3.2 below)

C.3.1 Low-voltage customers[41]

These customers have a number of tariffs to choose from:

The General Purpose Tariff--this tariff consists of a small standing charge, a charge for each kWh of energy used up to a certain level, and a lesser charge for each kWh used above that level. Night storage heating is charged separately and at a much lower rate. As with all of tariffs discussed here, there is also a Lower Power Factor Surcharge which "can generally be avoided by installing power-factor correction capacitors. "

The General Purpose Nightsaver Tariff--this is similar to the previous tariff, but allows more flexible use of the very low-cost night electricity.

The Flat Rates of Charge Tariff--again a similar tariff, but with separate charges for off-peak usage of electricity as well as for night storage heating. This tariff is restricted to existing users.

The Maximum Demand Tariff (described in more detail below)--this tariff seeks to encourage users to eliminate any daytime peaks in their electricity load by

introducing a charge for the maximum power demanded during the daytime.

C.3.2 Medium- and high-voltage customers[42]

Customers in this group do not have a choice of tariff--the Maximum Demand Tariff is compulsory. This tariff has 4 components: (1) ***Demand Charges***, which are based on the customer's maximum demand and are graded according to the season, the level of demand and the supply voltage; (2) ***Service Capacity Charges***, which are dependent on the customer's supply capacity/maximum demand and are also graded; (3) ***kWh Charges***, which are energy charges and are dependent on the level of energy used, the season, the supply voltage and, most importantly from our viewpoint, the time of use during the day/night; (4)***Lower Power Factor Surcharge***---self-explanatory--Install appropriate power-factor correction capacitors.

C.4 Economic incentives for night energy storage

Using the charge structures described in the relevant ESB literature[41,42], a spreadsheet was organised to compute the savings that are typically possible for both General Purpose-type tariffs and average Maximum Demand tariffs through the application of energy storage technologies of varying efficiencies. The results are shown in the graphs of Figures C.1 and C.2.

The basic assumption underlying all of the calculations is that all the daytime electricity required is purchased during the night at reduced rates. Of course, this means that the electrical infrastructure must be able to carry the complete daytime energy

Fig C1 Energy Cost Reductions possible using Energy Stores of Varying Efficiency--General Purpose Tariff

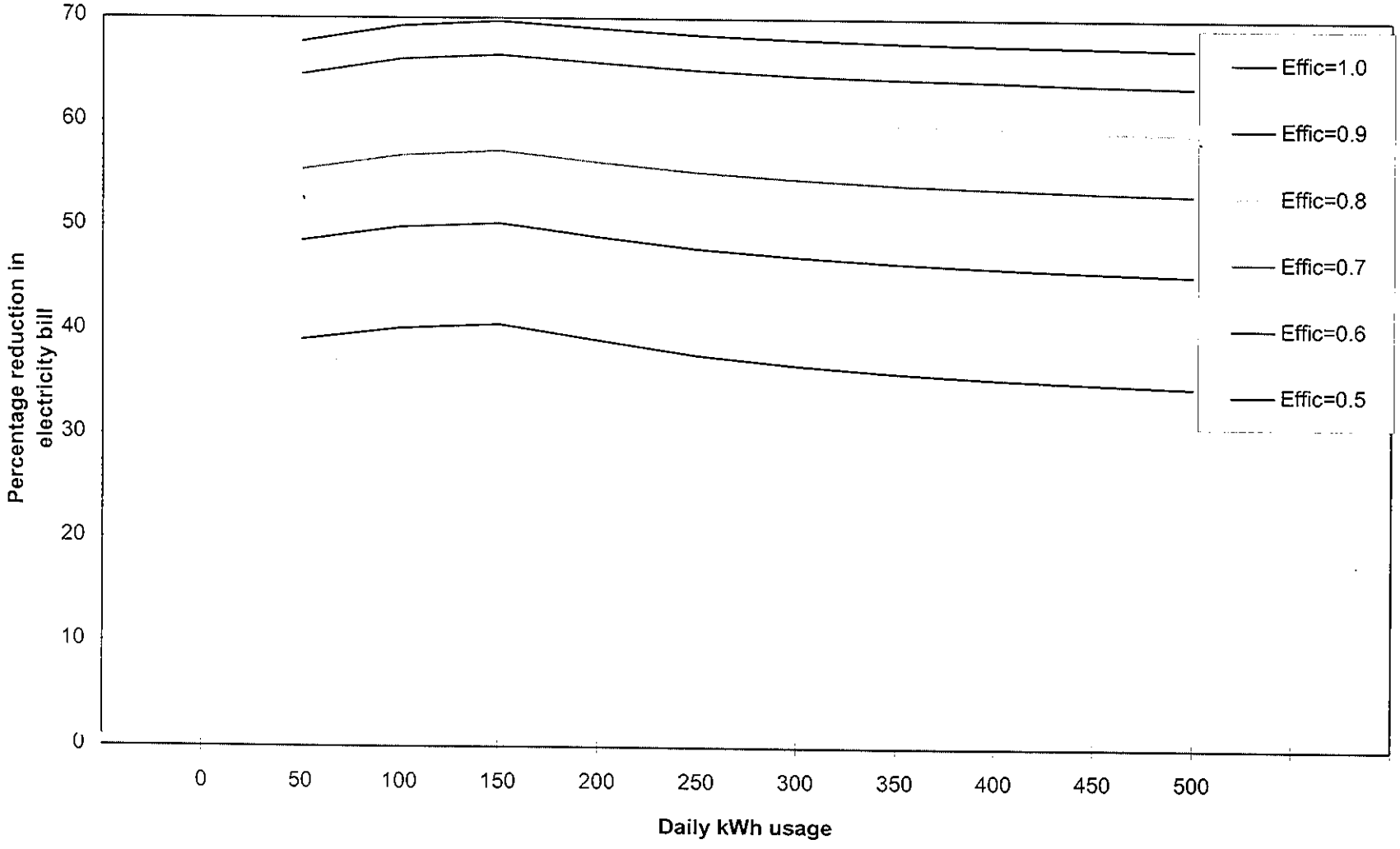

Fig C.2 Energy Cost Reductions possible using Energy Stores of Varying Efficiencies--Maximum Demand Tariff

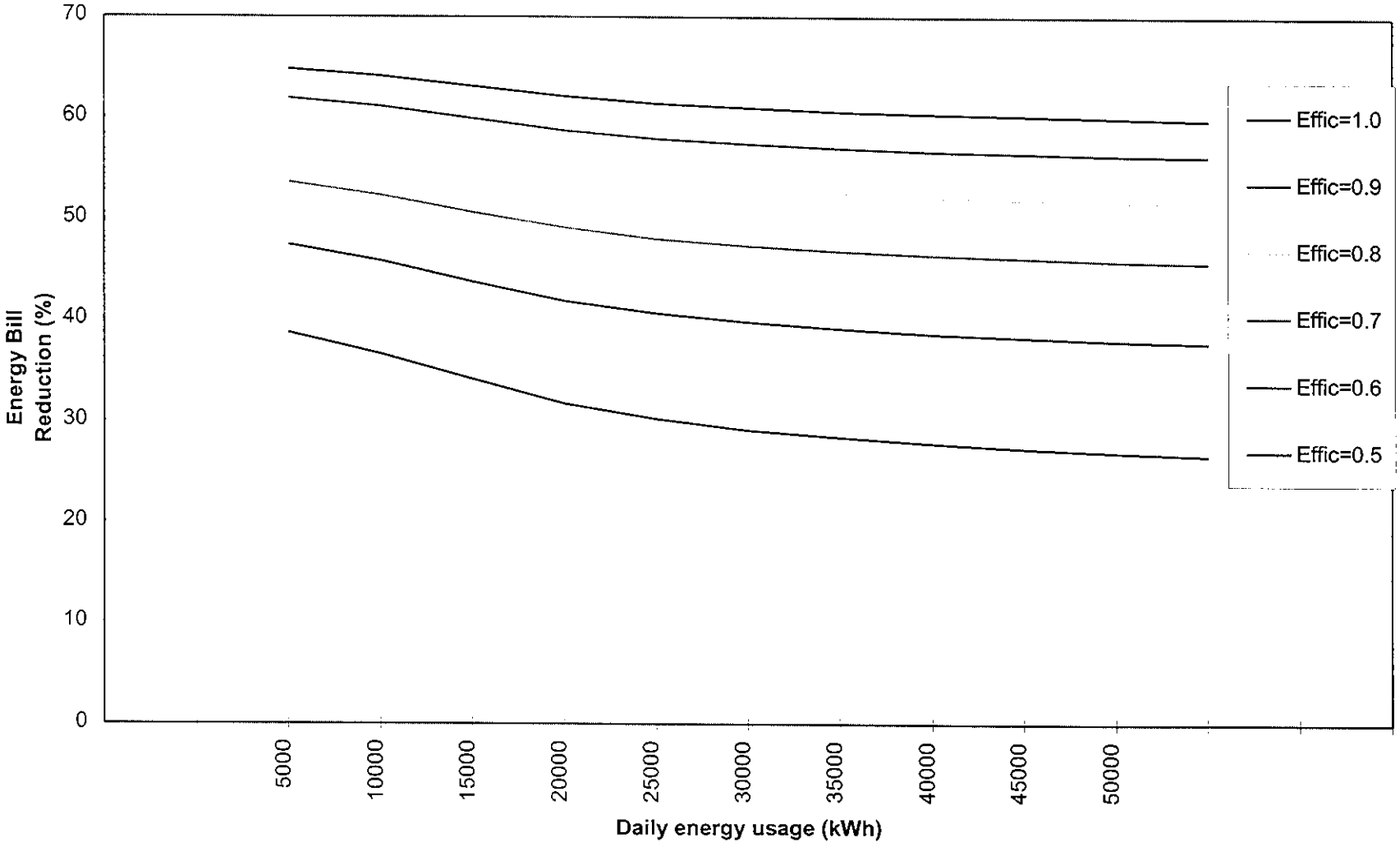

requirements, plus any night-time requirements, plus enough energy to compensate for the inefficiency of the energy store. If this is not possible, the cost evaluation process should be repeated to include infrastructural improvement costs

C.5 Viability of flywheel energy storage systems

As can be seen from the graphs, huge annual savings are possible even for storage efficiencies as low as 0.6-0.7. This is especially true in the case of General Purpose Tariffs because of the especially large difference between the cost of night and day electricity and in the case of the Maximum Demand Tariff when the average loading is low compared to the maximum demand (A loading of 0.3 is assumed in the Maximum Demand Savings Chart of Figure C.2). For both of these cases, the effective average cost of a night kWh compared to a day kWh may be above five pence. If the energy storage system is used more than 250 days in the year, the saving would be over £10 per kWh per year for a storage efficiency in excess of 80 percent. Obviously, the financial viability of a night-storing EMB will depend on the capital cost per kWh. This issue is evaluated in more detail in the main text (Section 2.4.2).

Appendix D

APPLICATION GUIDELINES FOR THE PROPOSED SHAFT-SUPPORTED EMB

D.1 Introduction

A shaft-supported EMB for use in standby applications is described in detail in the main body of text from Section 3.2 onwards. It comprises several off-the-shelf components (See Figure 3.9): a flywheel and support bearings, an induction motor with a mechanical coupling to the flywheel shaft, appropriate excitation capacitors, a circuit breaker and/or a contactor and contactor control circuitry. As well as those components, a suitable mounting arrangement would be required for the motor-flywheel assembly and an electrical panel would be needed for the circuit breaker etc. This appendix describes the specification of each of the off-shelf-components for applications in which values for all the relevant parameters in the following list are available:

Minimum Operating Frequency tolerated by the load--f_{min}

Maximum Operating Voltage tolerated by the load--V_{max}

Minimum Operating Voltage tolerated by the load--V_{min}

Minimum Operating Voltage/Frequency ratio--V/F_{min}

Minimum Operating Time of standby system--T_{min}

Lumped Parameters of motor equivalent circuit (R_1, X_1, X_m, R_c, R_2,X_2)

The minimum values of the load impedance--R_L+jX_L

D.2 Specifying the induction motor

There are several important aspects to the choice of induction motor:

- **Synchronous speed** Generally, the highest possible synchronous speed would be desirable so as to minimise both the mass and the size of the flywheel (Sec Appendix A). There is one proviso though--that aerodynamic losses, which are approximately proportional to speed cubed, are acceptable.
- **Rated voltage** The voltage of the machine will probably be determined by the supply voltage at the EMB installation point, which typically might be in the range of standard low-voltage mains supplies (i.e. 220-240 V per phase). Of course, depending on the choice of excitation capacitor (See Section D.3 below), the voltage in the self-excited mode could rise significantly above the nominal machine rating for a short time. This might not be a problem, however, if total current is not much greater than the rated current and if the wiring insulation can withstand the excess. (Consultation with the manufacturer may be in order depending on the size of the overvoltage.) Ultimately though, if the rated voltage of the machine is less than the parameter V_{max} defined in D.1, then V_{max} should then be set equal to the V_{max}.

- **Rated current** The simplest way of specifying a rated current is to divide Vmax by the minimum load. The load current should then always be less than the rated current even with an inductive load, because the voltage/frequency ratio of the machine will always be decreasing following the establishment of the self-excitation.

- **Parameters** The induction motor parameters might also be considered because of their influence in determining the self-excitation characteristics and the total efficiency of the system. Ideally, the motor would have low leakage reactances and a high efficiency.

D.3 Sizing the excitation capacitors

As explained in Chapter 4 and in Appendix E, it is possible to predict the operation of the self-excited induction generator knowing the characteristics of the electrical load, the motor and the excitation capacitance. Of course, the exact value of excitation capacitance will not be known, but various values can be tried until the value that gives an output voltage curve (similar to that shown in Figures 4.11-12) whose maximum voltage is less than V_{max} and whose minimum voltage before voltage collapse is greater than V_{min} is found. For example, if V_{max} = 265 V, V_{min} = 150 V and f_{min} = 37.5 Hz, and Figures 4.11-12 were the output characteristics for minimum load, it might be concluded that 17 microfarads would appear to be near the optimum value of capacitance, whereas 30 microfarads is unsuitable on every count.

D.4 Sizing the flywheel

The size of the flywheel effectively dictates the deceleration rate. A relationship that allows determination of a suitable flywheel can be found by considering the total deceleration as being composed of 3 different components: an aerodynamic drag deceleration (α_{aero}), a bearing friction deceleration (α_{fric}) and an electrical torque component (α_{elec}) i.e.

$$\frac{dw_m}{dt} = \alpha_{aero} + \alpha_{fric} + \alpha_{elec}$$

$$\Rightarrow \int dt = \int \frac{dw_m}{\alpha_{aero} + \alpha_{fric} + \alpha_{elec}}$$

This integral is not easily solvable even if a simple model is used for aerodynamic drag and friction (See Section 4.3.6) because the electrical torque is not a predictable function of the mechanical speed (w_m). It is possible to solve this equation, however, by replacing the integral with a series:

$$t \cong \sum \frac{\Delta w_m}{\alpha_{aero} + \alpha_{fric} + \alpha_{elec}}$$

Decelerations due to aerodynamic drag and friction can be found by measuring the deceleration curve of the system following disconnection of the electrical power (See Figure 4.14). In fact, once one set of those measurements has been taken, it may not have to be repeated for other flywheels or vacuums if a simple model constructed from the measurements were considered accurate enough for performance prediction (Section 4.3.6).

It only remains, therefore, to find the electrical deceleration. These are related to the following values of the induction machine equivalent circuit: the referred rotor current (I_2), the referred rotor resistance (R_2), the slip (s), the stator electrical frequency (w_e), the number of poles (p) and the number of phases (n) by the following equation:

$$\alpha_{elec} = \frac{n.p.I_2^2.R_2}{s.w_e.J}$$

All of the parameters required to compute the time taken for the flywheel to decelerate from synchronous speed to the de-excitation speed are now computable. (In fact, most of the values in the equation are calculated in the spreadsheet calculations shown in Section E.3, and an additional column at the end of the major calculation table would be eminently suited to the computation of α_{elec}.) The flywheel inertia should then be adjusted to ensure that the specified minimum operating time (T_{min}) is exceeded so as to allow for simulation inaccuracies and slight parameter changes with time.

D.5 Choosing the Circuit Breaker/Contactor-Contactor Controller

The simplest version of the shaft-supported standby EMB system would only require a standard circuit-breaker interface with the mains. This circuit breaker would be sized so as to be able to withstand the starting current of both the motor-flywheel and the load. In the event of a mains failure, the circuit breaker should trip quickly, leaving the EMB to power the load. Unfortunately, when the mains returns, the circuit breaker would have to be manually reset. In addition, the flywheel would have to be relatively small in order to permit start-up at a single attempt.

If the circuit breaker were to have a reclosing function, it could be controlled so as to open in the event of a power failure and to close when power returns. However, as such circuit breakers did not seem to be readily available, this function could be effected using a contactor with a motor current overload and an automatic reset. Another advantage of the latter approach is that flywheel acceleration could be controlled by opening and closing the contactor, thereby avoiding the possibility of motor overheating and allowing the installation of a bigger flywheel. It might also be possible to periodically turn the motor power to the EMB off and on to maximise

system efficiency but the savings available, especially if a high-efficiency motor were used, would probably not offset the risk of damaging the contactor and the consequent reduction in system reliability.

APPENDIX E

A MODEL FOR THE SELF-EXCITED INDUCTION GENERATOR

E.1 Introduction

As explained in Chapter 4, Salama and Holmes[36] performed a comprehensive and generalised analysis of the self-excited induction generator. That analysis is valid both for the generator in its use in a flywheel energy storage system and as well as for its most popular use, namely, as the electrical generator in autonous wind and hydro generation schemes. However, rather than duplicate the many complex equations produced by Salama and Holmes[36] to create a model for a self-excited-induction-generator-based flywheel energy storage system, it was decided to modify their approach in order to simplify the simulation process. This new approach, which is equally as accurate, is described below.

E.2 Analysis

The following analysis is based on the well-known induction machine equivalent circuit shown, which for the purposes of this analysis is best represented as four parallel impedances (Figure E.1). This circuit is similar to the circuit examined by Salama and Holmes[36], but with core losses included and with some changes in nomenclature.

Figure E.1 The lumped-parameter per-phase equivalent circuit of the three-phase self-excited induction generator reduced to parallel impedances

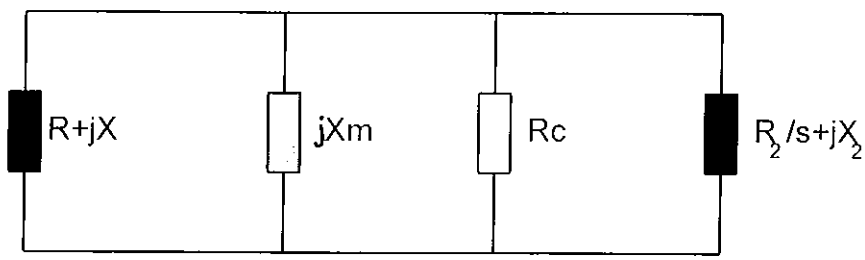

where R + jX is the combination of the following impedances:

the equivalent series load impedance (R_L+jX_L),

the excitation capacitive reactance (-jX_C)

and the stator resistance (R_1) plus leakage reactance (jX_1).

and

X_m is the machine's nonlinear magnetising reactance

R_c is core loss

R_2 is the referred rotor resistance

X_2 is the referred rotor reactance

s is the machine slip

The total primary impedance therefore, as seen from the air gap, (R + jX) is

$$R_1 + jX_1 + (-jX_C) \| (R_L + jX_L)$$

$$= R_1 + jX_1 + \frac{X_C.X_L - jX_C.R_L}{R_L + j(X_L - X_C)}$$

$$= R_1 + jX_1 + \frac{(X_C.X_L - jX_C.R_L).(R_L - j(X_L - X_C))}{R_L^2 + (X_L - X_C)^2}$$

$$= R_1 + jX_1 + \frac{X_C^2.R_L + jX_C(X_C.X_L - X_L^2 - R_L^2)}{R_L^2 + (X_L - X_C)^2}$$

$$= R_1 + \frac{X_C^2.R_L}{R_L^2 + (X_L - X_C)^2} + j\left(X_1 + \frac{X_C(X_C.X_L - X_L^2 - R_L^2)}{R_L^2 + (X_L - X_C)^2}\right)$$

$$= \quad R \quad + \quad j\,(X)$$

Now the peculiarities of the self-excited induction generator mean that the sum of the parallel admittances equals zero, a fact that can easily be seen by applying Kirchoff's current law. Hence:

$$\frac{1}{R + jX} + \frac{1}{R_C} + \frac{1}{jX_M} + \frac{1}{R_2/_S + jX_2} = 0$$

where R_2 is the referred rotor resistance, jX_2 is the referred rotor reactance and s is the slip of the mechanical rotation speed with respect to the speed of the rotating magnetic field (Mathematically defined below).

$$\Rightarrow \qquad \frac{R - jX}{R^2 + X^2} + \frac{1}{R_C} - \frac{j}{X_M} + \frac{R_2/s - jX_2}{(R_2/s)^2 + X_2^2} = 0$$

Equating real terms with real terms and imaginary with imaginary:

$$\Rightarrow \qquad \frac{R}{R^2 + X^2} + \frac{1}{R_C} + \frac{R_2/s}{(R_2/s)^2 + X_2^2} = 0 \qquad \textbf{Model Equation One}$$

and $$\frac{jX}{R^2 + X^2} + \frac{j}{X_M} + \frac{jX_2}{(R_2/s)^2 + X_2^2} = 0, \qquad \text{which can be rewritten as:}$$

$$X_M = -\left(\frac{X}{R^2 + X^2} + \frac{X_2}{\left(\frac{R_2}{s}\right)^2 + X_2^2} \right)^{-1} \qquad \textbf{Model Equation Two}$$

These two equations are neat expressions that, when solved, could be used to predict the behavior of any self-excited induction machine. Salama and Holmes[36] derived similar equations and then proceeded to solve for the slip (s) in the first equation before applying the result to the second equation to find a value for X_M. This is a logical approach and appeared to work well. However, to solve for s, the authors multiplied out the first equation to obtain a very complex polynomial of degree 7, the reason for the high degree being the fact that slip affects the electrical frequency and, hence, the impedance of the capacitors and inductors.

In the present work, it was felt that an iterative approach would be a far simpler way of solving for s. Accordingly, the first equation was first of all rearranged:

$$\frac{R}{R^2+X^2}+\frac{1}{R_C}+\frac{R_2/s}{\left(R_2/s\right)^2+X_2^2}=0$$

$$\Rightarrow \qquad \frac{R}{R^2+X^2}+\frac{1}{R_C}=-\frac{s/R_2}{1+\left(s.X_2/R_2\right)^2}$$

$$\Rightarrow \qquad s=-R_2.\left(1+\left(s.X_2/R_2\right)^2\right).\left(\frac{R}{R^2+X^2}+\frac{1}{R_C}\right)$$ **Iterative slip equation**

This equation can also be written in terms of the electrical frequency ω_e and the mechanical frequency ω_m using the following relation:

$$\omega_m=\frac{1-s}{p}.\omega_e \qquad \text{or} \qquad s=1-\frac{p.\omega_m}{\omega_e}$$

So: $$1-\frac{p.\omega_m}{\omega_e}=-R_2.\left(1+\left(\left(1-\frac{p.\omega_m}{\omega_e}\right)\frac{X_2}{R_2}\right)^2\right).\left(\frac{R}{R^2+X^2}+\frac{1}{R_C}\right)$$

And: $$\omega_e=\frac{p.\omega_m}{1+R_2.\left(1+\left(\left(1-\frac{p.\omega_m}{\omega_e}\right)\frac{X_2}{R_2}\right)^2\right).\left(\frac{R}{R^2+X^2}+\frac{1}{R_C}\right)}$$

Or: $$\omega_e=\frac{p.\omega_m}{1+R_2.\left(1+\left(\left(\omega_e-p\omega_m\right)\frac{L_2}{R_2}\right)^2\right).\left(\frac{R}{R^2+X^2}+\frac{1}{R_C}\right)}$$ **Iterative freq equation**

The result of either of the iterative equations could be used to provide an appropriate input for Model Equation Two which, in turn, would give a value of magnetising reactance. However, as explained in Section 4.1, it was felt that the iterative frequency equation would have better stability characteristics, so it was chosen ahead of the iterative slip equation. In its actual iterative form, the iterative frequency equation is as follows:

$$\omega_e(i+1) = \frac{p.\omega_m}{1 + R_2.\left(1 + \left((\omega_e(i) - p.\omega_m)\frac{L_2}{R_2}\right)^2\right).\left(\frac{R(i)}{R^2(i) + X^2(i)} + \frac{1}{R_C}\right)}$$

In other words, the (i+1)th estimate of the electrical frequency is found from the ith estimate of the electrical frequency and the effective resistive load and inductive load. Having found the frequency to within a satisfactory tolerance, it is then possible to calculate the magnetising reactance of the machine using Model Equation 2. Then, knowing the magnetising curve of machine, it is possible to find the air gap voltage, from which all important parameters can be found, eg. output voltage, current and efficiency, over the complete speed range.

The layout of a spreadsheet that does exactly over a range of speeds is given below. The results from the spreadsheet are shown to compare favourably both with the results of Salama and Holmes (Section 4.2.1) and with experimental results in (Section 4.3.4).

E.3 Spreadsheet simulation

A spreadsheet was organised to iteratively calculate the important output characteristics throughout the speed range of the self-excited-induction-generator-based electromechanical battery from basic machine, load and excitation capacitance data. This spreadsheet is shown below loaded with data taken from the paper of Salama and Holmes[38] for the purposes of comparing the proposed iterative method with the exact method adopted by Salama and Holmes. This comparison is described extensively in the main body of the thesis (Section 4.2.1).

In the first section of the spreadsheet, data necessary to compute the various output characteristics is inputted. This data is inputted in three different subsections:

Section I.I is dedicated primarily to the input of data for the purpose of computing the parameters of the induction machine equivalent ciruit. The data input is from the blocked rotor test, the dc-resistance test and the no-load test. If the parameters of the induction machine are known already, there is no need for much of this section or the corresponding calculations. In the sample spreadsheet shown below, the parameters were already known, so the test data shown, which is for a previous system is irrelevant and invalid.

In Section I.2, the values of the electrical load and excitation capacitance are inputted. The present spreadsheet setup expects a load in which any resistive and inductive elements are given as the equivalent series values while any capacitive load is given as a parallel equivalent value just like the excitation capacitors.

Section I.3 is dedicated to the magnetising curve of the induction machine. Measurements of input current and power for descending values of voltage are accepted in the first three columns. These measurements are then used to provide data on the variation of magnetising inductance with flux linkage for the induction machine. This data will subsequently be used to determine the operating air-gap voltage. (Because the sample spreadsheet shown below is a comparison with data given by Salama and Holmes[38], it was possible to directly input the data for air-gap voltage and magnetising reactance by reproducing the curve given in their paper--the reproduced curve is shown in Figure E.2)

Section 2 presents the calculations of the spreadsheet. In Section 2.1, the machine parameters are usually calculated (but not in this case because they are already known and are written in directly). Section 2.2 contains the main body of calculations in a large table. The results shown is for machine described by Holmes and Salama[38]. The formulae used to make the calculations in the table are given at the end

Fig E.2 The variation in air-gap voltage with magnetising reactance

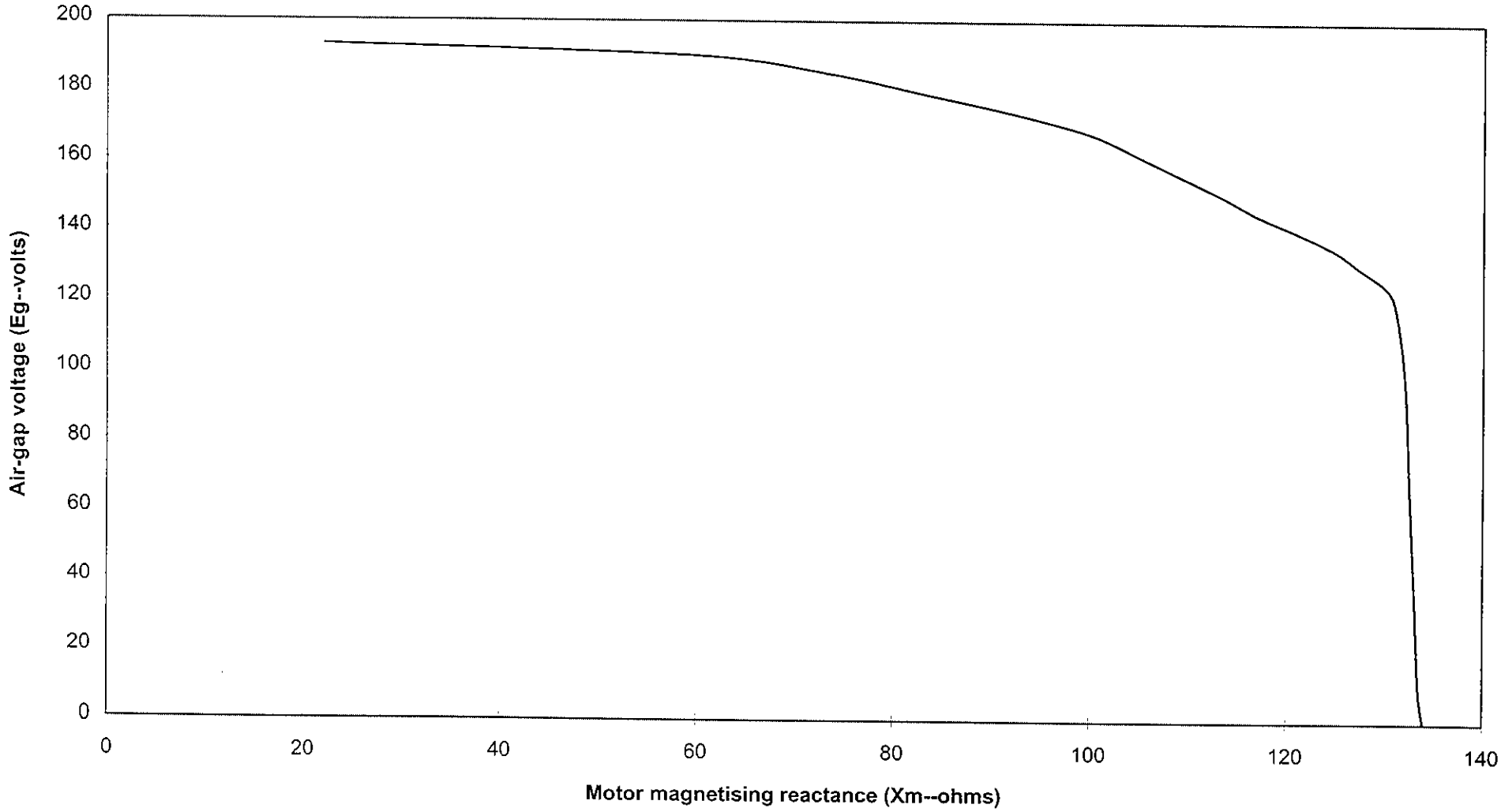

Input information

Section 1.1 *Induction machine data*

[illegible]

Synch. speed [illegible] [illegible]

[illegible]

Blocked-rotor test
Per phase values

[illegible]

[illegible]

[illegible]

[illegible]

[illegible]

[illegible]

No-load test data at rated voltage
(Per phase values only)

Voltage	=	234.3	V
Current	=	1.555	A
Power	=	51.5	W

Section 1.2 *Electrical load and excitation capacitance*

Series resistance per phase	=	200	ohms
Series inductance per phase	=	0	henries
Excitation capacitance	=	0.00009	farads
Load Capacitance	=	0	farads

Section 3.1 Calculation of machine and load parameters

Stator resistance (R1)	=	8.50	ohms				
Stator leakage reactance (X1)	=	15.72	ohms	L1	=	0.050	henries
Rotor leakage reactance (X2)	=	18.06	ohms	L2	=	0.058	henries
Z1 (ie R1+jX1)	=	17.87	ohms				
Core loss resistance (Rc)	=	##########	ohms				
Magnetising reactance (Xm)	=	133.70	ohms				
Rotor resistance (R2)	=	3.95	ohms				
Pole pairs (p)	=	2					
Total shunt capacitance	=	0.00009	farads				

INPUT MEASUREMENTS				PARAMETER CALCULATION				
Voltage (V)	Current (A)	Power (W)		Air-gap voltage (Eg)	Core-loss Resistance (Rc)	Magnetis'g Reactance (Xm)	Magnetis'g Inductance (Lm)	Flux linkage (Sig)
				193.000		22.000	0.070	0.615
				192.500		29.000	0.092	0.613
				192.000		36.000	0.115	0.611
				191.500		42.000	0.134	0.610
				191.000		48.000	0.153	0.608
				190.500		54.000	0.172	0.607
				190.000		60.000	0.191	0.605
				187.500		68.200	0.217	0.597
				185.000		74.000	0.236	0.589
				182.500		80.200	0.255	0.581
				180.000		85.700	0.273	0.573
				177.500		89.250	0.284	0.565
				175.000		93.000	0.296	0.557
				172.500		97.000	0.309	0.549
				170.000		99.750	0.318	0.541
				167.500		102.750	0.327	0.533
				165.000		105.400	0.336	0.525
				162.500		107.750	0.343	0.518
				160.000		111.000	0.354	0.510
				155.000		115.500	0.368	0.494
				150.000		120.000	0.382	0.478
				145.000		124.000	0.395	0.462
				140.000		126.000	0.401	0.446
				135.000		128.000	0.408	0.430
				130.000		130.000	0.414	0.414
				120.000		132.000	0.420	0.382
				110.000		132.000	0.420	0.350
				100.000		132.000	0.420	0.318
				90.000		132.500	0.422	0.287
				80.000		132.500	0.422	0.255
				70.000		132.500	0.422	0.223
				60.000		133.000	0.424	0.191
				50.000		133.000	0.424	0.159
				40.000		133.000	0.424	0.127
				30.000		133.500	0.425	0.096
				20.000		133.500	0.425	0.064
				10.000		133.500	0.425	0.032
				0.000		134.000	0.427	0.000

Section 2.2 Determination of the output characteristics of the machine (single iteration only)

Rotation Speed (RPM) [w_m]	Estimated Initial Electrical Frequency (r/s) [$w_e(0)$]	Computed Initial Slip (-) [s(0)]	Computed Initial Shunt Capac. Reactance (ohms) [$X_c(0)$]	Computed Initial Series load Resistance (ohms) [R(0)]	Computed Initial Series load Reactance (ohms) [X(0)]	First Iteration Electrical Frequency (r/s) [$w_e(0)$]	First Iteration Slip (-) [s(1)]	First Iteration Shunt capac. Reactance (ohms) [$X_c(1)$]	First Iteration Series load Resistance (ohms) [R(1)]	First Iteration Series load Reactance (ohms) [X(1)]	Machine Inductance (henries) [Lm]	Machine Flux linkage (V.s)	Air-gap Voltage (V)	Load Voltage (V)	Load Current (A)	fficiency (-)
1500	300.0	-0.047	37.0	15.1	-20.8	287.1	-0.094	38.7	15.7	-22.9	0.162	0.608	174.6	238.6	1.19	0.413
2450	277.5	-0.094	40.0	16.2	-24.6	280.0	-0.085	39.7	16.1	-24.2	0.162	0.608	170.3	228.4	1.14	0.433
1400	270.3	-0.084	41.1	16.6	-25.9	272.2	-0.077	40.8	16.5	-25.6	0.166	0.608	165.6	217.7	1.09	0.449
1350	262.5	-0.077	42.3	17.1	-27.4	264.1	-0.071	42.1	17.0	-27.1	0.172	0.607	160.2	206.4	1.03	0.466
1300	254.3	-0.070	43.7	17.6	-29.0	255.7	-0.065	43.5	17.5	-28.7	0.181	0.607	155.1	195.9	0.98	0.483
1250	245.9	-0.065	45.2	18.2	-30.7	247.0	-0.060	45.0	18.1	-30.4	0.191	0.605	149.5	185.1	0.93	0.501
1200	237.2	-0.060	46.8	18.9	-32.5	238.2	-0.055	46.6	18.8	-32.3	0.204	0.605	144.1	175.1	0.88	0.519
1150	228.3	-0.055	48.7	19.7	-34.5	229.2	-0.051	48.5	19.6	-34.3	0.220	0.597	136.8	163.1	0.82	0.538
1100	219.2	-0.051	50.7	20.6	-36.7	220.0	-0.047	50.5	20.5	-36.5	0.239	0.589	129.6	151.7	0.76	0.558
1050	210.0	-0.047	52.9	21.6	-38.9	210.6	-0.044	52.8	21.5	-38.8	0.260	0.581	122.4	140.8	0.70	0.578
1000	200.6	-0.044	55.4	22.7	-41.4	201.2	-0.041	55.2	22.7	-41.3	0.286	0.565	113.7	128.6	0.64	0.599
950	191.1	-0.041	58.1	24.1	-44.0	191.6	-0.038	58.0	24.0	-43.9	0.316	0.549	105.3	117.2	0.59	0.620

A	B	C	D	E
Rotation Speed (RPM)	*Estimated Initial Electrical Frequency (r/s)*	*Computed Initial Slip (-)*	*Computed Initial Shunt Capac. Reactance (ohms)*	*Computed Initial Series load Resistance (ohms)*
Ws	300	1-(p*$A137*0.1047/B137)	= (1/(B137*C_))	=_R1+D137^2*RL/(RL^2+(B137*LL-D137)^2)
A137-Ws/30	$G137*$A138/$A137	=1-(p*$A138*0.1047/B138)	= (1/(B138*C_))	=_R1+D138^2*RL/(RL^2+(B138*LL-D138)^2)
A138-Ws/30	$G138*$A139/$A138	1-(p*$A139*0.1047/B139)	= (1/(B139*C_))	=_R1+D139^2*RL/(RL^2+(B139*LL-D139)^2)

F

Computed Initial Series load Reactance (ohms)
B137*LL+((-LL/C)*(LL*B137-D137)+D137*RL^2)/(RL^2+(B137*LL-D137)^2)
B138*LL+((-LL/C)*(LL*B138-D138)+D138*RL^2)/(RL^2+(B138*LL-D138)^2)
B139*LL+((-LL/C)*(LL*B139-D139)+D139*RL^2)/(RL^2+(B139*LL-D139)^2)

G	H
First Iteration Electrical Frequency (rad)	*First Iteration Slip (-)*
(1+(R2*(1+((B137-p*A137*0.1047)*L2 / R2)^2))*(1/Re +E137/(E137^2+F137^2)))^(-1)*p*A137*0.1047	=1-(p*$A137*0.10471976/G137)
(1+(R2*(1+((B138-p*A138*0.1047)*L2 / R2)^2))*(1/Re +E138/(E138^2+F138^2)))^(-1)*p*A138*0.1047	=1-(p*$A138*0.10471976/G138)
(1+(R2*(1+((B139-p*A139*0.1047)*L2 / R2)^2))*(1/Re +E139/(E139^2+F139^2)))^(-1)*p*A139*0.1047	=1-(p*$A139*0.10471976/G139)

I	J	K
First Iteration Shunt capac. Reactance (ohms)	*First Iteration Series load Resistance (ohms)*	*First Iteration Series induc. Reactance (ohms)*
-(1/(G137*C_))	R1+I137^2*RL/(RL^2+(G137*LL-I137)^2)	=G137*L1_+((-LL/C_)*(LL*G137-I137)+I137*RL^2)/(RL^2+(G137*LL-I137)^2)
-(1/(G138*C_))	R1+I138^2*RL/(RL^2+(G138*LL-I138)^2)	=G138*L1_+((-LL/C_)*(LL*G138-I138)+I138*RL^2)/(RL^2+(G138*LL-I138)^2)
-(1/(G139*C_))	R1+I139^2*RL/(RL^2+(G139*LL-I139)^2)	G139*L1_+((-LL/C_)*(LL*G139-I139)+I139*RL^2)/(RL^2+(G139*LL-I139)^2)

L	M	N
Machine Inductance (henries)	*Machine Flux linkage (V.s)*	*Air-gap Voltage (V)*
-(((G137*K137/(J137^2+K137^2)+G137^2*L2 /((R2/$H137)^2+(G137*L2)^2))^-1)	=VLOOKUP(L137,H$46:I$83,2)	G137*M137
-(((G138*K138/(J138^2+K138^2)+G138^2*L2 /((R2/$H138)^2+(G138*L2)^2))^-1)	=VLOOKUP(L138,H$46:I$83,2)	=G138*M138
-(((G139*K139/(J139^2+K139^2)+G139^2*L2 /((R2/$H139)^2+(G139*L2)^2))^-1)	=VLOOKUP(L139,H$46:I$83,2)	=G139*M139

O	P
Load Voltage (V)	*Load Current (A)*
N137*((J137^2+K137^2-J137* R1-K137*L1 *G137)^2+(K137* R1-G137*L1 *J137)^2)^0.5/(J137^2+K137^2)	=O137/(RL^2+(G137*LL)^2)^0.5
N138*((J138^2+K138^2-J138* R1-K138*L1 *G138)^2+(K138* R1-G138*L1 *J138)^2)^0.5/(J138^2+K138^2)	=O138/(RL^2+(G138*LL)^2)^0.5
N139*((J139^2+K139^2-J139* R1-K139*L1 *G139)^2+(K139* R1-G139*L1 *J139)^2)^0.5/(J139^2+K139^2)	=O139/(RL^2+(G139*LL)^2)^0.5